NCU-T-78-011 C. 2

CIRCULATING COPY
Sea Grant Depository

Sediment Dynamics and Shoreline Response at Drum Inlet, North Carolina

J.W. Forman, Jr.
J.L. Machemehl

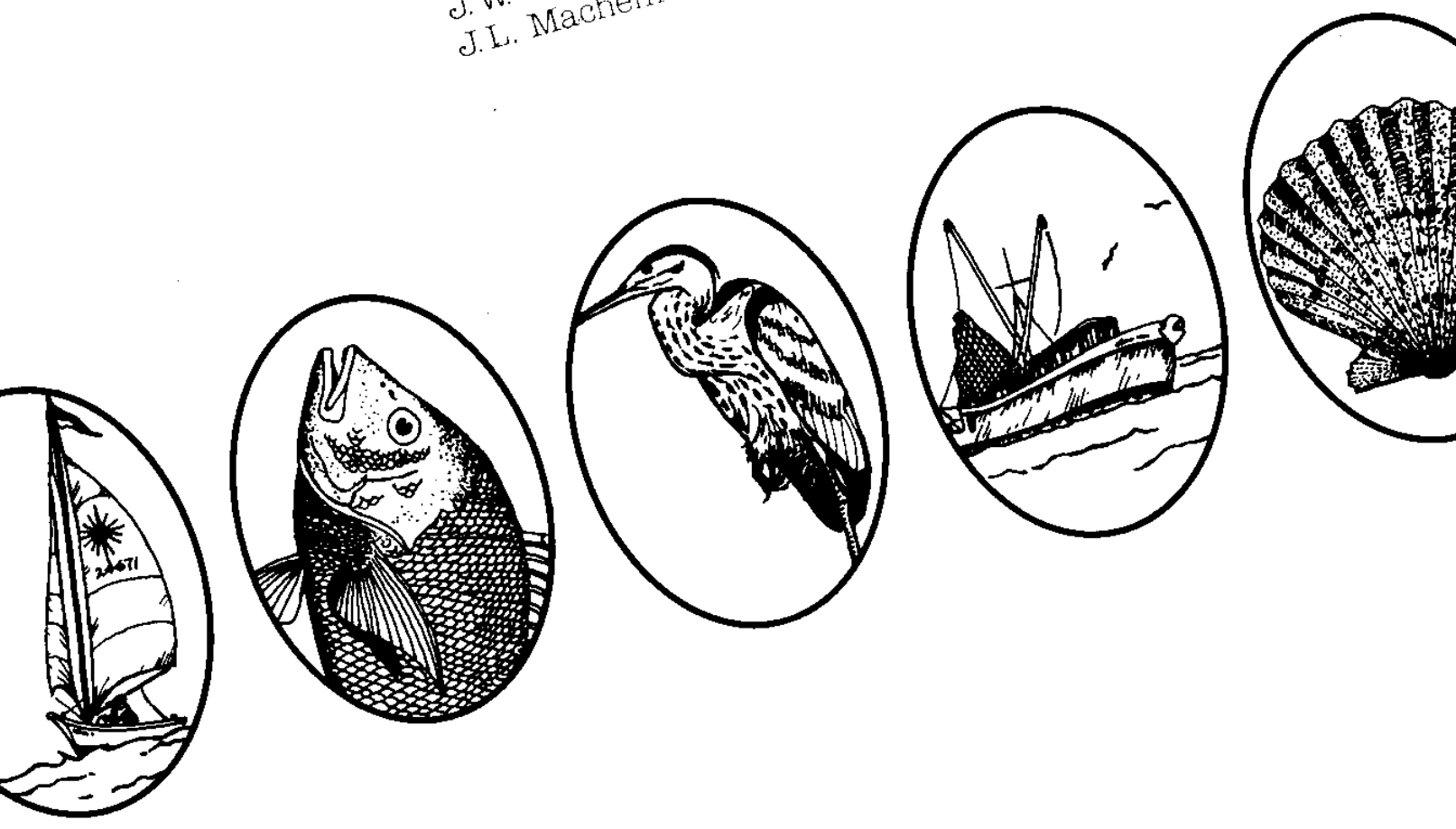

UNC Sea Grant College Program
105 1911 Building
North Carolina State University
Raleigh, NC 27650

SEDIMENT DYNAMICS AND SHORELINE RESPONSE AT DRUM INLET, NORTH CAROLINA

by

James William Forman, Jr.
Department of Civil Engineering

and

Jerry L. Machemehl
Department of Marine Science and Engineering
North Carolina State University
Raleigh, North Carolina 27650

This work was sponsored by the Department of Marine Science and Engineering and the Office of Sea Grant, NOAA, U.S. Department of Commerce, under Grant No. 04-8-M01-66 and the North Carolina Department of Administration. The U.S. Government is authorized to produce and distribute reprints for governmental purposes notwithstanding any copyright that may appear hereon.

Department of Marine Science
and Engineering Publication No. 78-7

UNC Sea Grant College Working Paper 78-2

December, 1978

ABSTRACT

A study of Drum Inlet was conducted to develop a hypothesis of sediment movement at the inlet, to determine the stability and predict the future of the inlet, to determine the response of the barrier island to the presence of the inlet, and to develop a sediment budget and establish shoaling rates for the inlet and flood tidal shoals.

Aerial photographs (October ,1971 to March ,1977) of the inlet and the adjacent barrier islands were analyzed to determine the volume of shoreline erosion and accretion of the barrier island occurring during the study period, the patterns and rates of growth of the flood tidal shoals and the movement rates of primary bedforms across the flood tidal shoals.

A flourescent tracer study was conducted in August ,1977 to determine the rates and patterns of sediment movement in high and low energy zones at the inlet. The maximum ebb and flood current velocities and the current directions were measured in the inlet main channel, distributary channels and at selected points in the low energy shallow shoal area. Sediment core samples from eight locations at varying distances from the inlet mouth were analyzed to determine grain size distributions of the inlet sediments.

Correlation of aerial photographs and field data revealed a pattern of sediment circulation in the inlet. It was found that the inlet mouth and adjacent beaches served as sources of sediment moving in and out of the inlet system. The sediments from the inlet mouth and the head of the flood tidal delta moved across the shallow flood-current dominated shoal areas into ebb dominated distributary channels where it was recirculated back to the inlet mouth.

It was found that the presence of the inlet caused severe erosion of 1.5 miles of shoreline adjacent to the inlet mouth. Nodal points, 3000 feet south of the inlet centerline and 5000 feet north of the inlet centerline, were found. The nodal points were characterized by little change in beach position compared to other points in the study area. The overall net shoreline erosion that occurred during the study period was 5.5 million cubic yards.

The sediment budget analysis which considered the contributions of littoral drift, beach erosion, sediment trapping and bypassing provided an order of magnitude value of the shoaling rate. It was found that approximately 13 percent of the material supplied to the inlet was trapped on the shoals. This volume rate of shoaling amounted to 360,000 cubic yards per year. This value was in close agreement with the calculated volume of material on the shoals.

The stability of the inlet was determined by comparing rates and patterns of growth of inlet features and by calculating the ratio of tidal prism to littoral drift volume proposed by Bruun and Gerritsen (1960) and Bruun (1966). By the end of the study period the beaches, inlet throat, and flood tidal shoals had reached a relatively stable configuration. This implied that there was substantial flushing of littoral material from the inlet. From these anlaysis and a ratio of tidal prism to littoral drift volume equal to 23 ($\Omega/M < 100$ indicates poor stability), it was determined that the inlet stability was fair and that shoaling would continue at a rate much less than in the early life of the inlet.

ACKNOWLEDGEMENTS

The authors express their appreciation to the Department of Marine Science and Engineering and the UNC Sea Grant Program, NOAA, for partial support of the study. The authors also express their appreciation to Civil Engineering and Marine Science students, John Gerstenlauer, Larry Watson, Joseph Hardee, John Reeves, Robert Tang and James Boone for their time and effort in the field work. The study would have been impossible without their assistance. A special thanks is extended to Mr. Limberios Vallianos and his staff at the U.S. Army Corps of Engineers, Wilmington District, for their time and assistance and for the data they provided to this study.

TABLE OF CONTENTS

LIST OF TABLES

LIST OF FIGURES

Page

INTRODUCTION

Drum Inlet is located in Carteret County, North Carolina approximately 22 miles north of Cape Lookout and 22 miles south of Ocracoke Inlet (see Figure 1). The Inlet divides Core Banks, which are part of the Cape Lookout National Seashore. The nearest town, Atlantic, North Carolina is located across Core Sound approximately 2 miles northwest of the Inlet and 30 miles from Beaufort, North Carolina,on Highway 70 east.

The Inlet was opened in December, 1971,by the U. S. Army, Corps of Engineers to provide navigational access to Rayleigh Bay from Core Sound and to maintain favorable salinity levels in Core Sound.

The Problem

Since the opening of Drum Inlet, the growth of extensive flood-tidal shoals rendered the inlet useless for navigation. Maintenance of a navigable channel proved uneconomical due to the rapid shoaling rate of both flood and ebb tidal shoals.[1] Erosion of the beaches adjacent to the Inlet threatened to reduce the width of the already narrow protective barrier island. Development of information concerning the hydraulics and sediment dynamics of the Inlet, beaches and shoals is important for the planning and design of man-made tidal inlets. The engineer must be able to predict the long range affects of a man made inlet in the planning and design process.

---

[1] Limberos Vallianos, personal communication.

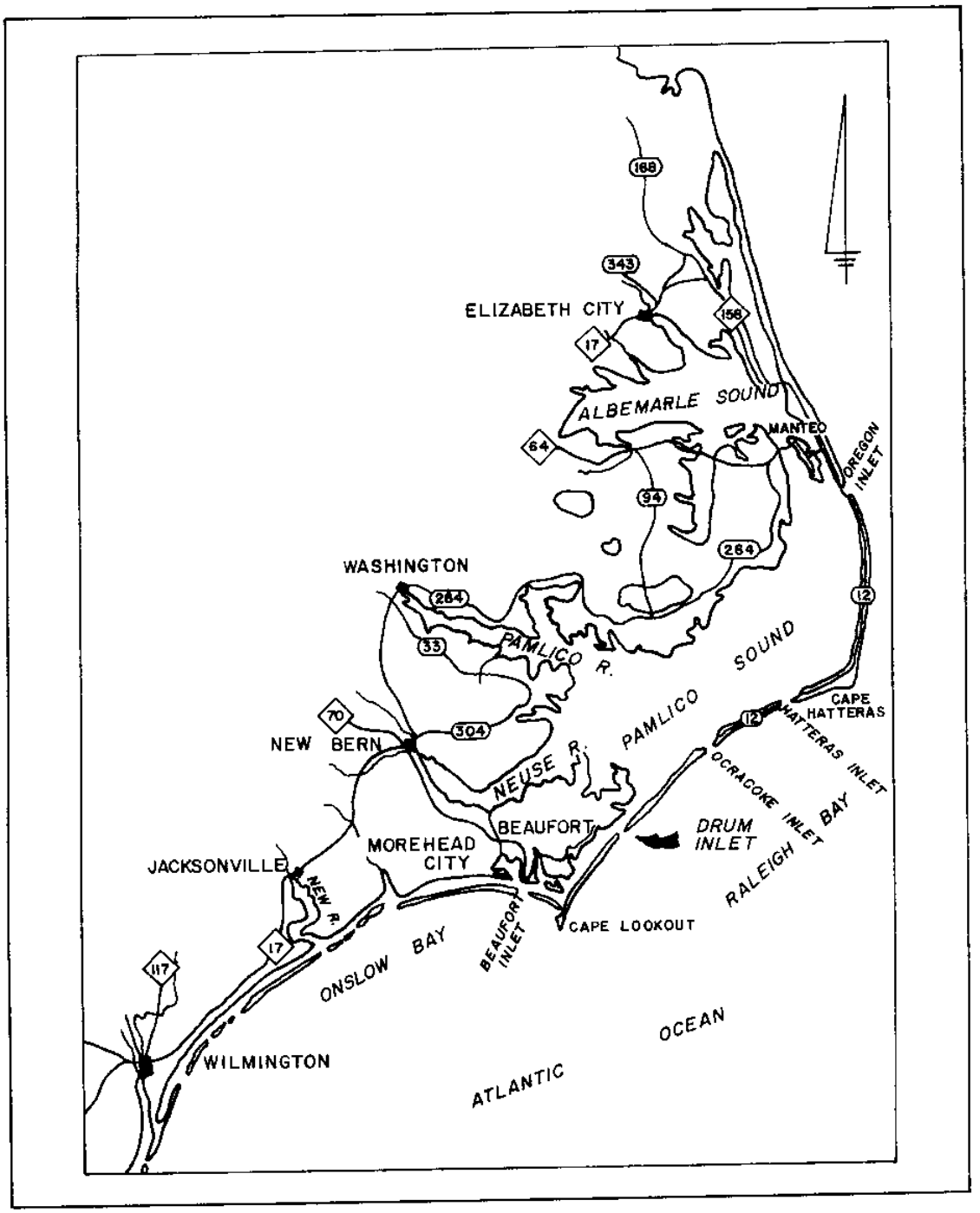

Fig. 1. Study Area Location Map

Objectives of Study

The objectives of this study were:

(1) to develop a hypothesis of sediment movement at Drum Inlet based on the analysis of erosion and deposition trends observed in aerial photographs and field measurements of currents, sediment distributions and movement of flourescent tracer in high and low energy zones;

(2) to determine the response of the barrier island to the presence of the Inlet by studying sequential aerial photographs of the Inlet and barrier islands since the opening of the Inlet;

(3) to devise a sediment budget for the Inlet system accounting for littoral drift, trapping of sediment on the flood shoals and bypassing; and

(4) to determine the stability and predict the future of the inlet and the flood tidal shoals by studying growth patterns using aerial photographs and field measurements.

REVIEW OF LITERATURE

Inlet Shoaling and Delta Formation

How and why inlets shoal

Shoaling occurs at inlets for a variety of reasons. According to Bruun and Gerritsen (1960), shoaling in inlets will occur due to:

(1) an elongation of the inlet channel or channels,

(2) large storm-driven sediments of littoral material deposited in the inlet,

(3) division of the main channel into multiple channels or development of additional channels from natural or artificial causes,

(4) changes in bay areas due to construction of dams or canals.

Inlet configurations are continuously attempting to reach an equilibrium state. The cross-sectional area of an inlet gorge will change until it reaches an equilibrium size. It can then maintain this stable area for a period of time. If shoaling occurs, the flow must increase and maintain the inlet cross-sectional area without elongation or choking will occur in the inlet. The cross-sectional area must increase with elongation of the inlet channels to prevent choking.

During flood flows littoral material is transported into the bay by flood currents. Depending on the inlet configuration, some material

will be returned seaward and some will remain at the end of flood channels building up shoals. Bay shoals will tend to develop mainly towards the end of flood channels. Sea shoals will do the same, but will have a different configuration due to wave current interactions. The dimensions of these shoals are a function of the flow capacity of an inlet (tidal prism).

According to Dean and Walton (1975) there is no limit to the equilibrium volume of the flood shoals. The existence of the shoals may play a primary role in causing an inlet to migrate. This can be especially true where there is a high volume of littoral drift. As material accumulates on the updrift side of the inlet, the hydraulics of the channels becomes less efficient causing increasing competition of downdrift channels. The result is a downdrift migration of the inlet. In the case of barrier islands, the inner shoals may become part of the outer shores by continuing inlet migration and shoreline erosion. If the inlet does not migrate, the inner shoals may eventually reach an equilibrium volume. In this case, an upward bottom slope will develop toward the inner bay. In equilibrium to this slope, is a downward seaward gradient that produces a force opposing the movement of any additional material into the bay shoals.

Several researchers have discussed the effects of tidal range, wave energy, inner shelf slope, tidal currents, bay area, and hydrological properties on the morphology of tidal inlets. Hayes (1975) demonstrated that the tidal range affects tidal inlet-lagoon system significantly. Micro-tidal coasts (tidal range less than 6 feet) are characterized by long narrow barriers seaward of shallow lagoons. Shoals

exist mainly on the lagoon side of the inlet. Meso-tidal coasts (tidal range between 6 and 12 feet) typically have lagoons consisting mainly of marsh. The bulk of sand is usually stored on a seaward semi-circular shoal. Macro-tidal coasts are generally characterized by funnel shaped embayments which are responsible for large tidal wave amplifications. These bays usually have long linear or S-shaped shoals oriented nearly parallel to the axis of the bay. The coasts of North Carolina are micro-tidal.

Nummendal (1977) discusses the response of inlet morphology to inner shelf slope, wave energy and the hydrologic properties of the lagoon. He states that lagoons with a large percentage of open water result in inlets that have flood dominated currents. Lagoons that are primarily marsh filled will generate ebb dominated flows.

Wave climate is parameterized in terms of the deep water energy flux and wave height frequencies. The onshore directed vector of wave energy flux is used as an indicator of the potential for shoreline modification. Wave dominated inlets typically have small ebb tidal deltas pushed against the shore, wide throats with several sand bodies and large flood shoals.

The variation of wave energy and tidal range is attributed to the magnitude of the inner shelf slope.

Delta formation

Most of the work done in the study of delta formation deals with the major river deltas. Yangs (1976) hypothesis of minimum unit stream power states that for subcritical flow with bed forms in the lower flow regime an alluvial channel will adjust its velocity, slope, roughness

and geometry so that a minimum stream power is used to transport a given sediment load and water discharge. Unit stream power is defined as the rate of potential energy expenditure per unit weight of water. The minimum unit stream power in an alluvial channel is affected by changes in the water discharge, sediment concentration, particle size and water temperature. An alluvial channel will adjust its velocity, slope and depth by way of scour or deposition and changing roughness in order to maintain a balance between the rate of sediment load imposed and the rate of work done (i.e. between the sediment concentration and the unit stream power).

Silvester and La Cruz (1970) investigated delta morphology of 53 major river deltas. Their results were a quantitative attempt to develop relationships between delta morphology and environmental conditions. They studied delta characteristics such as delta length, area, maximum width, ratios between maximum width and number of distributary mouths and ratios between maximum width and the number of distributaries. Of importance here are results indicating that both delta length and area are directly correlated to water discharge. They also determined that as discharge increased there were fewer but larger distributaries. Another important result was that the most important upstream controls on delta morphology are water discharge, flow velocity and sediment load.

Schumm (1977) discusses a model test done by Chang. The growth of a model delta was observed under varying sediment loads. This experiment is of special interest because of the similarity to the tidal delta studied in this report. It was found that major differences in

the delta shape resulted from changes in the sediment concentration. There was noticeable elongation of the delta during erosion of the head. This occurred during a decrease in sediment load. The result was a low width to length ratio. A much higher width to length ratio occurred with an increased sediment load. Sediment is stored near the delta head and then when erosion occurs the material is moved to the landward reaches of the delta causing elongation. It is predicted from these tests that, in nature, delta area and length will decrease with an increased sediment load and that erosion and lengthening of the delta will occur with decreased sediment loads.

Inlet Stability

All inlets change their configuration in response to changing natural forces. It is important to be able to determine the hydraulic characteristics that control the stability of inlets. There are several theories that concern the stability of inlets; however, these theories are only approximations subject to revision as additional inlet studies provide more accurate information.

O'Brien (1960, 1966) presented a relationship which correlates the cross-sectional area of an inlet gorge with the tidal prism. This formula is:

$$a_c = b\Omega^N \tag{1}$$

where a_c is the cross-sectional area of the gorge measured below mean sea level in $(\text{feet})^2$, and Ω is the tidal prism as volume of water stored in the bay between high and low waters corresponding to the

diurnal or spring tide range in cubic feet. The values of b and N are shown in Table 1.

TABLE 1

VALUES FOR O'BRIEN'S COEFFICIENTS, b AND N

Tidal Inlets	b	N
Two jetties	4.69×10^{-4}	0.85
No jetties	7.00×10^{-5}	1.0

O'Brien (1975) states that:

> Intuitively, these relationships seem questionable for a number of reasons:
>
> (1) There appears to be no effect for the size of sand forming the channel and adjacent shores,
>
> (2) The range of tide enters only as it affects the tidal prism. The percentage variation in flow area between HW and LW is large at small inlets subjected to a large range of tide,
>
> (3) The net and gross rate of littoral drift is not effective,
>
> (4) Both unimproved and improved inlets are included,
>
> (5) Lagoons with two inlets conformed if the summations of the flow areas was used, and
>
> (6) The inlets to both lagoons and estuaries followed the same relationship. There appears to be no affects of fresh water flow or of sediment transport.

Jarrett (1976) has evaluated data from 162 Pacific, Atlantic and Gulf Coasts inlets without jetties and with one or two jetties and determined more accurate values of b and N for O'Brien's relationship. The values of b and N obtained by Jarrett are shown in Table 2.

TABLE 2

VALUES FOR b AND N FOR O'BRIEN'S TIDAL PRISM AREA RELATIONSHIP*

Inlets	b	N
Atlantic, Gulf, Pacific Coasts		
All	5.74×10^{-5}	0.95
One or no jetties	1.04×10^{-5}	1.03
Two jetties	3.76×10^{-4}	0.86
Atlantic Coast		
All	7.75×10^{-6}	1.05
One or no jetties	5.37×10^{-6}	1.07
Two jetties	5.77×10^{-5}	0.95
Gulf Coast		
All	5.02×10^{-4}	0.84
No jetty	3.51×10^{-4}	0.86
Two jetties	Insufficient data	
Pacific Coast		
All	1.19×10^{-4}	0.91
One or no jetties	1.91×10^{-6}	1.10
Two jetties	5.28×10^{-4}	0.85

*Jarrett, 1976.

Bruun and Gerritsen (1960) and Bruun (1966) proposed the ratio of Ω/M as a measure of inlet stability where M is the annual gross littoral drift. Values of Ω/M for different degrees of stability are:

$\frac{\Omega}{M} > 200$ good stability

$200 > \frac{\Omega}{M} > 100$ fair stability

$\frac{\Omega}{M} < 100$ poor stability

Johnson (1973) studied Pacific Coast inlets and concluded that, "Wave power appears to be the single most important factor affecting inlet stability." He discusses O'Brien's closure criteria C_1 which is the ratio of the wave energy to the tidal energy per tidal cycles, or

$$C_1 = \frac{E_s \, T \, w}{\Omega \, (2 a_o) \, \gamma} \tag{2}$$

in which E_s is wave power in foot pounds per foot of beach per second; w is the width of inlet gorge channel, in feet; a_o is the tidal amplitude, in feet; and γ is the unit weight of water in pounds per cubic foot. O'Brien reasoned that if wave energy is such that if the closure criteria is greater than a critical value, the elapsed time to closure, measured from the beginning of wave energy intensity E_s, should depend on a ratio of C_1/C_{crit} and the volume of the inlet to be filled by littoral drift. If C_1/C_{crit} is less than 1 the inlet remains open and if C_1/C_{crit} is greater than 1 the inlet tends to close if the storm exceeds a critical time.

Johnson was unable to apply this criteria to the study inlets because of insufficient data. Instead, he used a simplified procedure of comparing the potential tidal prism with the estimated annual wave power. The results were represented in graphic form with a line separating the inlets that have closed from the ones that have remained open. That line is represented by the equation:

$$W_p = 7.32 \times 10^{11} \, \Omega_p \, 0.20 \tag{3}$$

where W_p is the annual wave power in deep water near each inlet in foot pounds per foot per year and Ω_p is the potential tidal prism.

O'Brien and Dean (1966) proposed a stability index which represented the ability of an inlet to resist closure due to deposition. The stability index β is defined as:

$$\beta = \int_{a_p}^{a_E} (V_m - V_t)\, d a_c \tag{4}$$

where V_m is the maximum velocity in the inlet throat, V_t is the critical velocity for sand transport, a_c is the cross-sectional area in the inlet gorge, a_p is the value of a_c at peak of the V_m curve and a_E is the value of a_c at the intersection of the curve with the O'Brien's equilibrium velocity curve. A definition of this equation is given in Figure 2.

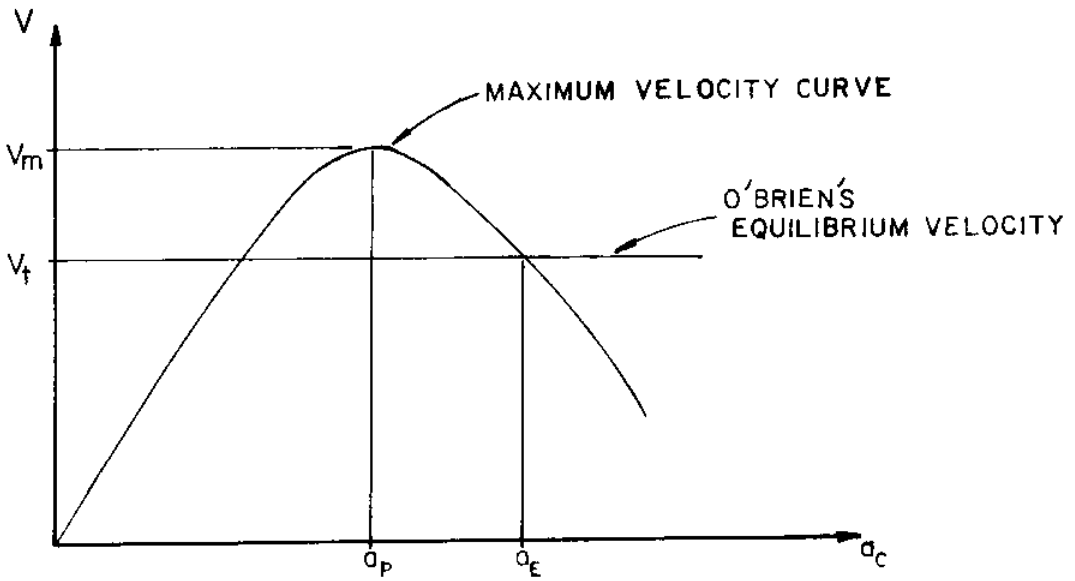

Fig. 2. Graphic description of integration limits a_E and a_p (after Escoffier, 1977).

Escoffier (1940) compared the peak tidal current velocity V_m, with the critical velocity, V_{cr}, to determine if an inlet was self-filling, self-eroding or stationary in size. V_m is calculated by the equation:

$$V_m = c\left(\frac{aH}{2pL}\right)^{1/2} \{(1 + r^2) - r\}^{1/2} \qquad (5)$$

where $$r = \left(\frac{12054c}{M}\right)^2 \frac{a^3}{2pHL} ,$$

C is the Chezy coefficient in $(\text{feet})^{1/2}$ per second, a is the cross-sectional area of the channel in square feet, p is the wetted perimeter of the channel in feet, L is the channel length in feet, H is the mean tidal variation in the ocean in feet, and M is the water surface area of the bay in square feet.

If c, L, H and M are constants and a and p are functions of x (a measure of the size of the channel) equation 5 can be used to evaluate the stability of inlets. Figure 3 shows the relationship between the variables V and x. On each graph the horizontal line that represents $V_M = V_{cr}$ and the intersections with the V curve are stable inlet cross-sectional areas. If the V curve and the $V_M = V_{cr}$ line intersect as in Figure 3a, there are two points or roots, an unstable one at B and a stable one at D. Any deviation from the unstable root at B will set into action forces which will lead to further instability. Deviation from the stable root at D will set in motion forces that will try to restore the inlet to a stable condition. If the conditions of an inlet channel place it between B and D near point C in Figure 3a, the channel may erode to the stable root at D or fill

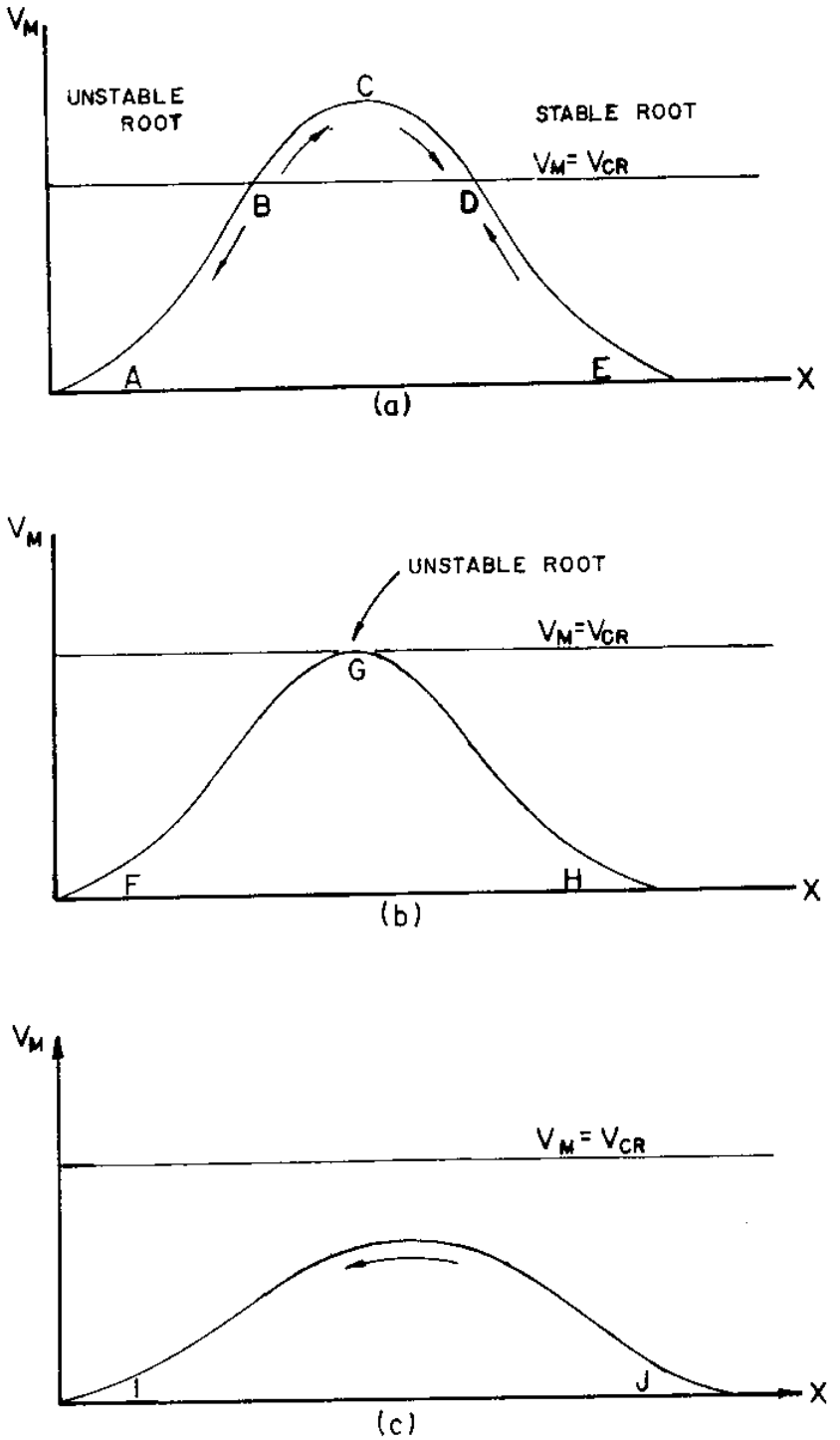

Fig. 3. Variations of Variables V_m and a_c (after Escoffier, 1940).

itself to the unstable root at B at which time the flushing capacity will decrease and the inlet will continue to fill and be represented on the V_M curve between A and B. Point D represents an inlet that is self-flushing and point B represents an inlet that is self-filling.

Figures 3b and 3c represent situations where a permanent inlet is not possible. In both cases, the tidal currents are not of sufficient strength to maintain a channel. The inlets will self-fill and choke to a closure condition.

Escoffier (1977) developed his expanded theory by using Keulegan's and O'Brien's formulas for maximum velocity. This allowed construction of a more usable diagram (Figure 4) with the equilibrium value of V_m not constant, but varying with the repletion coefficient. This coefficient summarized the effects of the channel and basin dimensions, of the roughness of the channel sides, and of the period and range of tidal fluctuations on the limits of the water-level changes in the basin. Escoffier then introduced a dimensionaless velocity ν defined as:

$$\nu = \epsilon \xi \tag{6}$$

where

$$\epsilon = \frac{C \sin \tau}{K}$$

and

$$\xi = \left(\frac{2 g L n^2}{1.486^2 R^{4/3}} + m \right)^{-1/2}$$

in which C is a dimensionaless number that is a function of K, τ is an angular measure of the lapse of time from slack tide in an inlet to mid-tide in the sea, L is the effective length of an inlet,

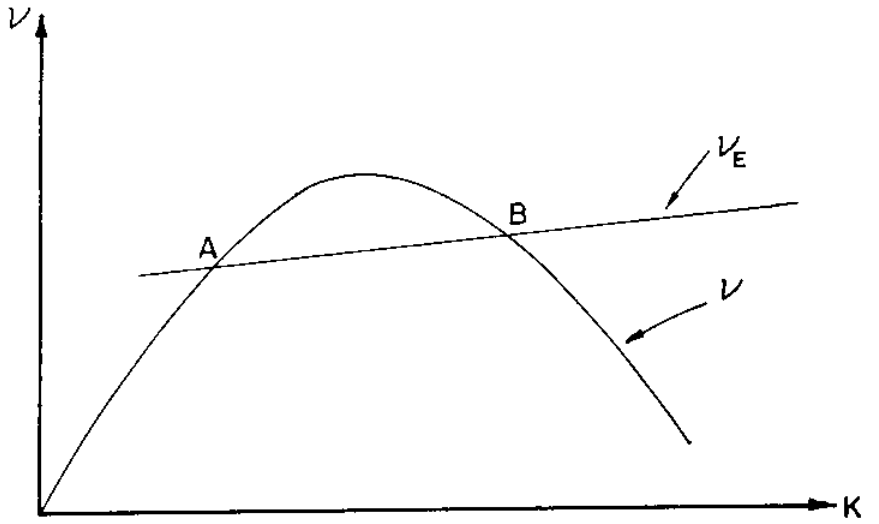

Fig. 4. ν_E and ν versus the repletion coefficient (after Escoffier, 1977).

n is the Manning roughness coefficient, R is the hydraulic radius in an inlet gorge, and m is the coefficient of combined entrance and exit losses. An equilibrium value of ξ_E is added as:

$$\xi_E = \frac{1}{\beta_*} K (\sin \tau)^{-N} \tag{7}$$

in which β_* is a dimensionaless number defined as:

$$\beta_* = \frac{b T \sqrt{2 g a_o}}{\pi} (2 A_b a_o)^{N-1}$$

where A_b = water surface area of the bay and b and N are coefficients from O'Brien's stability formula. From this an equilibrium

dimensionaless velocity is taken and defined as:

$$\nu_E = \epsilon \xi_E \quad . \tag{8}$$

ν and ν_E are then plotted as a function of the repletion coefficient, K, as shown in Figure 4. The intersections A and B in Figure 4 are points of equilibrium with A an unstable point and B a stable one. A deviation from point A sets in motion forces that will tend to increase the deviation. A deviation from B sets into action forces which tend to restore the inlet to equilibrium. If an increase in the size of the inlet results in a deviation of A, the velocity will increase. The resulting erosion will increase the gorge area. A deviation at B will cause the velocity to decrease, and the resulting accretion will decrease the cross-sectional area of the gorge causing a return back toward point B. A decrease in the cross-sectional area at point A will cause a decrease in the flow velocity resulting in a further area decrease until closure occurs. A decrease in area at Point B will cause an increase in the velocity resulting in scour and a return to equilibrium at Point B. The different positions of the ν curve in Figure 5 reflect the influence of waves and littoral drift volumes on the equilibrium size and stability of the inlet. The high position of the first curve is a reflection of small littoral drift or small wave power. The lower positions of the other ν curves reflect higher littoral drift or greater wave power. From this, Escoffier developed the stability index, λ , defined as:

$$\lambda = \left(\frac{\nu}{\nu_E}\right)_{\nu_{max}} \quad . \tag{9}$$

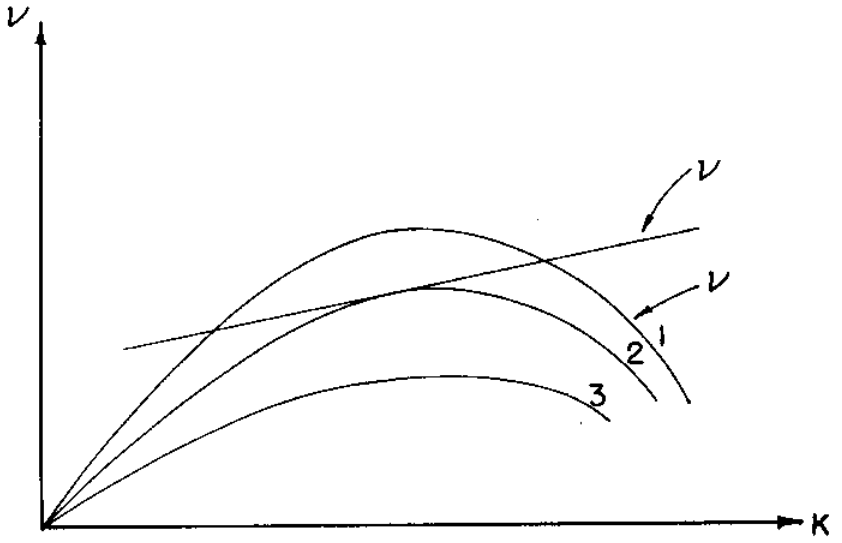

Fig. 5. ν_E and Various Values of ν Versus the Repletion Coefficient, K (after Escoffier, 1977).

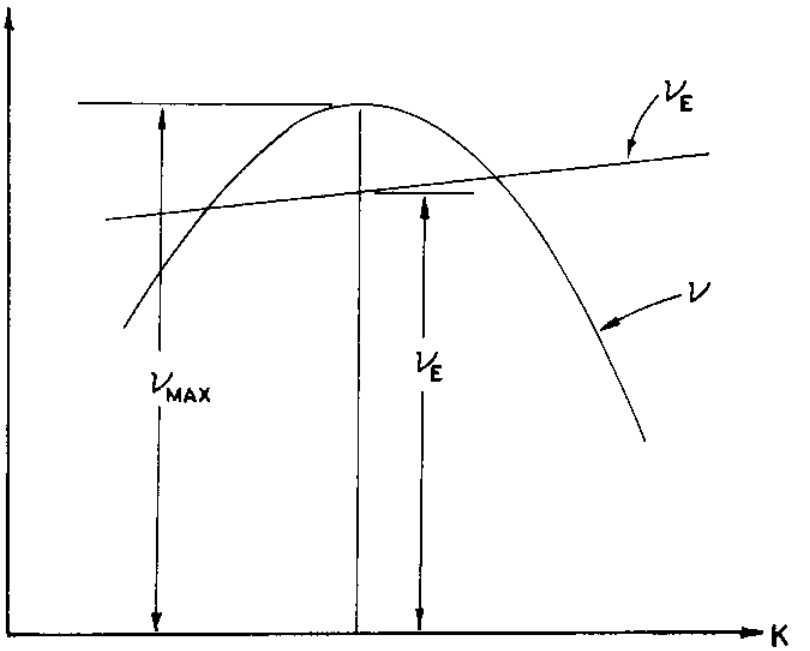

Fig. 6. Definition Diagram for the Stability Number, λ .

DESCRIPTION OF THE STUDY AREA

History of Old Drum Inlet

The most recent opening of Old Drum Inlet occurred during a hurricane of September, 1933 (House Doc. No. 414, 1937). There are records that indicate a Drum Inlet opened in 1799 and 1899. In addition, there was a Drum Inlet shown on the chart of James Wimble of 1738. The inlet served the commercial fishing industry of Core Sound until shoaling limited the drafts of boats that could use the inlet. In November, 1937, it was proposed to improve the inlet to accommodate the fishing industry and to increase fish populations in the Core Sound area.

After its most recent opening, Old Drum Inlet remained in a state of relative equilibrium for almost twenty years. The inlet maintained a controlling depth across the offshore bar of 7 feet from 1940 to 1953 (Snell, 1973). During the period 1954 to 1960 the inlet migrated 2400 feet to the southwest. This was probably caused by five hurricanes that passed within 50 miles during that period. Aerial photograph coverage available from 1940 to 1971 shows a migration of 6400 feet from a base location in 1940 (Vallianos).[2] A summary of inlet features, presented in Table 3, shows a rapid contraction on the inlet from March, 1955 ,to May, 1958. The inlet widened considerably

---

[2]Limberos Vallianos, personal communication.

TABLE 3

SUMMARY OF BASIC INLET FEATURES AT OLD DRUM INLET, OCTOBER, 1941 TO FEBRUARY, 1971*

Date of Aerial Photograph	Minimum Waterline Width of Inlet Throat (ft.)	Inlet Centerline** Position Relative to 1940 Position (ft.)
12 Oct. 1940	1,850	Baseline
23 Feb. 1943	1,100	Same
24 Jan. 1945	1,500	+1,000
29 Mar. 1955	1,310	+210
4 May 1958	850	+1,350
10 Oct. 1958	2,850	+600
16 Aug. 1959	600	+2,200
3 May 1962	1,408	+2,200
7 Apr. 1968	1,900	+5,400
11 Feb. 1971	0	+6,400

SOURCE: *Aerial photograph study by U.S. Army, Corps of Engineers, Wilmington District.

**Positive refers to a westerly position with respect to 1940 reference line.

during 1958 to its October width. Hurricane Helene (September, 1958) was probably responsible for this expansion. It is interesting to note the rapid contraction that occurred between October, 1958, and August, 1959. Temporarily open to small craft during the 1960's, the inlet finally became impassable in 1970. Seasonal storms during early 1971 completely closed the inlet.

Opening of New Drum Inlet

The loss of Old Drum Inlet inflicted an economic hardship on navigational interests in Carteret County, North Carolina. The economy of the Core Sound area is largely dependent on sport and commercial fishing (Snell, 1973). Valuable fish and mollusk species are taken in an area of Rayleigh Bay extending about 10 miles on either side of Drum Inlet and 25 miles offshore in the Atlantic Ocean. Access to these fishing grounds by sport or commercial fishing interests by way of Ocracoke of Beaufort Inlets involved a long round trip. This restricted activities and increased operating expenses. Small craft were almost excluded from activity due to the absence of a harbor of refuge. Productivity of shellfish beds in the Core Sound was especially vulnerable to salinity levels in the Sound. The absence of an inlet between Ocracoke and Cape Lookout reduced the salinity in the sound affecting shellfish populations.

In December, 1971, the U. S. Army Corps of Engineers opened a new Inlet, 2.1 miles southwest of the old location. The benefits of the project were: (1) to decrease the travel distance to Rayleigh Bay for Core Sound commercial and sport fishermen; (2) to increase seafood catches due to easier access to the fishing grounds; (3) to decrease spoilage of fish catches during the shorter return trip; (4) to provide a harbor of refuge for recreational and sports fishing craft; and (5) to restore the salinity balance in Core Sound and maintain favorable environmental conditions for development of the native shellfish populations (Snell, 1973).

The project consisted of dredging a channel 1.8 miles long by 7 feet deep by 150 feet wide in Core Sound extending from the north-south waterway connecting Pamlico Sound and Beaufort Harbor to the Outer Banks. The remaining distance through the barrier island to the ocean was a cut 9 feet deep by 150 feet wide. The final 350-foot-long cut was accomplished by explosive excavation.

The progression of development of the Drum Inlet system since the opening is most easily followed by a photographic record shown in Figures 7-12. Of interest in this report is the growth of flood tide shoals and sequential changes in the barrier island adjacent to the inlet. An explanation of the method used to make the basic photographic measurements is presented in the aerial photograph analysis section of this paper. The reference base for all measurements was a photograph of the inlet taken July 30, 1972. The reference inlet centerline is the centerline of the inlet throat from an aerial photograph of July ,1972. A summary of the basic inlet features is presented in Table 4. Of special interest, is the rapid growth of the flood tidal shoals between the time of the opening and November ,1975. After this there appears to be a slowing of the growth with very little additional lateral or longitudinal growth through March, 1977. The growth of the flood tidal shoals and barrier island changes are discussed in the air photo analysis portion of this study.

The width of the inlet throat measured at its narrowest point developed rapidly from the opening date through June, 1975. A reduction in width then occurred through November, 1975. After this, there appears to be a stabilization of the width. Compared to the Old Drum Inlet,

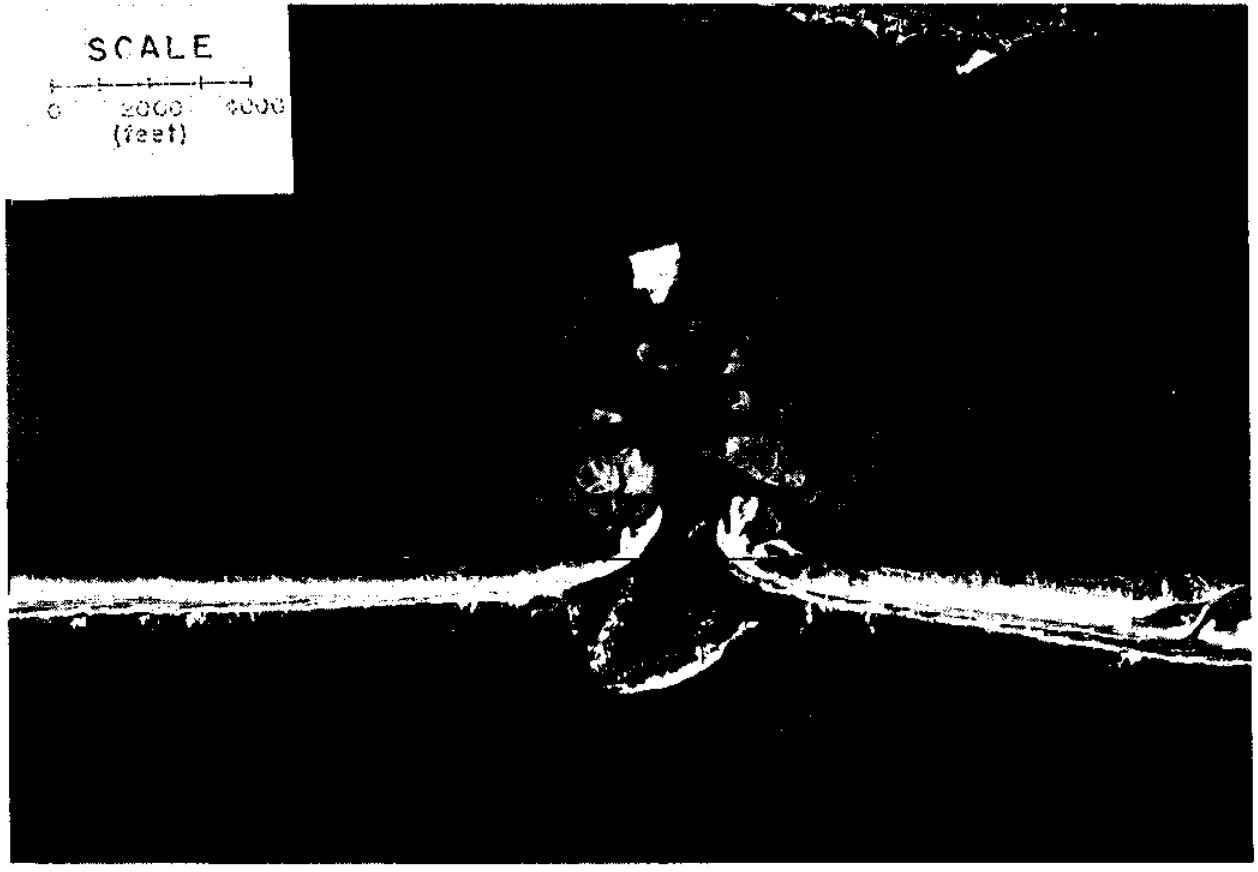

Fig. 7. Aerial Photograph, Drum Inlet, October 1973

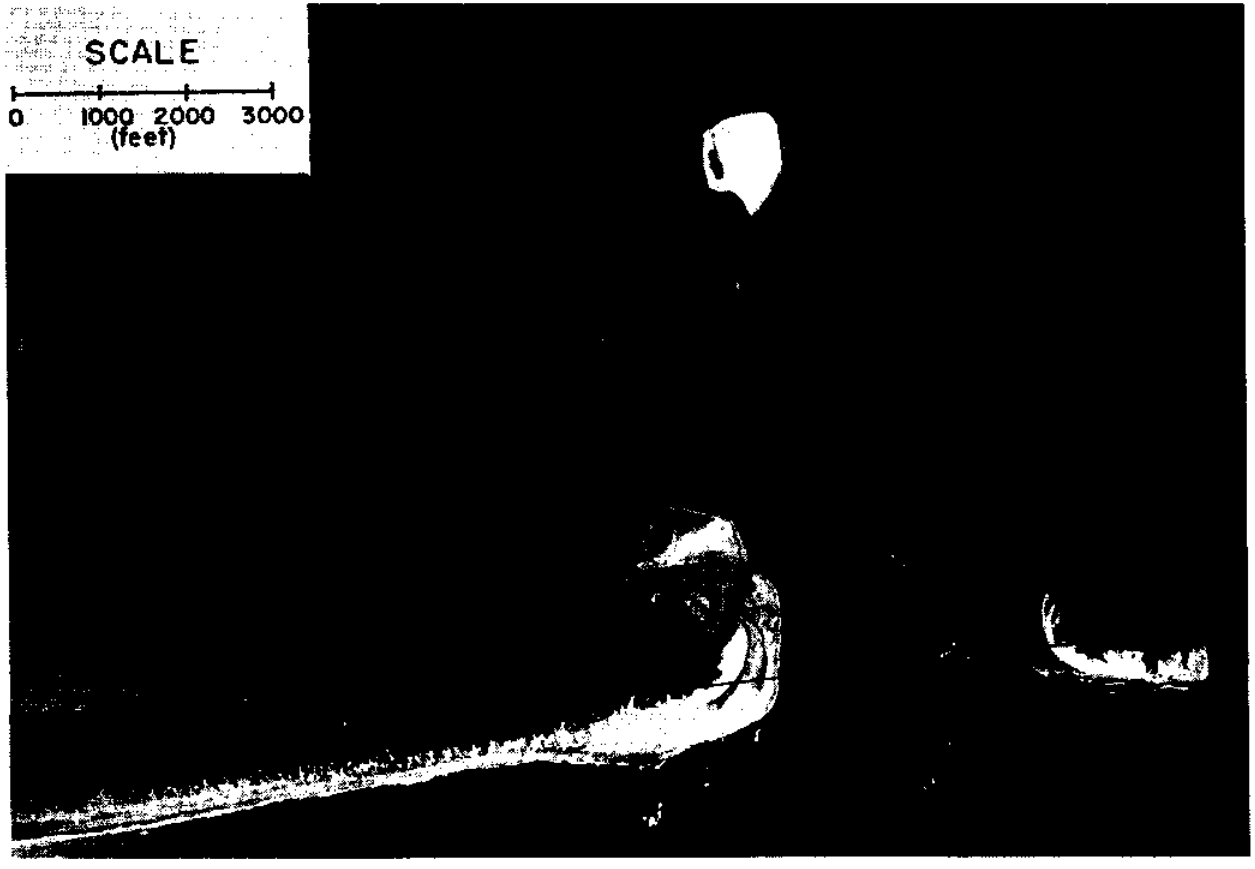

Fig. 8. Aerial Photograph, Drum Inlet, January 1975

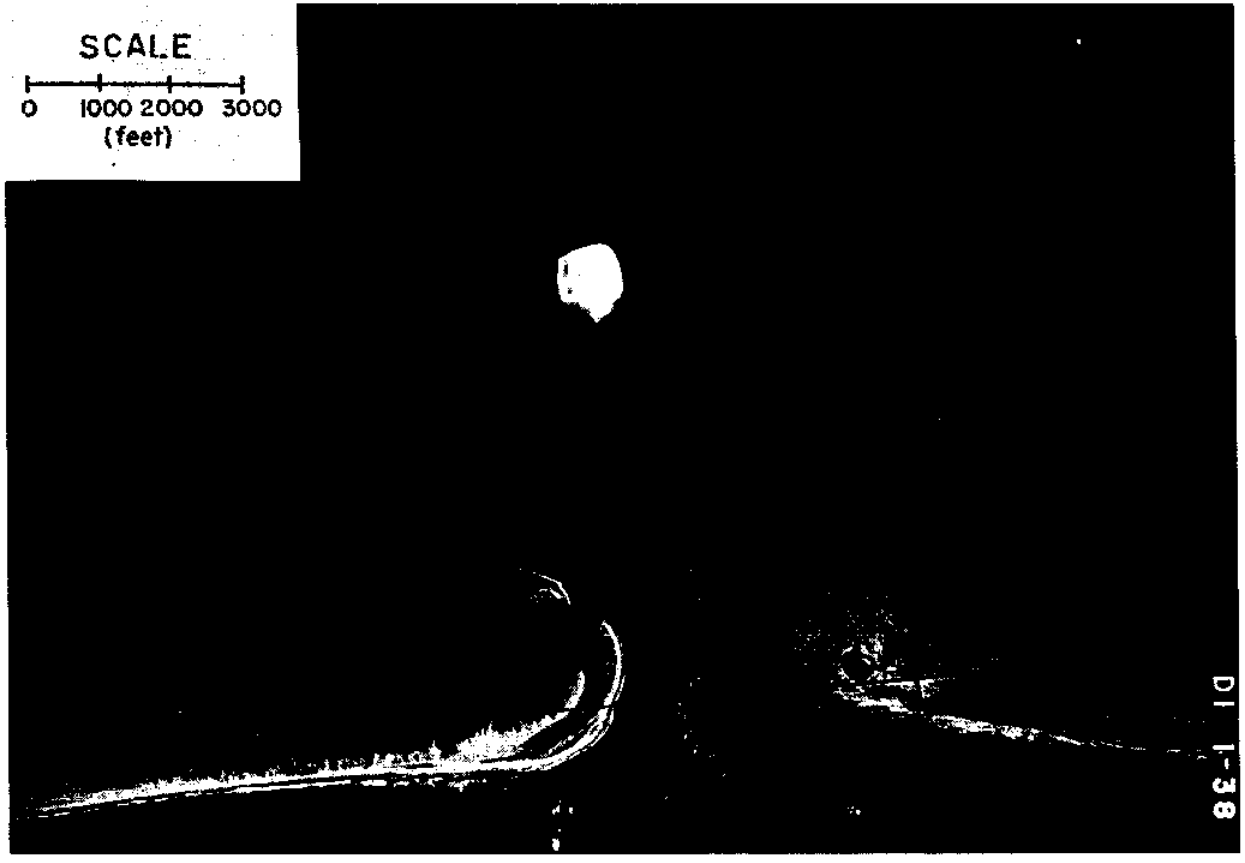

Fig. 9. Aerial Photograph, Drum Inlet, June 1975

Fig. 10. Aerial Photograph, Drum Inlet, November 1975

Fig. 11. Aerial Photograph, Drum Inlet, October 1977

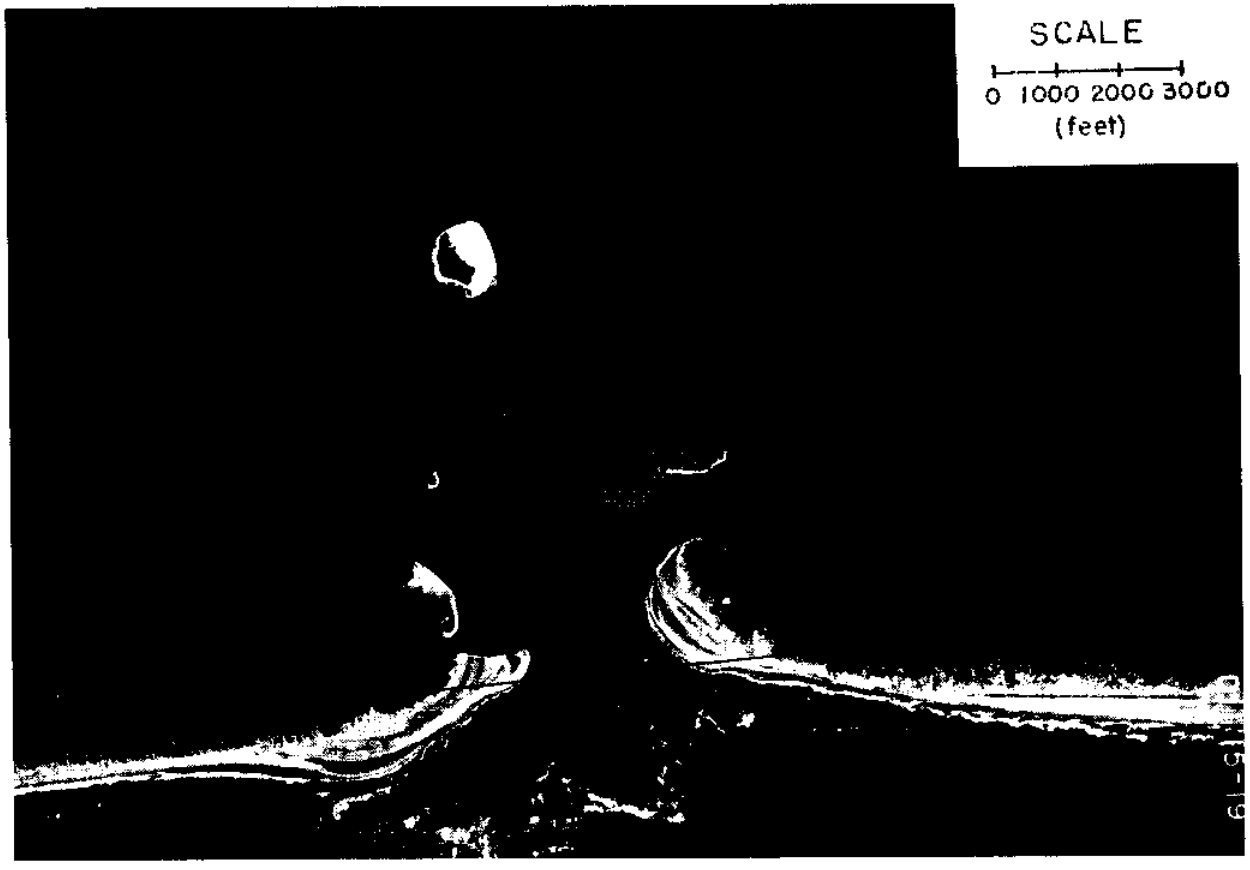

Fig. 12. Aerial Photograph, Drum Inlet, March 1977

TABLE 4

SUMMARY OF BASIC INLET FEATURES AT NEW DRUM INLET
FROM JULY 1972 TO MARCH 1977

Date of Aerial Photography	Location of* Inlet Centerline in Relation to 1972 Base (ft.)	Aerial Extent of Flood Tidal Delta	Width of Inlet Mouth at Narrowest Point (ft.)
Jul 72	Baseline	0.63	1050
Oct 73	+238	1.4	1159
Jan 75	-764	1.6	3024
Jun 75	-828	1.9	3096
Nov 75	-212	2.0	1557
Jan 76	-384	2.0	1883
Oct 76	-509	2.1	1931
Mar 77	-401	2.3	1702

*Positive indicates location of centerline southwest of 1972 baseline.

Negative indicates location of centerline northeast of 1972 baseline.

the new inlet migrated very little from the July, 1972, location. The change in the position of the inlet centerline can be attributed mainly to the widening of the inlet channel. The erosion of one bank and accretion of an opposite bank associated with migration did not occur on a scale great enough to be considered migration.

Oceanographic and Meteorological Background

Tidal characteristics

The periodic tides in Core Sound are caused by the semidiurnal tides in the Atlantic Ocean. The magnitude of the tides are greatly reduced due to the large area and shallow depths of the sound, as well as the limited amount of interchange provided by the inlets along the barrier islands. Mean tidal ranges for two ocean locations near Drum Inlet are shown in Table 5.

TABLE 5

ATLANTIC OCEAN TIDAL RANGES

Location	Mean Range*	Spring Range*
Hatteras	3.4 ft.	4.1 ft.
Cape Lookout	3.7 ft.	4.4 ft.

SOURCE: NOS Tide Tables, 1977.

*Ranges given above mean low water.

Ranges in the vicinity of Drum Inlet are approximately 3.6 feet for mean tide and 4.3 feet for spring tide. A summary of tide ranges for Atlantic and Davis, N.C., are given in Table 6. Meteorological

conditions affect the tides in Core Sound more than any other factor. The values in Table 6 are a comparison of mean daily water levels because the occurrence of winds and diurnal inequalities makes a comparison of periodic tides impossible. The mean daily water level range at Atlantic is 0.68 feet.

In the immediate vicinity of Drum Inlet the mean tidal range is approximately 2.0 feet. This is a very rough value obtained from photogrametric survey by the U. S. Army Corps of Engineers.

Wave climate

Wave climate affects shoal growth directly because with increased wave severity there is an increase in the amount of sediment suspended on the beach and set into the littoral drift. The wave climate at Cape Hatteras, generalized here for the Drum Inlet area, is shown as height versus direction and period versus direction roses in Figures 13 and 14. These roses were constructed using a method outlined by Walton (1973) with data from the U. S. Naval Weather Service Command (1975). These are deep water wave height and period values and must be corrected for refraction in order for the actual ocean wave climate affecting the inlet to be known.

Of interest here, are the onshore directed vectors of height and period. These vectors are responsible for the magnitude and direction of littoral drift along the coast. The major contributions are from the north, northeast and south.

TABLE 6

MEAN DAILY WATER LEVEL DATA AND RANGES BY MONTH - ATLANTIC AND DAVIS, N.C., 1975/1976*

Month	Mean Low Water Level*		Mean Water Level**		Mean High Water Level**		Daily Range**	
	Atlantic	Davis	Atlantic	Davis	Atlantic	Davis	Atlantic	Davis
May		0.23		0.76		1.35		1.12
Jun		0.25		0.75		1.33		1.08
Jul	0.34		0.75		0.96		0.62	
Aug	0.05		0.62		0.95		0.90	
Sep	0.53		0.86		1.14		0.61	
Oct	0.73	0.58	1.05	1.04	1.35	1.62	0.62	1.04
Nov	0.48	0.27	0.82	0.80	1.14	1.40	0.66	1.13
Dec		0.24		0.83		1.41		1.16
Jan	0.10	-0.16	0.45	0.32	0.81	0.85	0.71	1.01
Feb	-0.32		-0.04		0.30		0.62	
Mar		-0.33		-0.18		0.67		1.00
Apr	0.05	-0.04	0.38	0.44	0.72	0.96	0.67	1.00
May	0.02	-0.09	0.37	0.40	0.74	0.97	0.72	1.06
Jun	0.29		0.58		0.94		0.65	
Average	0.23	0.10	0.58	0.57	0.90	1.17	0.68	1.07

*Water level values in feet above or below NCVD - (+) Above and (-) Below.

SOURCE: Limberios Valianos, U.S. Army, Corps of Engineers, Wilmington District.

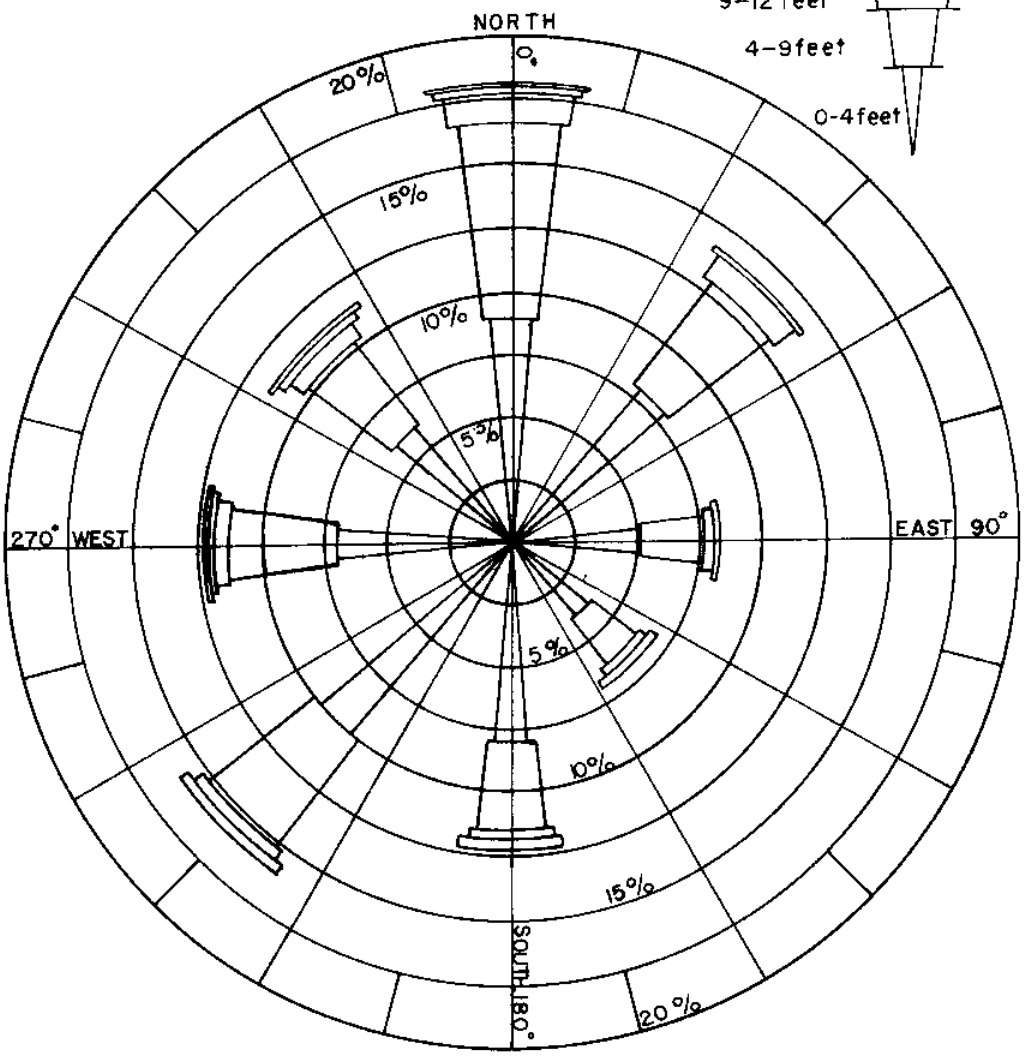

Fig. 13. Wave Height Frequency Versus Direction Rose

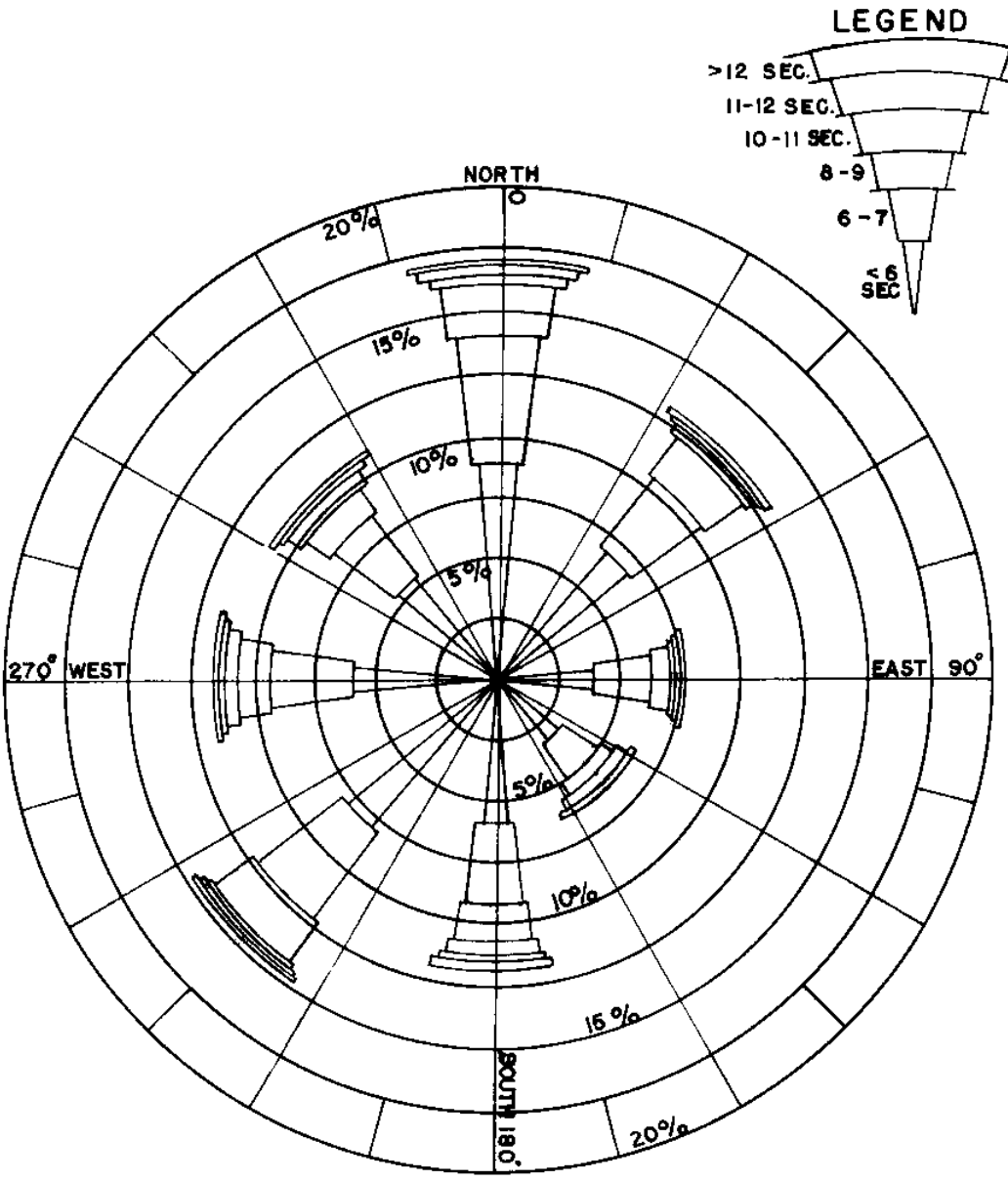

Fig. 14. Wave Period Frequency Versus Direction Rose

Wind conditions

Winds are the dominant factor affecting water level and wave climate in Core Sound. Results of wind observations over a 17-month study period are presented in Table 7. It can be noted from Table 7 that winds from the south to west vector are dominant in terms of direction and winds from the north to east vector are second in frequency of direction. It is also evident that winds of over 12 knots had the highest frequency from these two vectors. Long term wind records indicate that the prevailing winds along the North Carolina Coast are from the south to west vector with major north to east contributions during the winter months.

In discussions with local residents at Atlantic, N.C.,it was found that winds from the north to west vector caused a 1-to 2-foot tide at Atlantic depending on the velocity and duration of the wind. Winds from the south to west vector caused a negative tide up to 1.5 feet.

During the study period from August 18 thru August 23, 1977, the average wind speed varied from 6 to 10 miles per hour. A summary of the wind conditions during the study period is presented in Table 8.

TABLE 7

SUMMARY OF WIND OBSERVATIONS - CAPE LOOKOUT, N.C.*
APRIL 1975 - OCTOBER 1976

Direction	Number Observations**	Percent of Total	Average Speed (Knots)	Percent of Observations With Speeds 12 to 20 (Knots)	Percent of Observations With Speeds Greater Than 20 (Knots)	Average Speed of Those Greater Than 20 (Knots)
N	287	6.2	11.0	2.3	0.2	24.0
MME	218	4.7	12.8	2.3	0.3	23.5
NE	457	9.9	13.3	5.2	0.8	23.6
ENE	243	5.2	11.0	2.1	0.1	26.3
E	201	4.3	10.2	1.2	0.1	27.2
ESE	210	4.5	9.4	1.0	0.1	23.0
SE	240	5.2	9.4	1.3	0.1	23.7
SSE	219	4.7	10.6	1.4	0.2	26.6
S	357	7.7	11.3	2.7	0.3	24.0
SSW	398	8.6	11.8	3.8	0.4	23.1
SW	630	14.7	12.6	7.3	0.8	23.3
WSW	319	6.9	12.0	2.7	0.5	26.0
W	178	3.8	11.5	1.6	0.2	25.9
WNW	132	2.9	12.4	0.9	0.3	25.6
NW	256	5.5	11.9	2.1	0.3	25.0
NNW	234	5.1	12.2	1.9	0.4	24.4
TOTAL	4,579					

SOURCE: Limberios Vallianos, U.S. Army, Corps of Engineers, Wilmington District.

**Observations made at 0100, 0400, 0700, 1000, 1300, 1900, 2000 hours each day.

TABLE 8

SUMMARY OF WIND CONDITIONS DURING STUDY PERIOD, AUGUST 18 TO AUGUST 23, 1977*

Date	Maximum Velocity (mph)	Average Velocity (mph)	Direction of Maximum Velocity
Aug. 18	17	10.1	WSW (240°)
Aug. 19	13	9.8	NE (50°)
Aug. 20	12	9.1	NE (40°)
Aug. 21	10	7.0	E (90°)
Aug. 22	10	7.4	SE (150°)
Aug. 23	9	6.1	SSW (210°)

SOURCE: Personal communication with Carl Molis, National Weather Service, Buxton, N.C.

The winds of August 19 thru August 21 resulted in an additional tide in the Drum Inlet area of approximately 1.0 to 1.5 feet.

DESCRIPTION OF STUDY

An analysis of aerial photography and collection of data in the field were used in the study of inlet shoals. The air photo phase described the large scale spacial and temporal changes in the inlet system. The response of the barrier island to the presence of the inlet was examined by determining the volume of shoreline erosion or accretion that occurred over the study period for which sequential aerial photographs were available. The patterns of growth of the flood tidal shoals were examined by aerial photography. The changes in the lateral, longitudinal and aerial extent of the flood shoals were documented as well as the number of distributary channels. Air photos were also used to follow the movement of large sand dunes across the flood tidal shoals. The volumes of sediment on the flood tidal shoals were estimated and compared to the volumes eroded from the beaches.

The field study phase of this project consisted of a flourescent tracer study, collection of core samples for determining sediment characteristics and measuring current velocities at selected points in the inlet system. The tracer study was designed to determine the patterns of sediment movement in a high and low energy zone. The high energy zones were the north and south beaches adjacent to the inlet throat. These areas were designated high energy zones because they were under the direct influence of ocean waves and tidal currents. The area designated as the low energy zone was a relatively small grid area laid out

on one of the major flood tidal shoals. This area is only influenced by tidal currents and some very small waves. The locations of these study areas are shown in Figure 15.

The collection of core samples was used to determine the distribution of sediment sizes in the inlet system. Collection of samples was at selected points at varying distances from the inlet throat and at each grid point of the shoal study area.

Measurement of current velocities was carried out in the channels adjacent to the shoal study area (low energy area) and at points on the shoal study area. The maximum ebb and flood currents and the durations of the flood and ebb cycles were determined from these measurements.

A sediment budget was devised which accounted for the littoral drift and the volumes of sand that bypassed the inlet and were trapped on the flood tidal shoals.

The information developed from the aerial photographs and the field studies were correlated to satisfy the objectives of this study and to form a hypothesis of sediment movement in the inlet system.

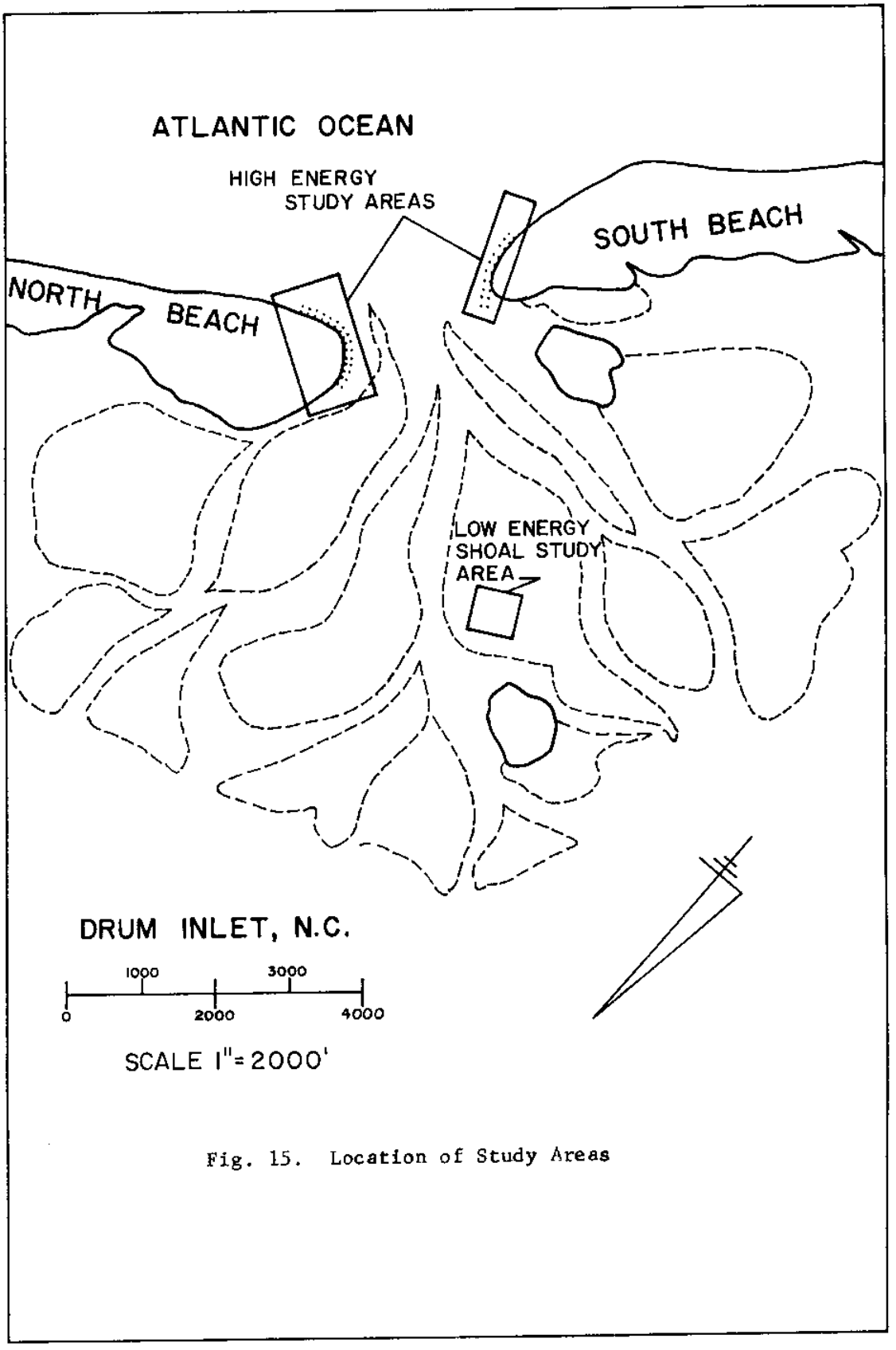

Fig. 15. Location of Study Areas

AERIAL PHOTOGRAPHY STUDY

Aerial photographs provide excellent documentation of the features on a coastline. They can provide information on the size and wave length of waves and direction of wave travel. The predominate direction of littoral drift, distribution of sediments resulting from erosion or deposition and the deposition patterns of shallow water sediment accumulations to depths of 8 to 10 feet are discernable on air photos.

Moffitt (1977) outlines a method to determine changes in shoreline location. The method involves carefully selecting permanent distinguishable points that appear on each sequential photo. These points are used to set up a coordinate system to be used to make measurements of shoreline erosion of accretion. Stafford (1968) developed a method of surveying coastal erosion using sequential aerial photos. The procedure consisted of selecting stable reference points on aerial photographs taken in different years and measuring the change in the position of transient beach features. The changes in the location of the beach, the dune line and the high water line were measured.

Analysis of sequential aerial photography in this study was done using methods outlined by Moffitt and Stafford. This study consisted of making measurements on photographs of the inlet and adjacent barrier island before the inlet was opened and of sequential photographs of the inlet complex taken in July, 1972, through March, 1977. The three part

study consisted of:

(1) determining the response of the barrier island to the presence of the inlet by measuring the erosion of the adjacent beaches,

(2) measuring the growth and determining the growth patterns of the flood tidal shoals and the inlet throat, and

(3) tracing the movement of selected major bedforms across the shoal study area.

Color photographs obtained from the U. S. Army Corps of Engineers, Wilmington District were used in this study.

Methods of Analysis

In order to make accurate measurements, the actual scale of each photograph had to be determined. The scale was determined by measuring distances between three different highway intersections visible in the photographs in the town of Atlantic, North Carolina. The exact distances for each set of highway features were measured on a U.S.C.G.S. seven minute topographic map, Atlantic, N.C., 1949. All map and photo measurements were made with a Theo Alteneder and Sons micro-rule. The photo distances measured were compared to the topographic map distances for the three sets of street features and a scale was calculated for each measurement. The actual scale was obtained by averaging the three calculated scales. The averaging was a way to reduce error since the street features used in each photograph

were always located near the edge of the photo where the horizontal distortion is the greatest.

In order to determine the changes in the beach and inlet features, a reference coordinate system was constructed on each photograph. The X axis was drawn connecting two cultural features on the barrier island, a U.S. Coast Guard boat slip north of the inlet and an unidentified building south of the inlet. The Y axis was a line perpendicular to the X axis representing the centerline of the inlet throat, measured on a photograph of July,1972, seven months after the opening of the inlet. The coordinate system was scaled for each photograph. An example of the coordinate system is shown in Figure 16.

Erosion measurements were made from the X axis to the apparent high water line or berm line at 1000-foot intervals from the Y axis. There were eight intervals north and south of the Y axis. Each 1000-foot section represented a cell when making the erosion calculations. The positions of the beach for each photograph were plotted and the area of erosion or accretion in each cell was calculated in square feet. The eroded volumes were determined using the relationship described by the Shore Protection Manual (1973) in which one square foot of beach surface area equals one cubic yard of beach material.

Measurements of changes in the inlet features were made relative to the X and Y axis. The area of the shoals was determined by planimetering the areal extent on each photograph. The landward extent of the shoals was measured from the X axis to the most landward reach of the shoals evident in each photograph. The lateral extent was measured parallel to the X axis to the most distant reaches of the shoals northwest

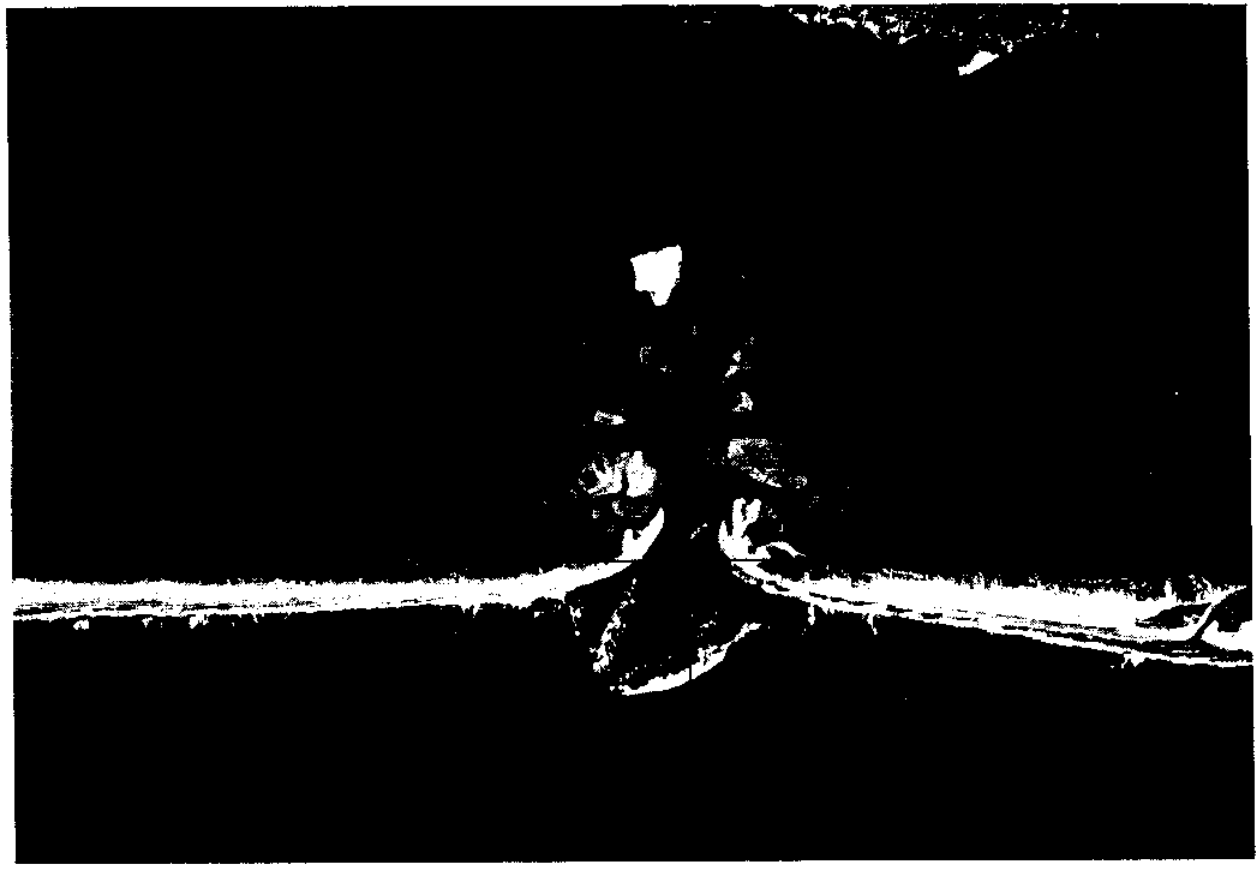

Fig. 16. Drum Inlet, October 1973, Locations of Reference X, Y Axis

and southeast of the Y axis. The location of the inlet centerline was the distance from the Y axis to a line parallel to the Y axis through the center of the inlet throat on each photo.

The movement of the sand waves across the shoal study area was measured along a line from the intersection of the X and Y axis 10 degrees south of the Y axis. The distance along the line from the X, Y intersection to the leading edge of each sand wave was measured. The rates of movement were calculated by dividing the distance of advance by the time between photographs.

Response of Barrier Island

It was found that following the opening of the inlet there was a very rapid rate of erosion north and south of the inlet throat. Most of the erosion can be attributed to the inlet attempting to reach a stable configuration. As shown in Figure 17, the shoreline eroded dramatically through June,1975. The position of the high water line relative to the Y axis of reference is plotted in Figures 18 and 19 for each sequent aerial photograph. The position of the beach appears exaggerated because of the small horizontal scale. The point where the beach position lines intersect the horizontal axis (zero distance from reference axis) represents the width of the inlet throat from the north and south high water lines. The solid line represents the contour of the barrier island prior to the opening of the Inlet. It is interesting to note that where the islands were eroding rapidly adjacent to the inlet throat, there was significant accretion further away from the inlet centerline.

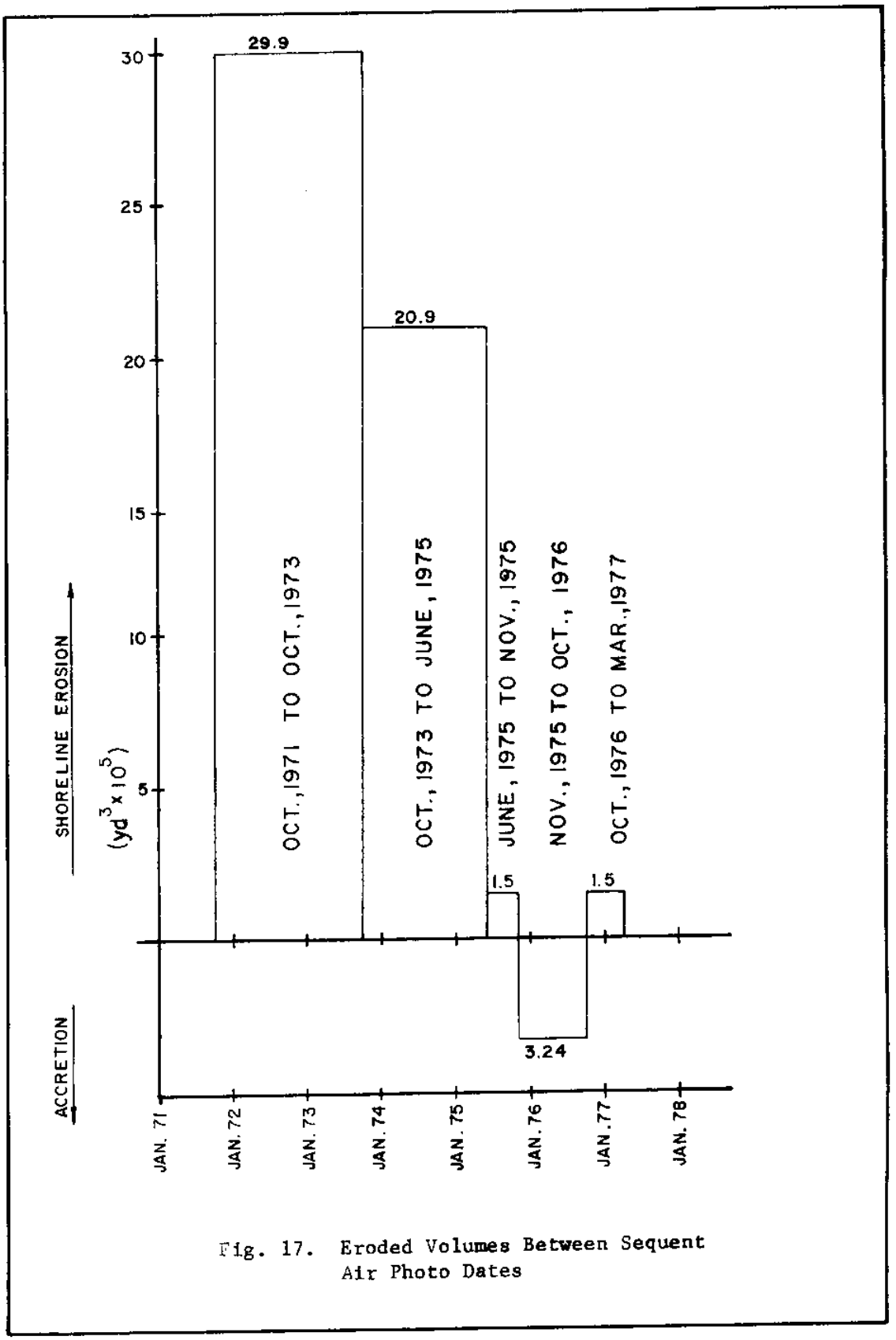

Fig. 17. Eroded Volumes Between Sequent Air Photo Dates

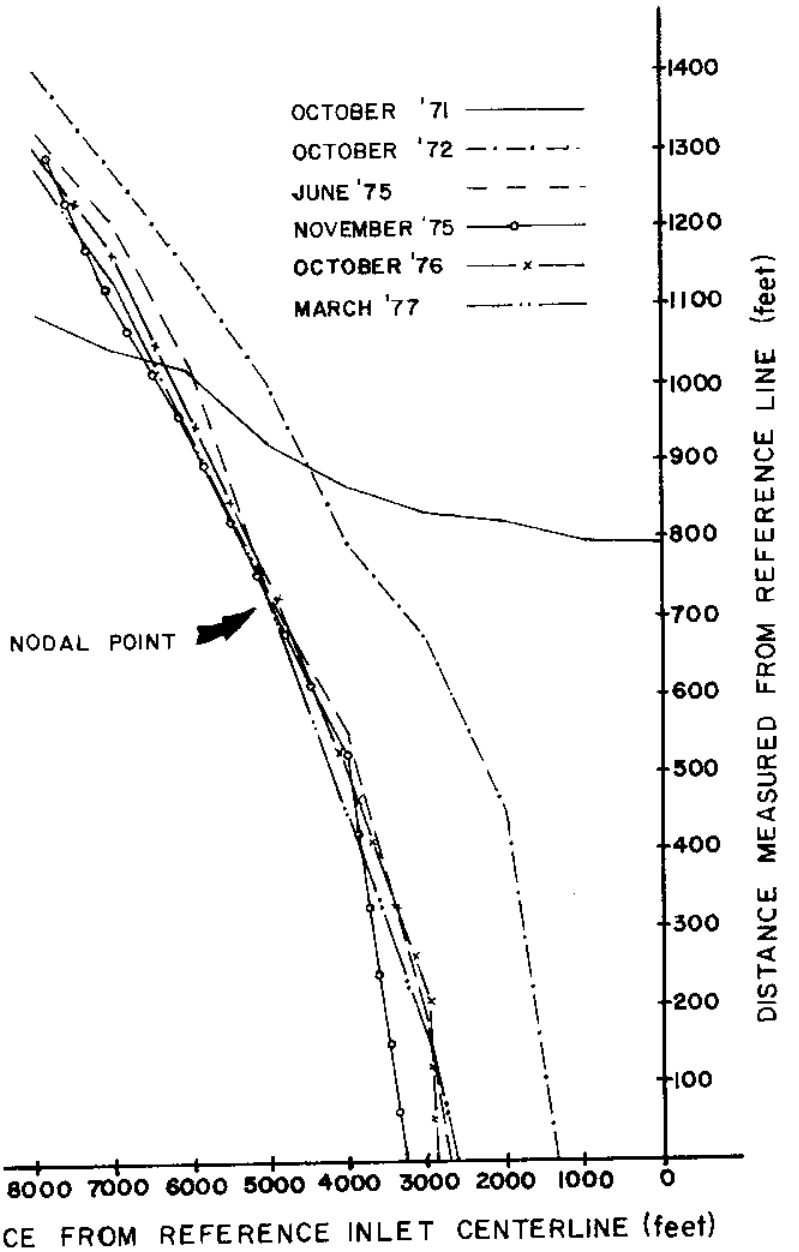

Fig. 18. Position of High Waterline on the South Beach on Sequential Air Photographs Dates Relative to Reference Line

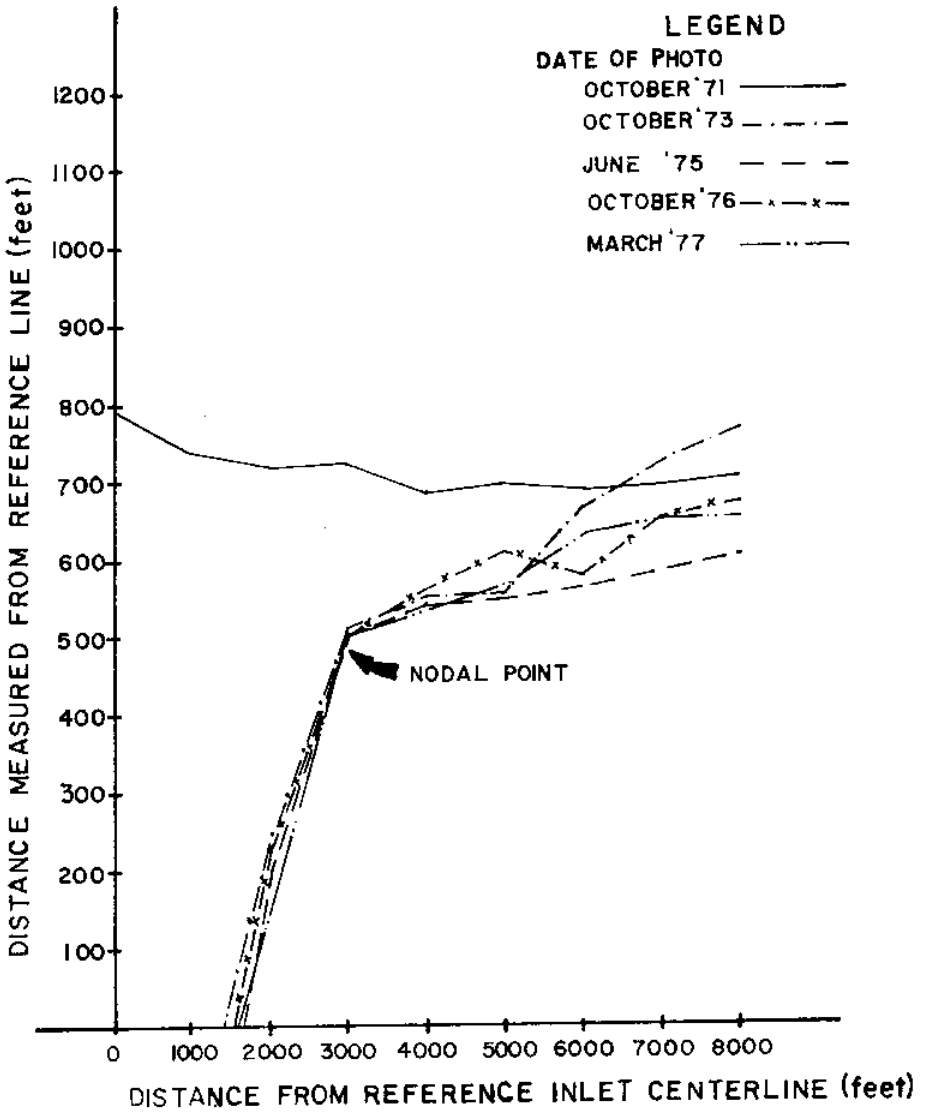

Fig. 19. Position of High Waterline on the South Beach on Sequential Air Photos Relative to Reference Line

After June ,1975 ,the position of the beach changed within a narrow range. Close evaluation of the diagrams shows that after the large amounts of initial erosion there was a nodel point 5000 feet from the inlet centerline on the north beach and 3000 feet from the inlet centerline on the south beach. These nodel points probably represent the points on the beach where the influence of the inlet is terminated. Inside these points the sand is drawn towards the inlet and outside the points the sand moves away from or towards the inlet depending on the direction of the littoral currents. According to the data there was an overall erosion of the shoreline of 5.5 million cubic yards during the study period. However, since June,1975,there has been a net accretion of the shoreline. A majority of the accretion took place beyond the nodel points. Figures 20 - 24 were taken from Figures 18 and 19 and show amounts of erosion and accretion for each 1000 feet cell north and south of the reference centerline between sequential photo dates. The north beach appeared to be much more unstable because the total erosion and accretion is greater than for the south beach. No measurements were made that could account for this instability.

Flood Tidal Shoal Study

The data obtained from the measurements of the features of the inlet and the flood tidal shoals are shown in Table 9. In order to examine the changes in the flood tidal shoals with respect to time, the dimensions of the basic features were plotted versus time for each sequent photograph in Figure 25. It is interesting to note the rapidly changing conditions through October,1976. Although the landward growth

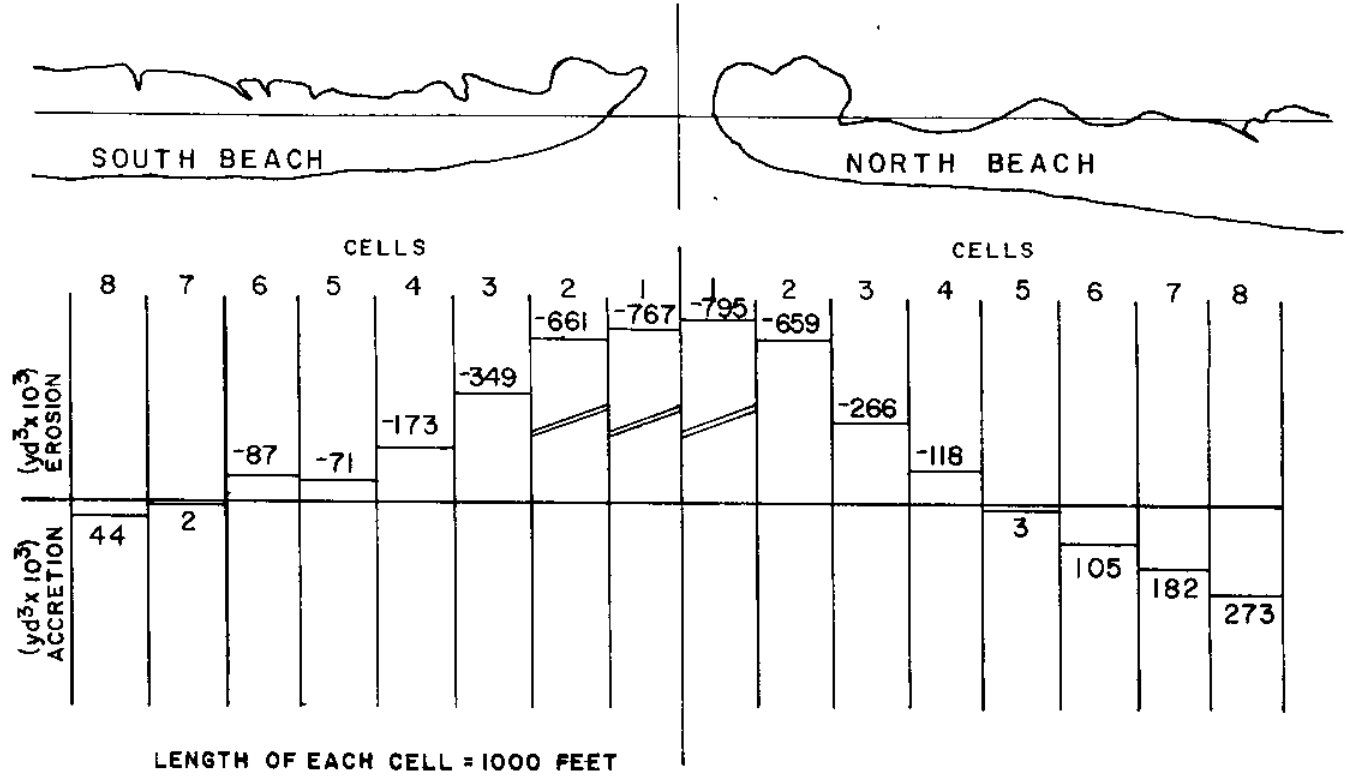

Fig. 20. Volumetric Shoreline Changes for each 1000 Cell from October 1971 to October 1973

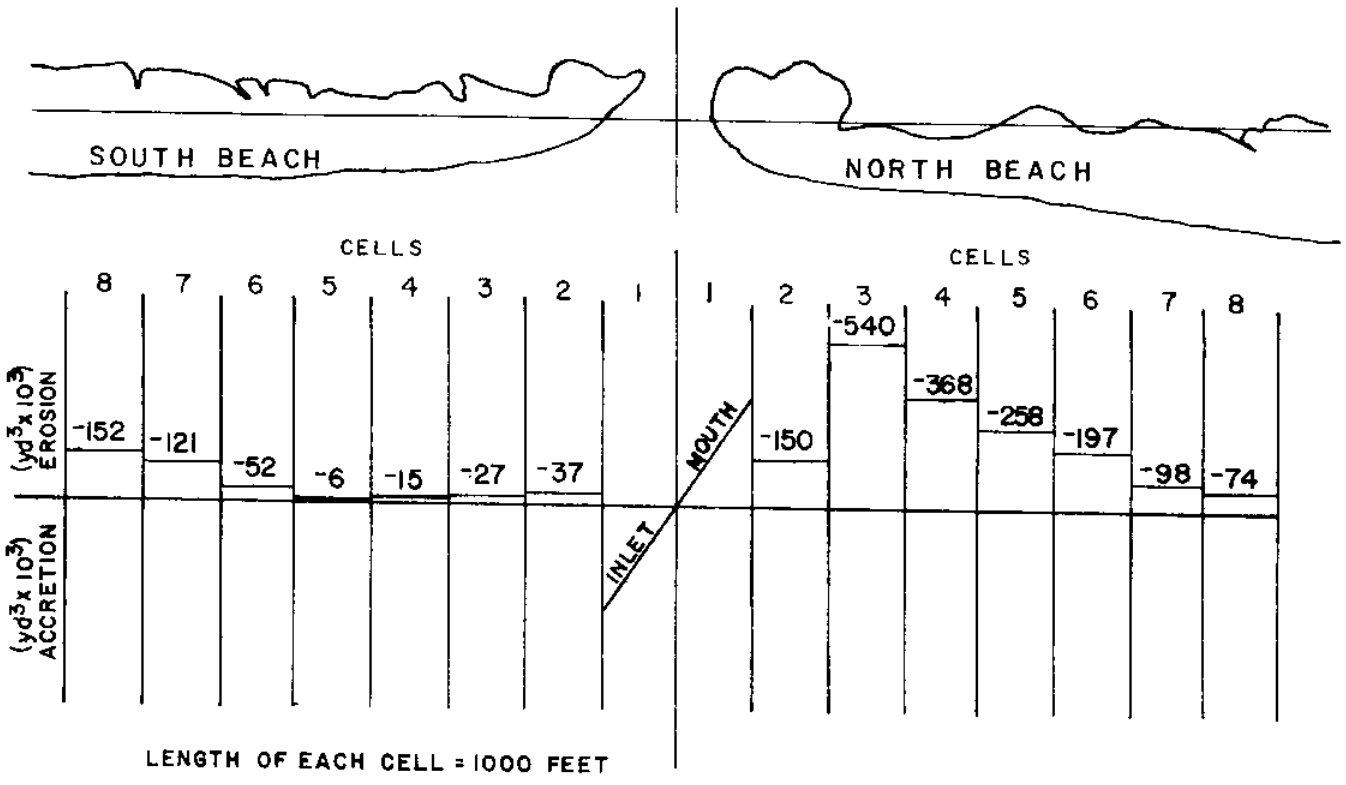

Fig. 21. Volumetric Shoreline Changes for each 1000 foot Cell from October 1973 to June 1975

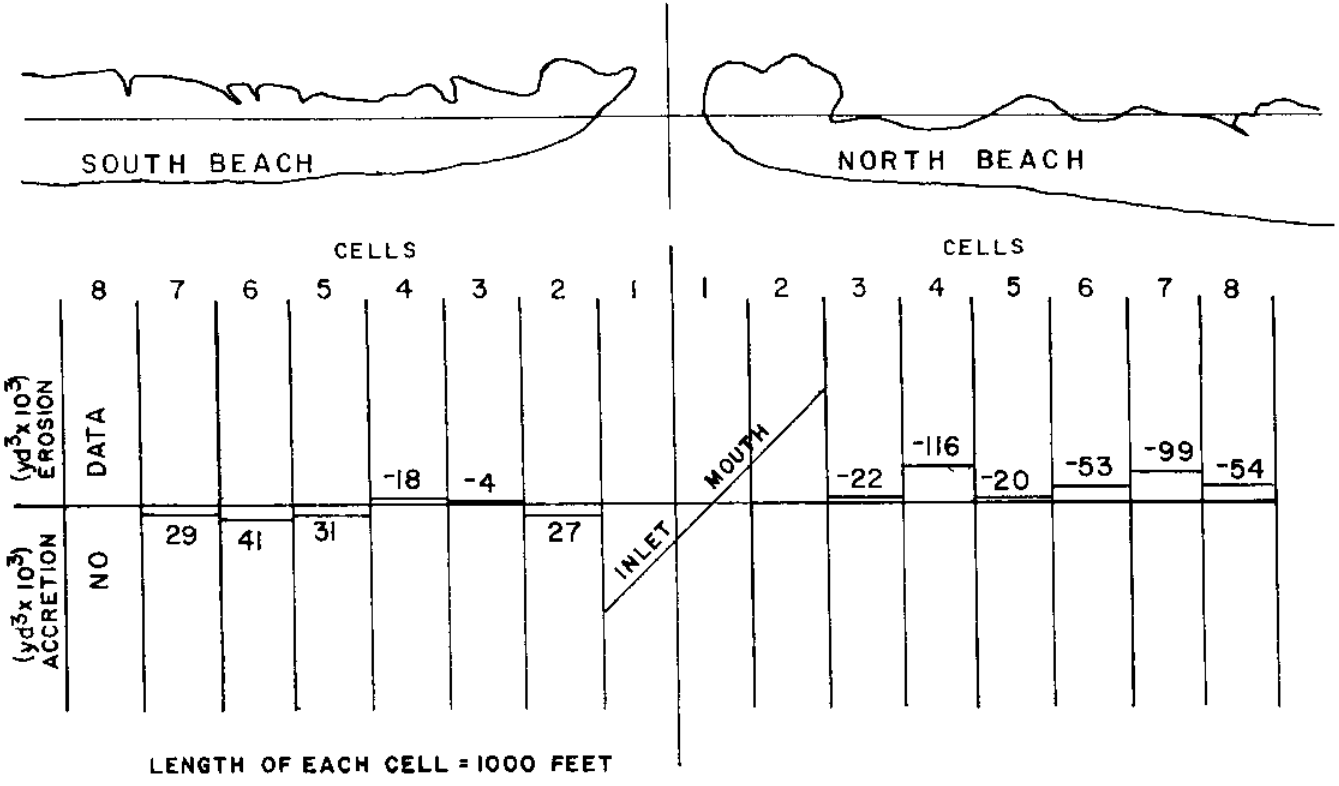

Fig. 22. Volumetric Shoreline Changes for each 1000 foot Cell from June 1975 to November 1975

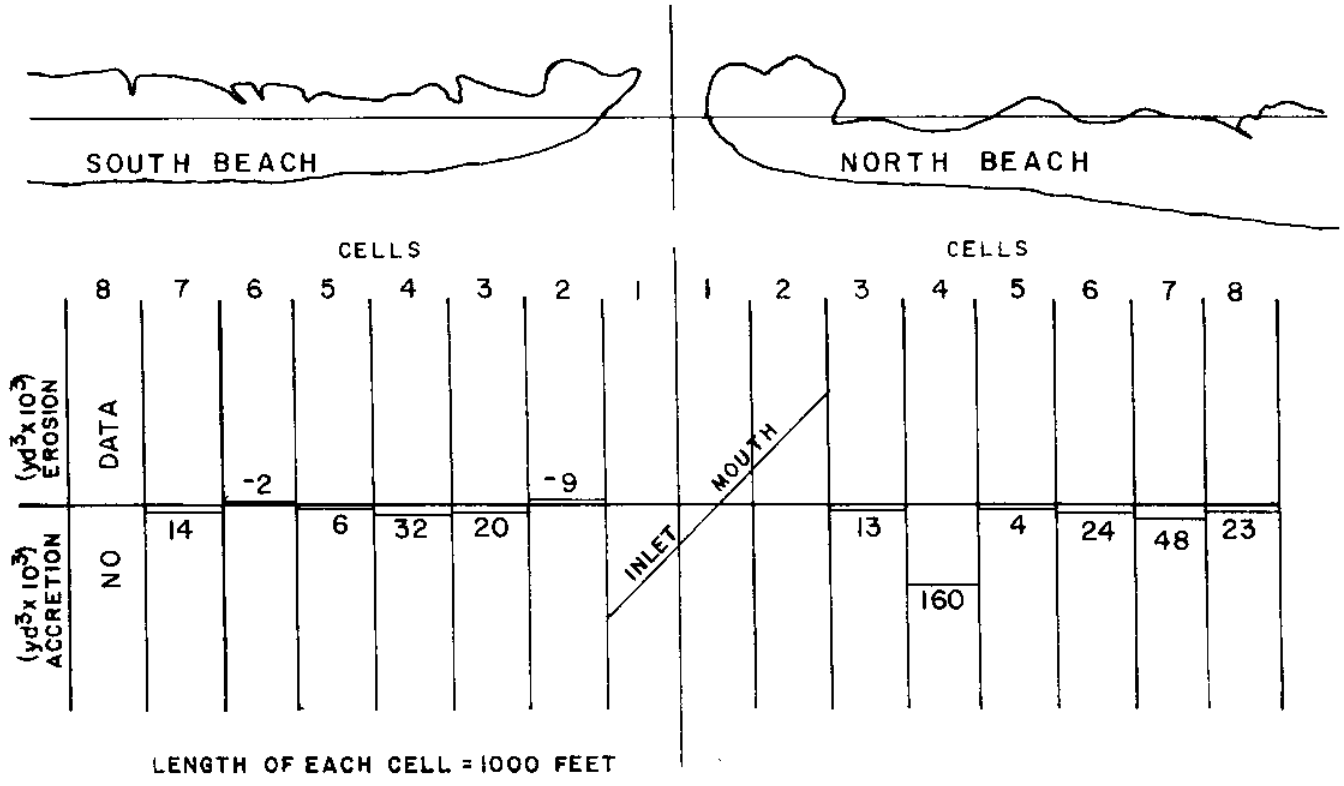

Fig. 23. Volumetric Shoreline Changes for each 1000 foot Cell from November 1975 to October 1976

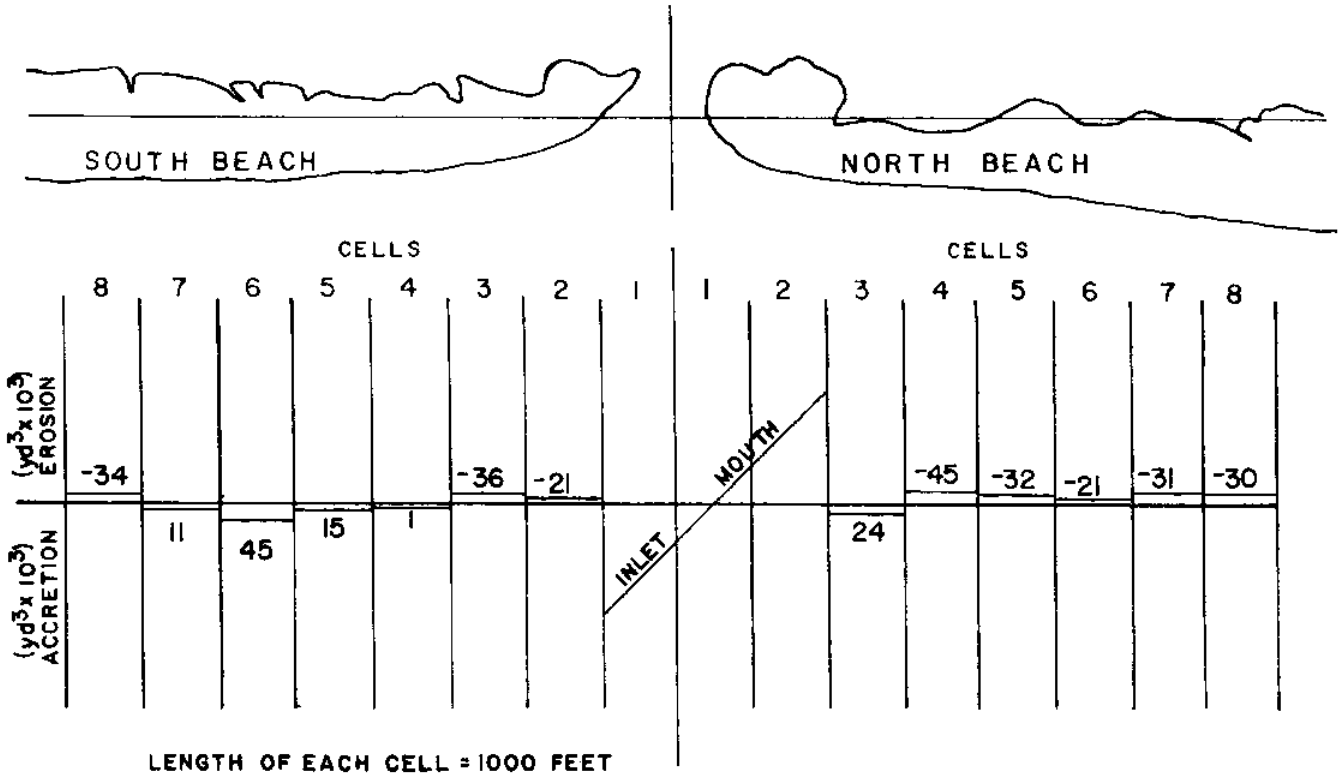

Fig. 24. Volumetric Shoreline Changes for each 1000 foot Cell from October 1976 to March 1977

TABLE 9

SUMMARY OF CHANGES IN INLET FEATURES OF NEW DRUM INLET

Date of Aerial Photograph	Location of Inlet Centerline Relative to 1972 Base (+SW, -NE) (ft.)	Area of Ebb Tidal Delta ($mi.^2$)	Area of Flood Tidal Delta ($mi.^2$)	Width of Inlet Mouth at Narrowest Point Measured from Apparent Waterline (ft.)	Number of Distributaries From Main Channel	Maximum SW extent of Floodtide Shoals - (Landward Reach) (mi.)	Maximum SW to NE extent Flood Shoals - (Lateral Extent) (mi.)
Jul 72	Base	None Apparent	0.63*	1050*	---	0.9*	1.0*
Oct 73	+238	None Apparent	1.4	1159	6	1.3	1.5
Jan 75	-764	None Apparent	1.6	3024	13	1.5	1.6
Jun 75	-828	None Apparent	1.9	3096	10	1.5	2.0
Nov 75	-212	0.08	2.0	1557	11	1.5	2.1
Jan 76	-384	0.007	2.0	1883	11	1.5	2.1
Oct 76	-509	0.06	2.1	1931	8	1.6	2.2
Mar 77	-401	0.05	2.3	1702	8	1.6	2.2

*Measured by Vallianos from unknown reference point.

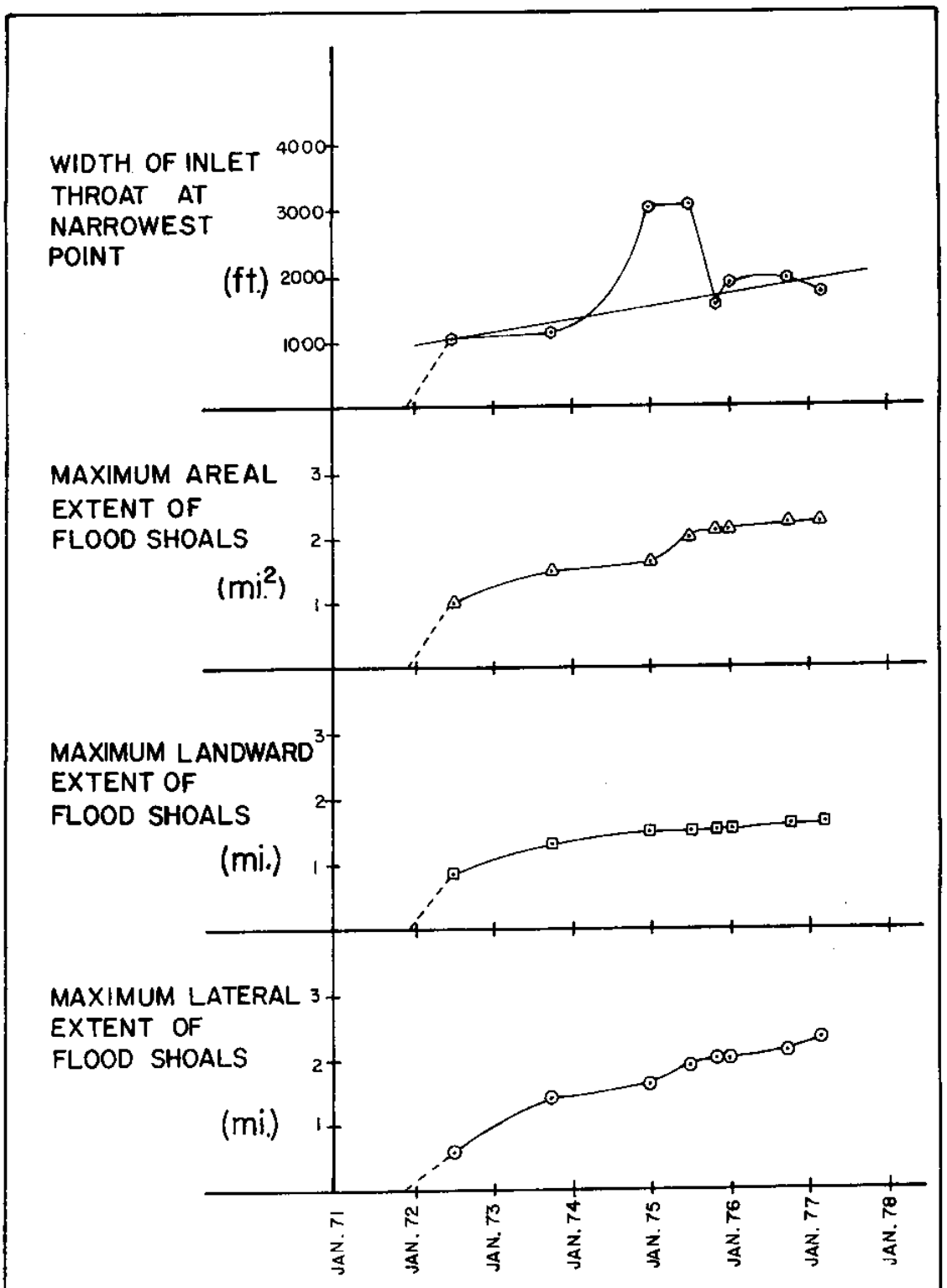

Fig. 25. Summary of Changes in Basic Inlet and Flood Tidal Shoal Features

stabilized early in 1975, there was marked stabilization of the other features after October,1976. Landward growth of the delta increased only slightly after January,1975,while lateral and areal growth increased considerably through March,1977.

Study of Movement of Primary Bedforms

The rate of movement of primary bedforms was measured using sequential aerial photographs over the period from May 6, 1975 to March 17, 1977. Figures 26 and 27 show the locations of the three sand waves studied. Of interest is the migration and deposition of the wave labeled 2 in Figure 26 into the channel indicated by the arrow. All three waves advanced at varying rates over the study period. The rates of advance are summarized in Table 10.

TABLE 10

RATES OF ADVANCE OF LEADING EDGE OF SAND WAVES IN STUDY AREA

Photo Dates	Rate of Advance (ft./day) Sand Wave Number			Days Between Photographs
	1	2	3	
5-6-75 to 6-15-75	0.13	4.08	-	40
6-15-75 to 11-18-75	4.5	0.72	-	156
11-18-75 to 10-21-76	0.6	Lost in Channel	-	337
10-21-76 to 3-17-77	1.37	-	1.9	147

Fig. 26. June, 1975 Photograph Indicating Location of Sand Waves Migrating Over Shoal Study Area

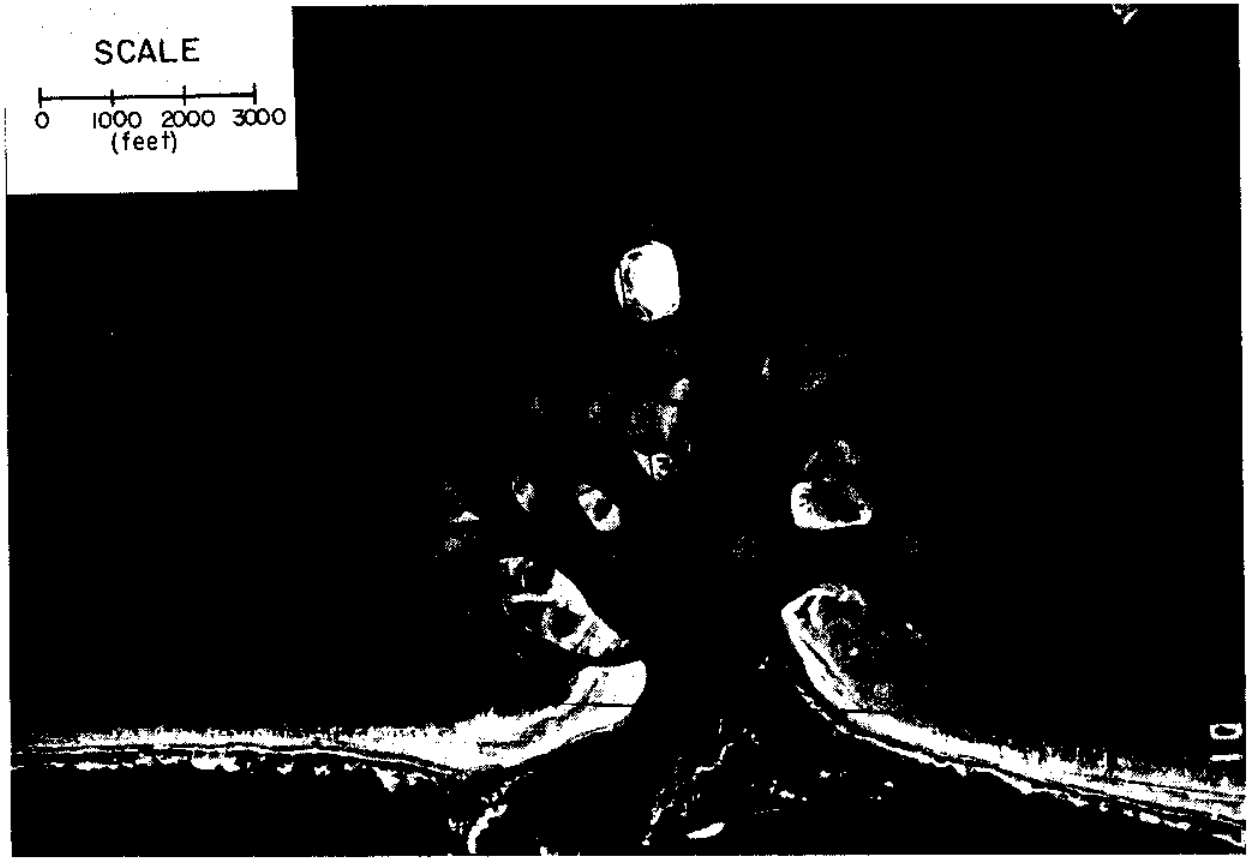

Fig. 27. October, 1976 Photograph Indicating Location of Sand Waves Migrating Across Shoal Study Area

FIELD STUDY

Flourescent Tracer Study

Flourescent tracer has been used for determining sediment movement patterns at tidal inlets at North Carolina State University. Masterson, Machemehl and Cavaroc (1973) used flourescent tracers to develop a pattern of sediment movement at Tubbs Inlet, North Carolina. The tracer mixture used was developed by MacArthur while the sampling technique was developed by Ingle.

Machemehl, Chambers and Bird (1977) used tracers to develop a pattern of sediment bypassing at Lockwood Folly Inlet, North Carolina. The MacArthur mixture was used, but sampling was done by taking core samples over the study area. This was done to allow for burial of tracer in the bed after multiple tidal cycles.

Flourescent tracer methods for this study were taken from these studies.

High energy zone study

Flourescent tracer material was introduced into the beach environments adjacent to the inlet mouth. The object of this phase of the field study was to determine the pattern of sediment movement in a zone exposed to ocean wave attack and tidal currents. The movement of the dyed sand was traced over one and one-half ocean tidal cycles. A description and detailed analysis of the study is presented in Appendix A.

North Beach study

After introduction, the tracer moved down the beach toward the sound side of the inlet mouth at a rapid rate. After two hours, the tracer was dispersed up to 100 feet into the surf zone (see Figure 62). However, samples taken near the high water line showed little or no evidence of tracer material. After approximately five hours, the tracer was dispersed down the beach in the surf zone up to 1200 feet from the introduction line (see Figure 63). Samplings one and one-half tidal cycles after introduction indicated that the tracer was moving towards the inlet as a wave of sand (see Figure 71).

The most interesting and unexpected finding was the discovery of fire orange tracer from the shoal study area on the north beach. This indicated that there was movement of sand out of the inlet from shoal areas a substantial distance from the inlet mouth. After the initial findings of the fire orange tracer, it was thought that there had been some contamination of the samples somewhere in the drying or analysis. However, continued findings in samples collected at different periods on the beach confirmed the findings and made the contamination idea improbable.

South Beach study

The rate of movement of the tracer material was higher on the south beach than on the north beach. No patterns of movement were evident from amounts of tracer found in samples collected during the different sampling periods. The tracer was dispersed over the entire grid area only one hour and twenty minutes after the introduction (see Figure 68). Data from the last sampling period on August 23 showed a

uniform distribution of the tracer on the grid area (see Figure 70).

As in the case of the north beach study, fire orange tracer from the shoal study area was found on the south beach in sufficient quantity to indicate some degree of flushing of material from the inner shoals.

Low energy zone study

Flourescent tracer sand was introduced on a small shoal area and the movement traced for nine tidal cycles (4½ days). The object of this phase of the field study was to document the movement of sand across a small portion of the flood tidal shoals and then generalize that movement for the entire shoal system. A detailed analysis of this study is presented in Appendix A.

It was found that sand moves across the shoal area with both flood and ebb currents. There were patterns of movement indicated by some of the tracer data. The fire orange tracer detected formed a "tongue like" pattern moving northwest across the shoal. The pattern advanced from approximately 300 feet long approximately five hours after introduction to approximately 500 feet long after two tidal cycles (see Figures 45 and 49). The blaze orange tracer detected formed a pattern oriented in a southerly direction. There was insufficient evidence to indicate any advancement of the pattern. The blaze orange also moved in a "tongue like" pattern towards the northwest parts of the grid (see Figures 52 and 58). There was indication from the analysis of the blaze orange tracer data that there was a substantial amount of sand transported on the shoal by the ebb currents.

The lightning yellow tracer appeared to disperse in all directions across the grid. Substantially more tracer was found north and northwest of the introduction line than in the southerly directions indicating a net northerly to northwesterly movement (see Figures 53 and 54). The horizon blue tracer detected followed the northerly and northwesterly trends of movement across the grid. Some traces were detected south of the introduction line in the ebb flow direction (see Figures 47, 53 and 54).

Figure 28 shows a summary of the patterns of flood oriented movement in the northeasterly and northerly directions across the grid. Close examination of Figure 28 shows that the dominant direction of flood movement was to the west and northwest portions of the grid. A higher density of all four tracer colors was found in this region. The general patterns indicated that sediments were carried by flood currents towards channels located to the west, northwest, north and northeast of the grid area.

Figure 29 shows the ebb oriented patterns of tracer movement across the shoal. The dominant direction of ebb movement across the shoal was south (see Figure 29). The general pattern was a dispersion of sediments towards the south to east directions. A comparison of Figures 28 and 29 shows that the amounts of sand transported by the ebb currents was not as great as that transported by the flood currents. This was due to the fact that much of the shoal is above the waterline and therefore, not exposed to ebb currents through much of the ebb portion of the tidal cycle. In spite of this fact, there was enough evidence to indicate that substantial amounts of sand are transported

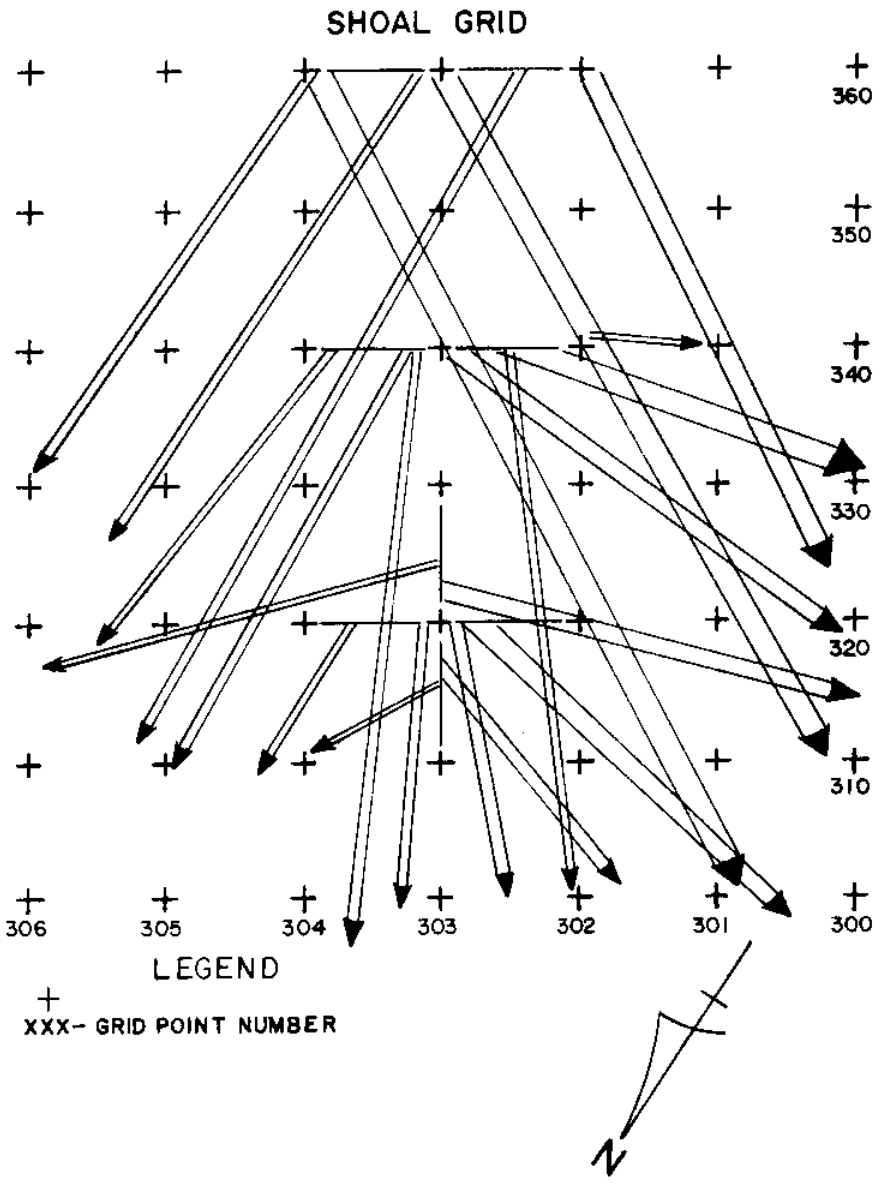

TRACER INTRODUCTION LINES DENOTED BY COLOR
FIRE ORANGE — FO, HORIZON BLUE —HB, LIGHTNING YELLOW-LY
BLAZE ORANGE — BO

ORIENTATION OF ARROWS SHOWS DIRECTION OF TRACER MOVEMENT
WIDTH OF ARROWS INDICATES RELATIVE VOLUMES OF TRACER FOUND

Fig. 28. Flood Oriented Movement Patterns of Tracer Sand Across the Shoal Study Area

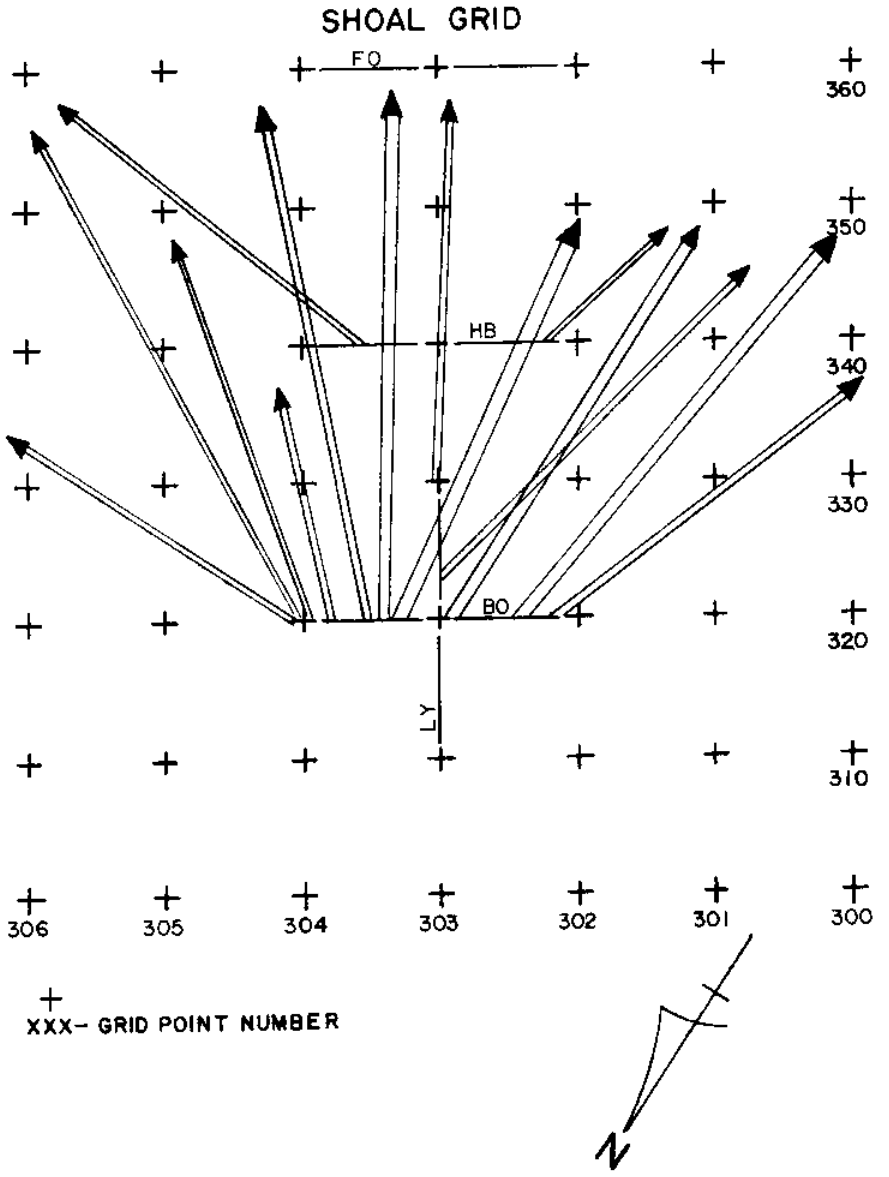

TRACER INTRODUCTION LINES DENOTED BY COLOR
FIRE ORANGE— FO, HORIZON BLUE— HB, LIGHTNING YELLOW— LY
BLAZE ORANGE— BO

ORIENTATION OF ARROWS SHOWS DIRECTION OF TRACER MOVEMENT
WIDTH OF ARROWS INDICATES RELATIVE VOLUMES OF TRACER FOUND

Fig. 29. Ebb Oriented Movement Patterns of Tracer Sand Across the Shoal Study Area

across the shoal during the ebb cycle to channels located near the southern and southeastern edges of the shoal area.

Sediment Characteristics Study

Core samples of sediment were collected at points in the inlet channels and distributaries and at each grid location in the shoal study area. The object of this phase of the field study was to determine the size distributions of the sediments in the inlet and across the shoal study area and to determine the relationship of size distribution to the hydraulic characteristics of the inlet system. A description of the study method used and the data obtained for each sample are provided in Appendix B.

Method of analysis

After oven drying, size analysis was performed on each sample by sieving. The sieving method consisted of:

(1) obtaining a 50 to 100 gram sample using a sand splitter,

(2) weighing each sieve before the sample was poured in,

(3) introducing sample to sieves and shaking in a Soil Test, Ro-Tap machine for ten minutes,

(4) weighing and recording the weight of the sieve plus the material retained to nearest 0.1 gram, and

(5) subtracting the pre-test sieve weight from the sieve plus sand weight to obtain the weight retained in each sieve.

The phi (ϕ) scale was used to measure grain size in this study. The scale was chosen because of its ease in making calculations. The sieves used in the sieve test were even phi numbers from -1ϕ to 4ϕ. A

conversion chart for converting ϕ units to millimeters and inches is presented in Table 17 in Appendix B.

Calculation of the statistical parameters of the grain size was done using a computer program modified for IBM 360/40 by Isophording (1970). Eight sieve sizes, -2 ϕ to 5 ϕ, were used in the calculation. The -2 ϕ and 5 ϕ weights retained were set equal to 0.0 in order to assure that the assumed normal distribution was closed at both ends. The program provided Folks statistics and textural description as described by Folks (1974). The statistics used in this study were the graphic mean and the graphic sorting (standard deviation) described by Folks. Analysis of the mean and sorting parameters provided the needed information to describe the distribution of sediments in the inlet.

Histograms showing the percent retained for each sieve increment, the graphic mean and the sorting are presented for each sample by station in Appendix B. Graphic means and sorting values are indicated on the figures for samples from stations 1, 2, 4, 5, 7 and 8 and representative samples from station 6, grid stations on the shoal study area.

Inlet channels and distributaries

The collection stations for core samples collected in the inlet channels are shown in Figure 30. Twenty-eight core samples were collected at seven different locations in the inlet system. The samples collected at station 1 were from above the high water line and at varying distances into the surf zone at the north beach study grid points N0 , N4 and N13. Samples collected in the surf zone ranged from 30 to 80 feet from the high water line. The same procedure was followed for

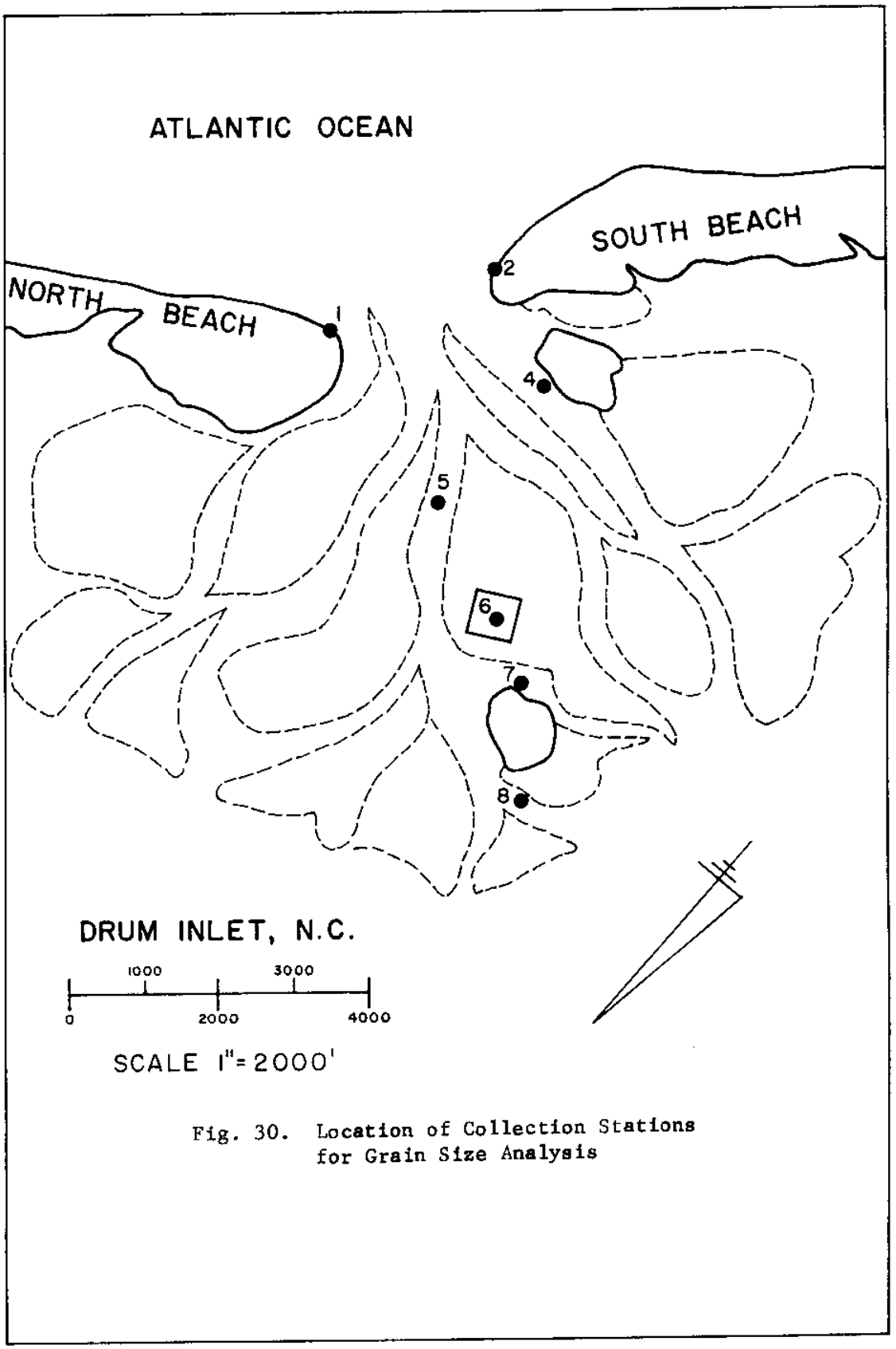

Fig. 30. Location of Collection Stations for Grain Size Analysis

samples from Station 2. Samples were collected at grid points S0, S5 and S10 and at adjacent points 100 feet seaward of the high water line. The sampling stations from the north and south beach grids are shown in Figures 41 and 42 in Appendix A. Samples from channel stations 4, 5, 7 and 8 were collected from the channel bottoms at siffer-ent depths. Samples from station 6 were from representative grid points on the shoal study area.

The data was analyzed by plotting the graphic mean versus the sorting for each sample (Figure 31). The points appeared to lie along a line related to the hydraulic energy at the locations where the samples were collected. The hydraulic energy is the sum of unidirectional flow energy and the wave energy at each specific location. Relating the energy to the sediment properties one sees that as the energy increases the graphic mean size increases and the sorting decreases. The points along the high energy section of the line represent samples taken at stations 1, 2, 4 and 5 and lie in blocks A and B in the figure. These samples represent the coarsest and most poorly sorted of all the samples. The beach samples in this group were taken at points in the surf zone. Sample points in blocks C and D were from stations 1, 2, 6, 7 and 8 and represent the finer and better sorted samples. The samples from the beach locations in this group were taken from above the high waterline. Other samples in blocks C and D were taken from distributary channels and the shoal study area at increasing distances from the inlet mouth.

Samples in blocks A and B came from areas in the inlet system where the tidal currents were the strongest and varied the most and

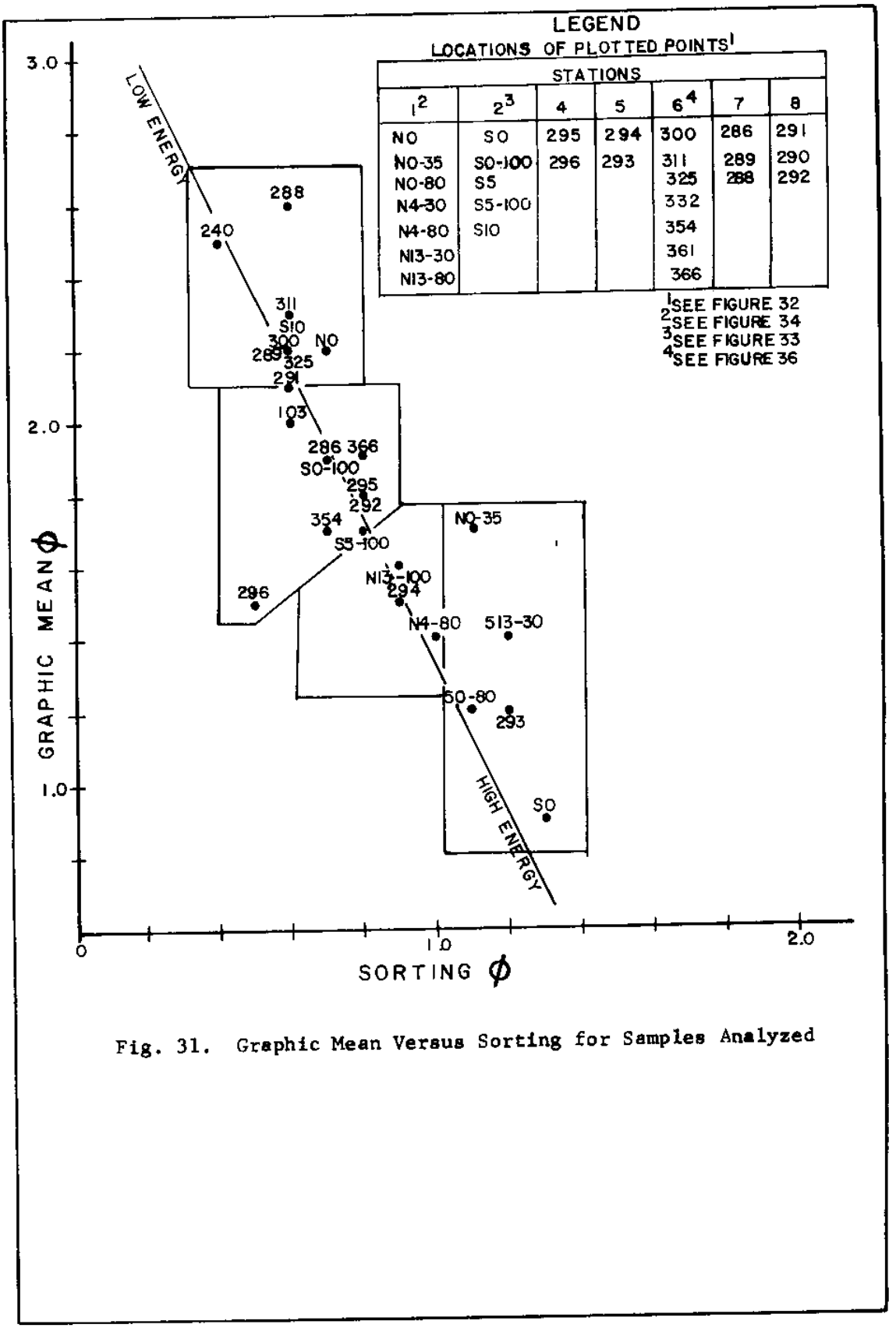

Fig. 31. Graphic Mean Versus Sorting for Samples Analyzed

where there was exposure to a combination of tidal currents and ocean waves. The most poorly sorted samples came from the surf zone on the north and south beaches and from station 5. One can see from an evaluation of Figure 31 that as the distance from the inlet mouth increases the mean size decreases and the sorting increases. The exception to this finding was that samples taken from high on the north and south beaches were more poorly sorted than the samples from the surf zone. Samples taken from the distributary channels and the shoal study area range from moderately to very well sorted. The best sorted sample was from the northwest side of the channel at station 8.

Shoal study area

Core samples were collected at each grid location and analyzed to determine the distribution of sediment sizes across the shoal study area. Figure 32 shows the graphic mean and the sorting of samples taken at each grid point.

The computer program provided the Folks (1974) textural description for each sediment sample. The description classified the sample as to the percentage of gravel sized particles in the sample. The gravel in this study were mainly small shell fragments. The two classifications found on the shoal study area were sand, s, and slightly gravely sand, (g)s. The locations of the different classifications are indicated in Figure 33. Histograms for representative samples for the four different areas are in Appendix C.

It is interesting to note that the average mean and sorting for samples collected in the channel bottom northwest of the shoal grid

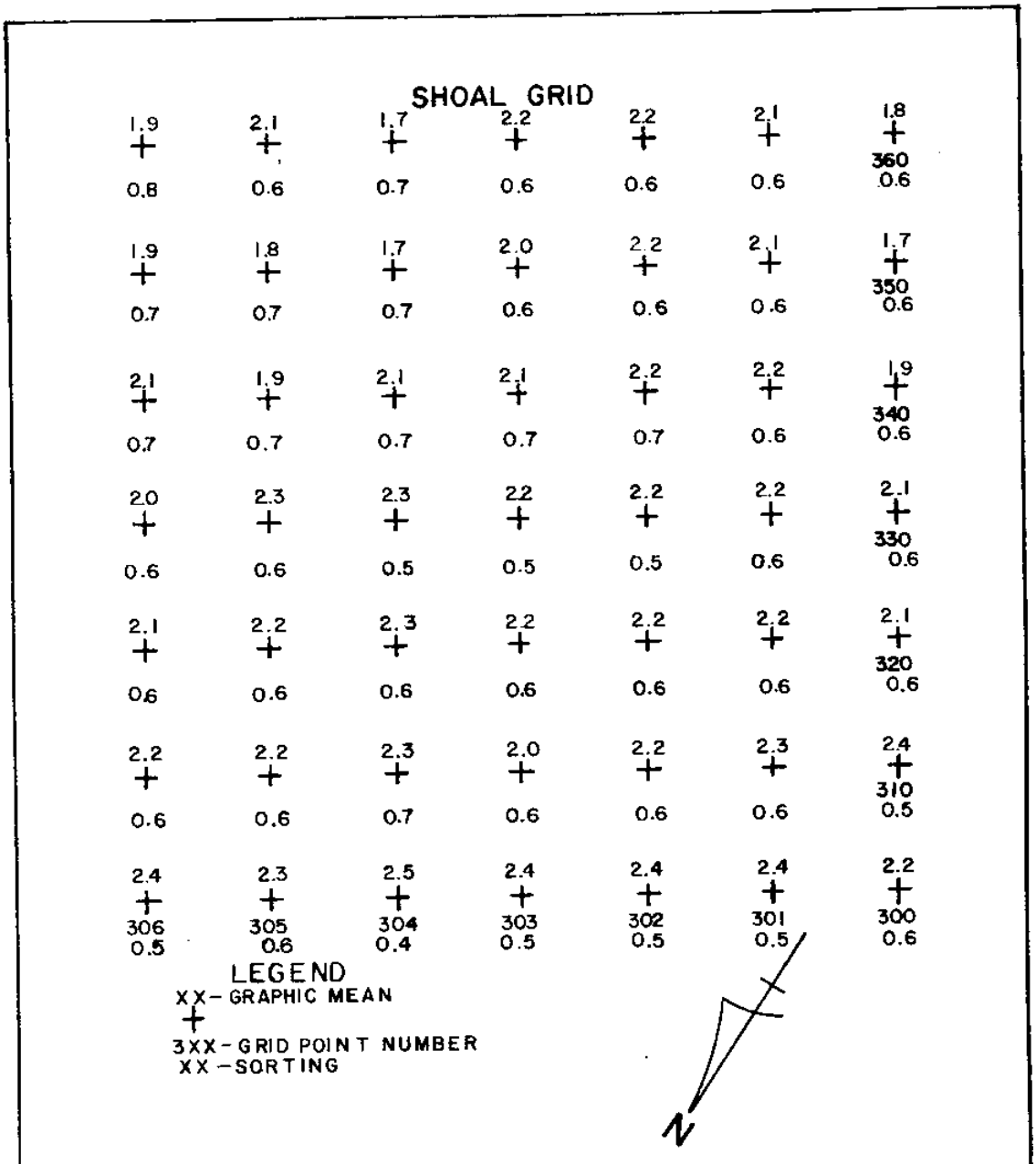

Fig. 32. Graphic Mean and Sorting Values for Core Samples taken at each Grid Point on Shoal Study Area

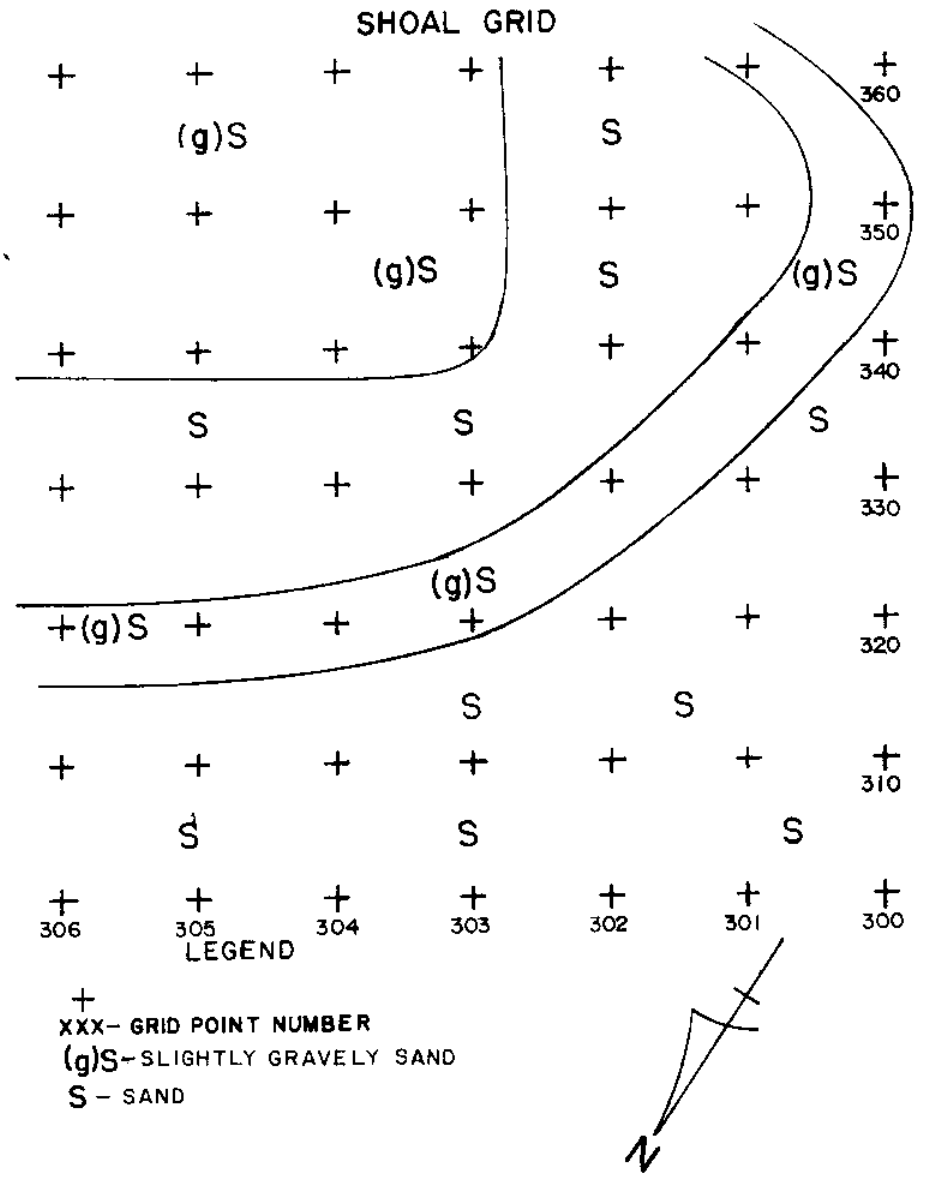

Fig. 33. Variation of Folks Textural Classifications Across the Shoal Study Grid

area (station 7) were 2.2 ϕ and 0.6 ϕ, respectively. These values are the same as the average mean and sorting of all the samples from the shoal area. This indicates that the shoal is probably the source of sediments found on the channel bottom.

Generally the mean increased and the sorting decreased from the northwestern edge of the grid to the eastern corner. The sediment near the northwestern edge of the grid was classified as sand. The sediments with a higher percentage of gravel sized material were present near the eastern corner of the grid (see Figure 33). Much of the variation detected in grain size on the shoal can be attributed to the thickness of the post-inlet shoal deposits. Observing the sediment layers in the core samples indicated that the shoals generally were made up of post-inlet light colored beach sands composed of quartz and shell fragments overlying very fine, dark colored sand of presumed pre-inlet origin. The thickness of the light colored sand layer varied across the shoal from over one foot thick to less than one inch. The thinnest layers of beach sand were near the northwestern edge of the shoal where sand waves were poorly developed. Elsewhere the thickness varied with position and sand wave profiles. The area of finer grain sizes between the two areas of more gravely material could be attributed to the presence of a washout area in front of a sand wave located between grid lines 340 and 350. Core samples taken in this area contained a higher percentage of pre-inlet sand due to the shallow depth of the beach sand caused by the washout. Figure 34 shows the sand wave and washout area between grid lines 340 and 350.

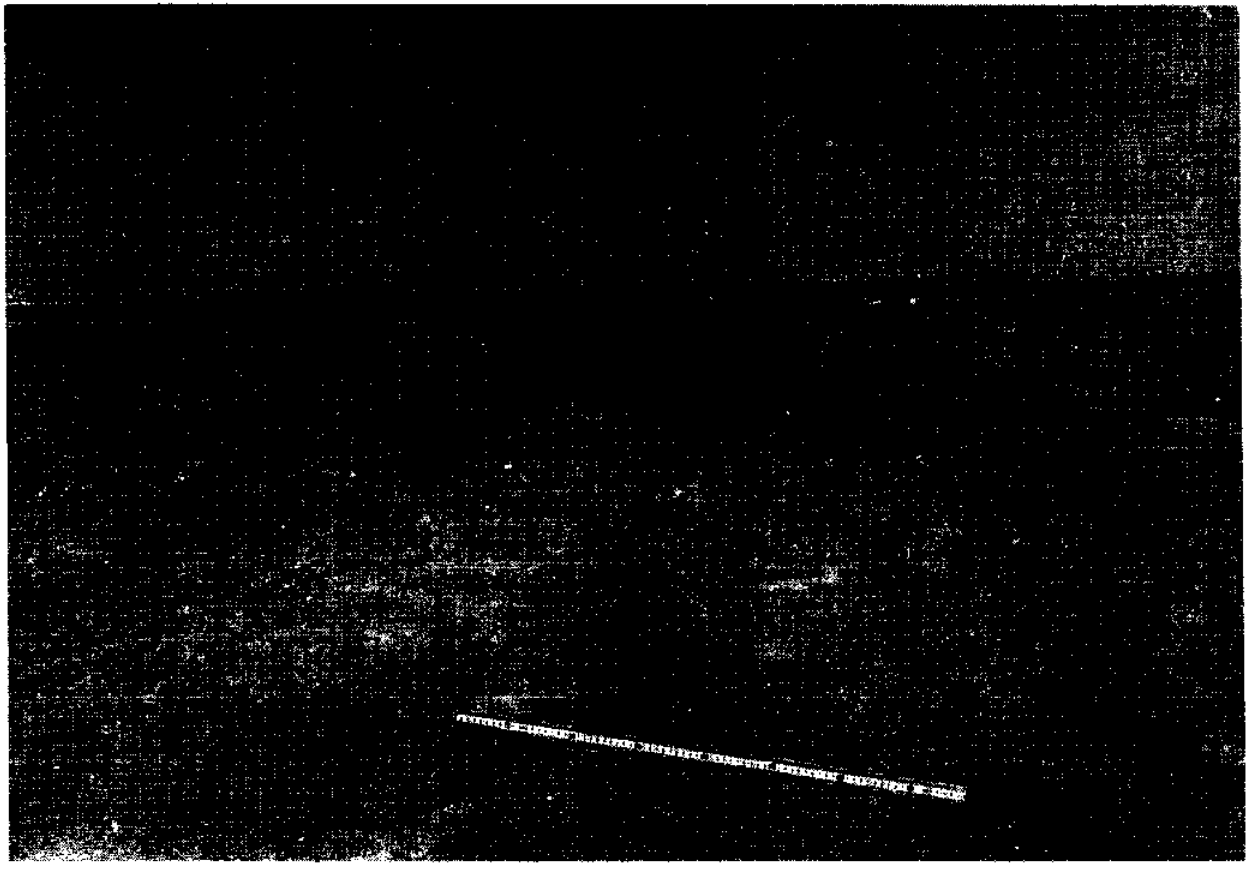

Fig. 34. Sand Wave and Washout Area near Grid Lines 340 and 350

Current Study

The object of the current study was to determine the duration and range of velocities at measurement stations located in the inlet channels and distributaries and at selected grid points on the shoal study area.

Inlet channels and distributaries

Current velocities and directions were measured at four locations in the main channel and distributary channels adjacent to the shoal study area. The channel measurement stations are shown in Figure 35. The study was conducted on August 21, 1977 from 0800 to 1930 hours. The velocity measurements were made at mid-depth with a Teledyne Gurley No. 622 hand held current meter by moving, by boat, from one location to the other during the study period. Directions were estimated using a hand held Brunton compass. The current velocities and directions measured are tabulated in Table 18 in Appendix C. The maximum and average ebb and flood velocities were determined from the data in Table 18. Current durations were determined from graphs of velocity versus time shown in Figure 36.

It was found that at all four locations the durations of the flood currents cycle were greater than for the ebb. At stations 4 and 5 (see Figure 35) the maximum measured ebb velocity exceeded the maximum flood velocity. A summary of the durations, maximum ebb and maximum flood velocities are presented in Table 11.

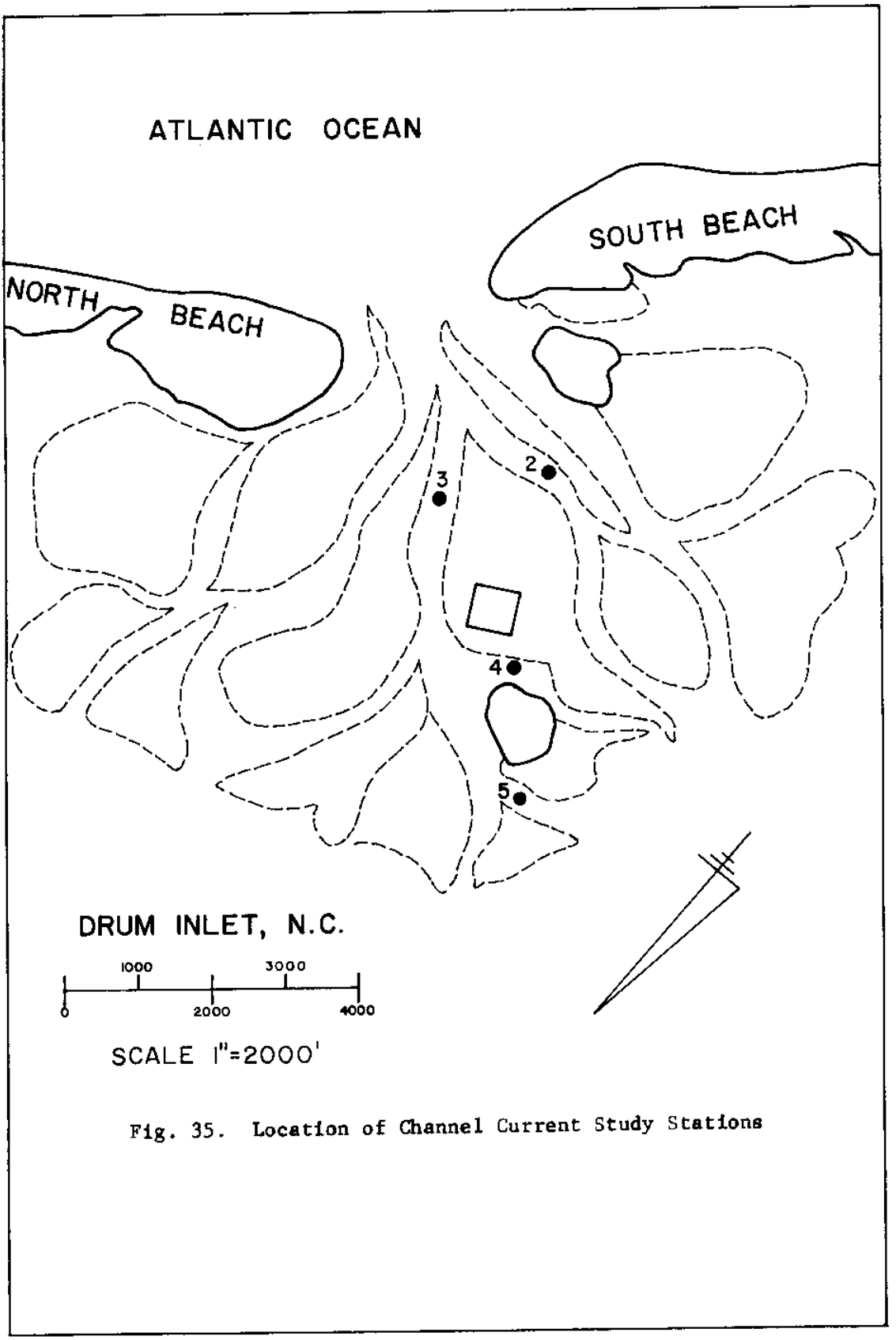

Fig. 35. Location of Channel Current Study Stations

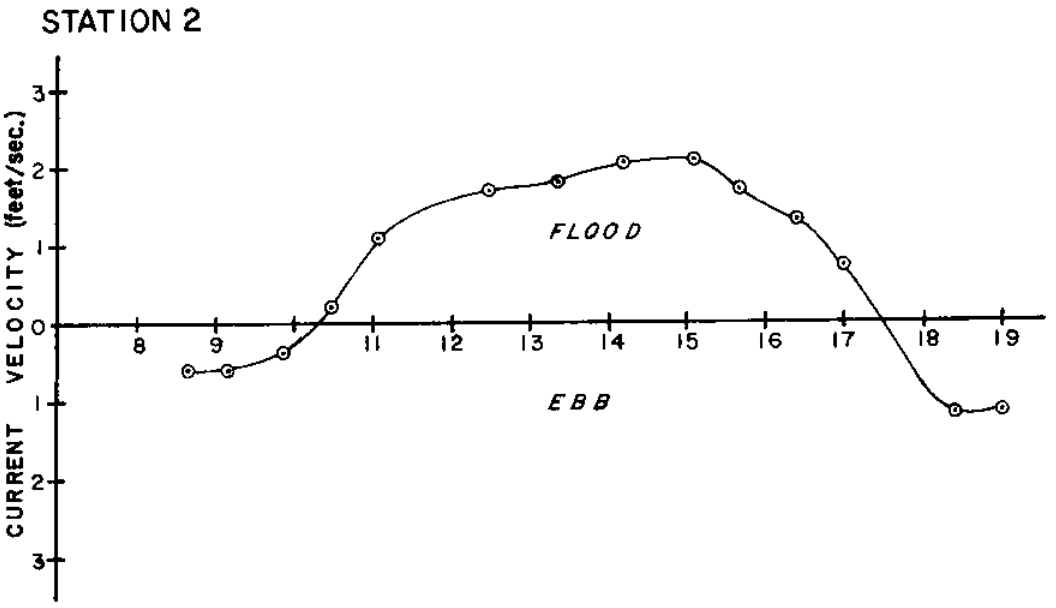

OCEAN TIDES HIGH 1149 HRS. 2358 HRS.
LOW 0506 HRS. 1755 HRS.

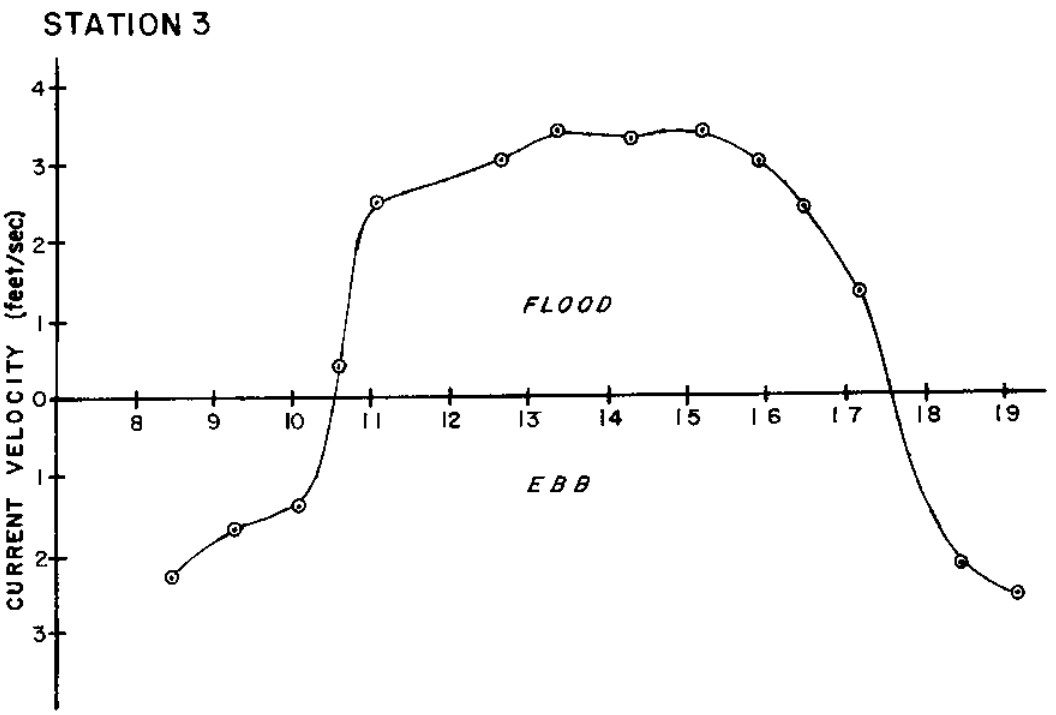

Fig. 36. Channel Current Velocities Versus Time

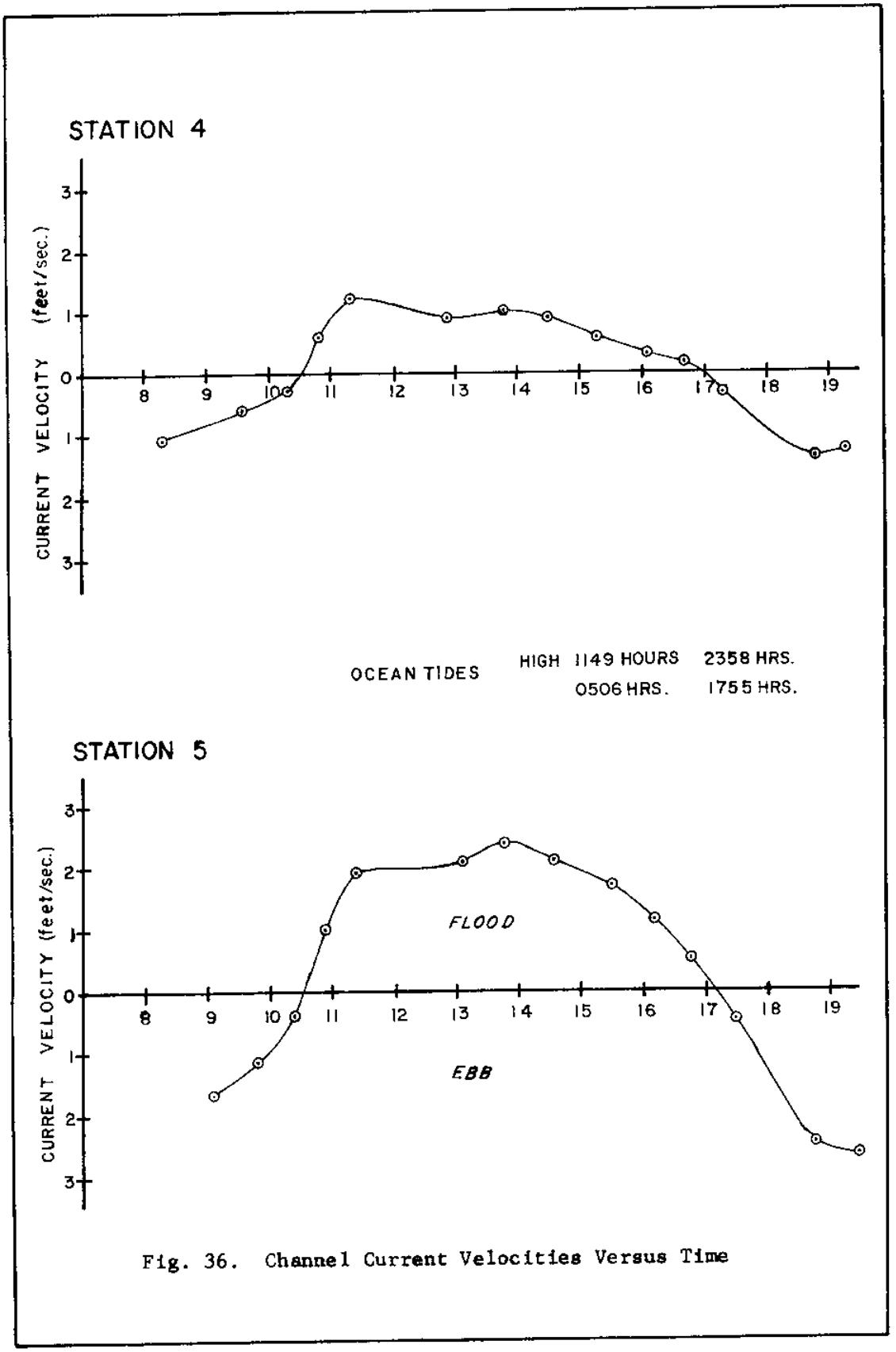

Fig. 36. Channel Current Velocities Versus Time

TABLE 11

SUMMARY OF CURRENT DATA FOR INLET CHANNEL STATIONS

Station	Max Flood (ft/sec)	Max Ebb (ft/sec)	Flood Duration (hrs)	Ebb Duration (hrs)
2	2.12	1.22	7.0	5.5
3	3.4	2.6	7.0	5.6
4	1.22	1.38	6.5	6.1
5	2.39	2.65	6.5	6.1

Shoal study area currents

Current velocities and directions were measured along the 340-346 and the 300 to 360 line of the shoal study grid. The location of the stations is shown on the grid in Figure 37. The velocity measurements were made with an A. Ott Kempton type 10152 current meter. The directions were estimated using a Brunton hand held compass. The velocity and direction measurements made over the shoal are tabulated in Table 19 in Appendix C. Graphs of the current velocity versus time for each station are presented in Figure 38.

It was found that at all stations, with the exception of 345, the maximum flood currents far exceeded the maximum ebb currents. This was the expected result since the depth during the maximum flood was always greater than during the ebb. In most places, the shoal area was above the water level in the inlet during a large portion of the ebb cycle. The large flood velocities along the 300 and 360 grid line can be attributed to the depth in that area being the greatest of any in

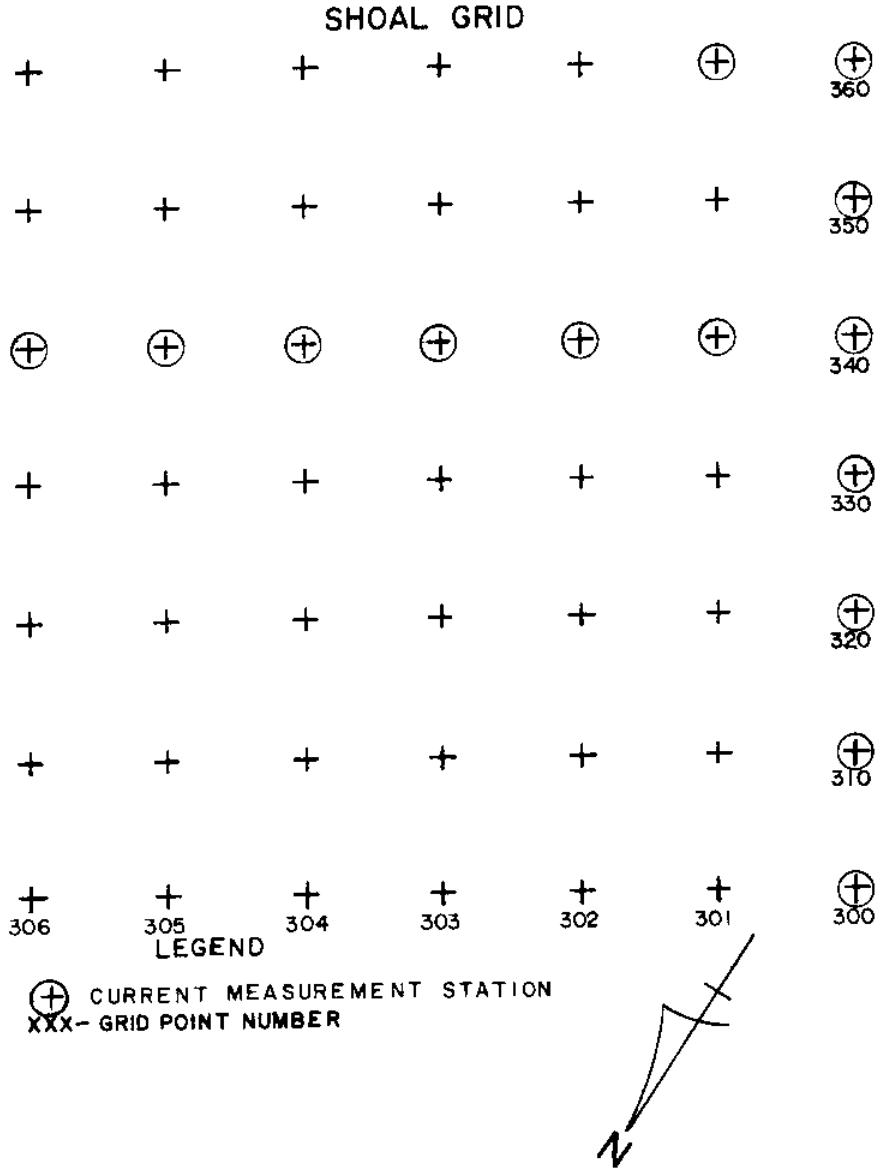

Fig. 37. Location of Current Measurement Stations on Shoal Study Grid

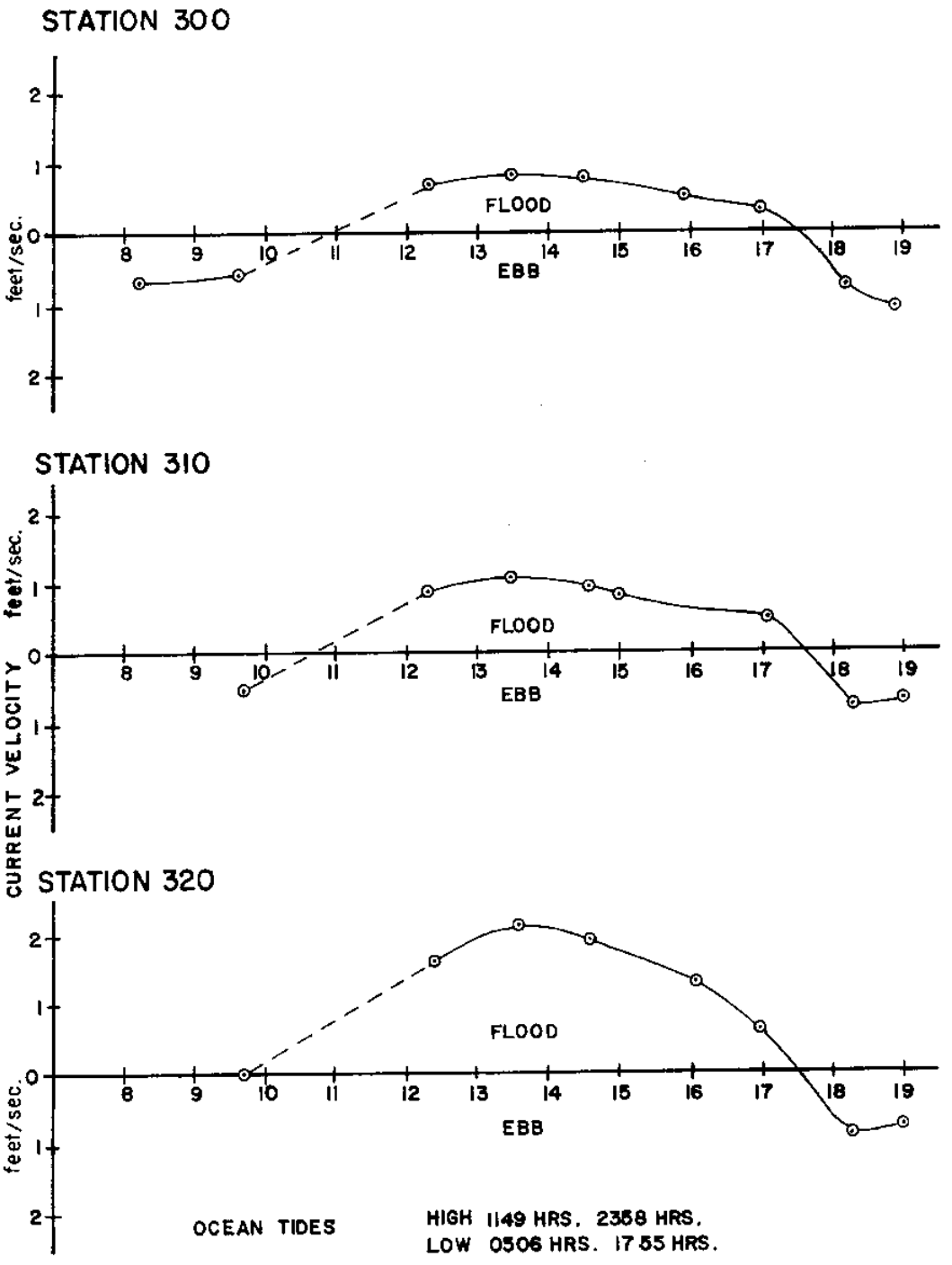

Fig. 38. Shoal Current Velocities Versus Time

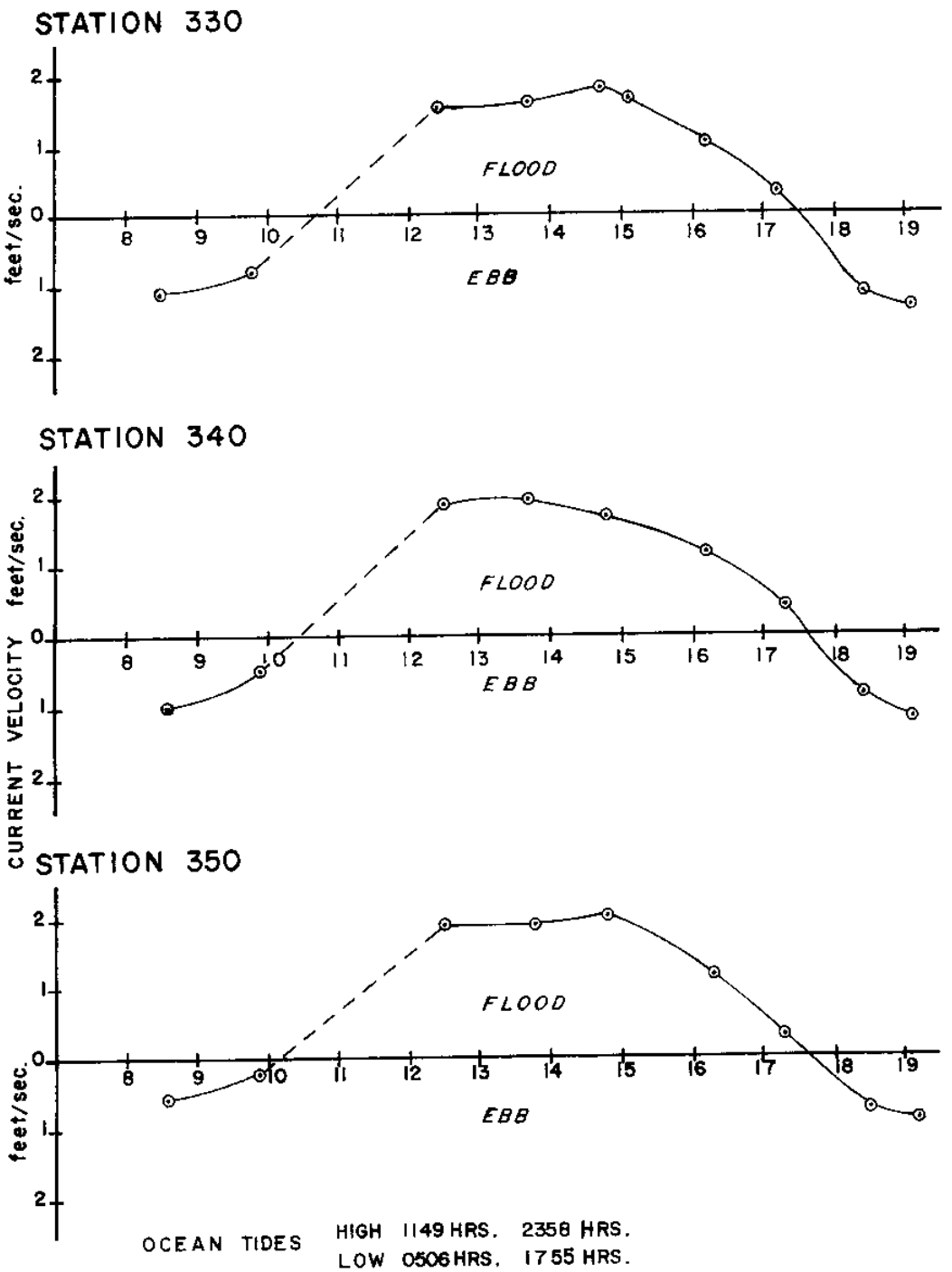

Fig. 38. Shoal Current Velocities Versus Time

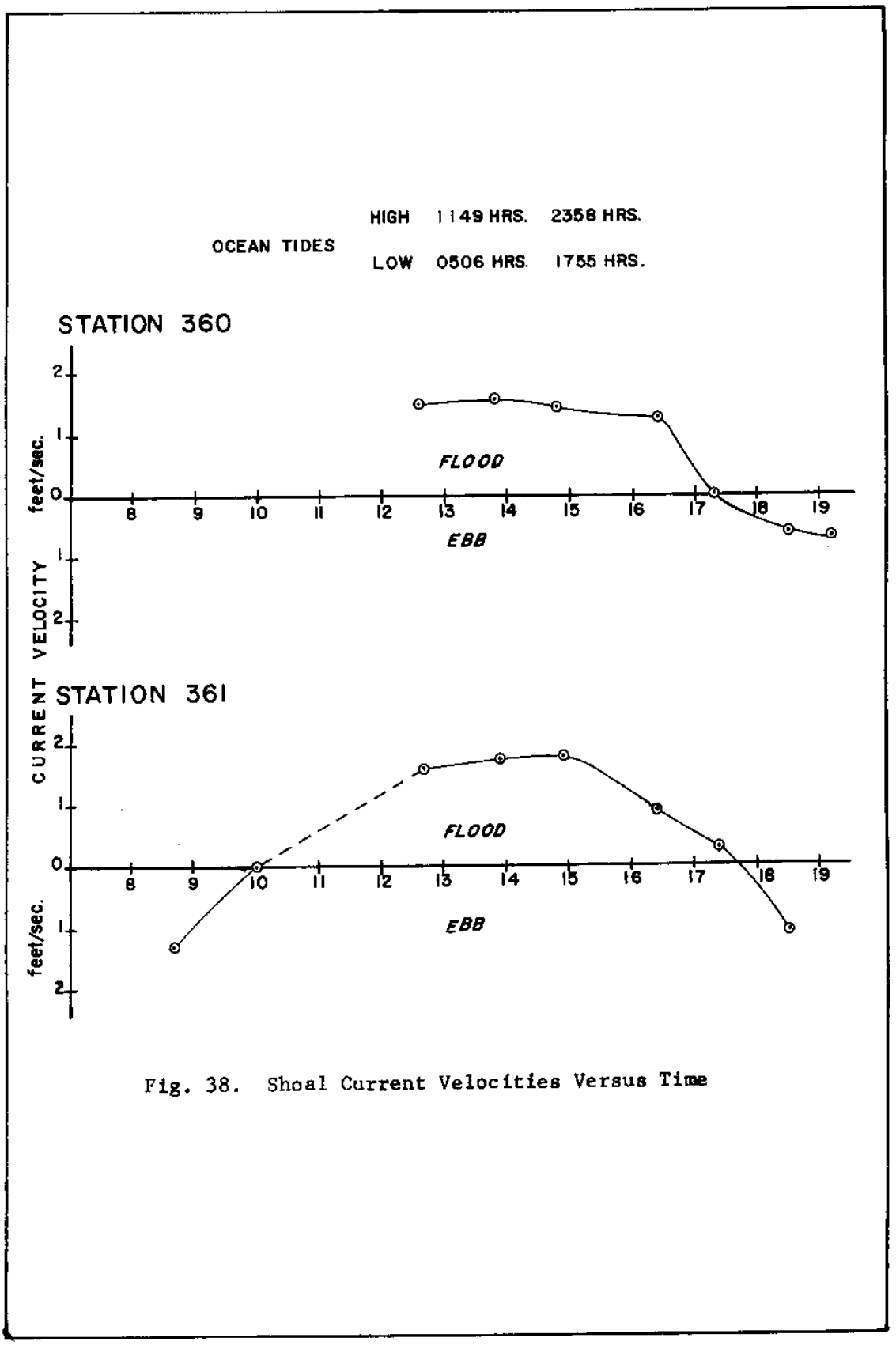

Fig. 38. Shoal Current Velocities Versus Time

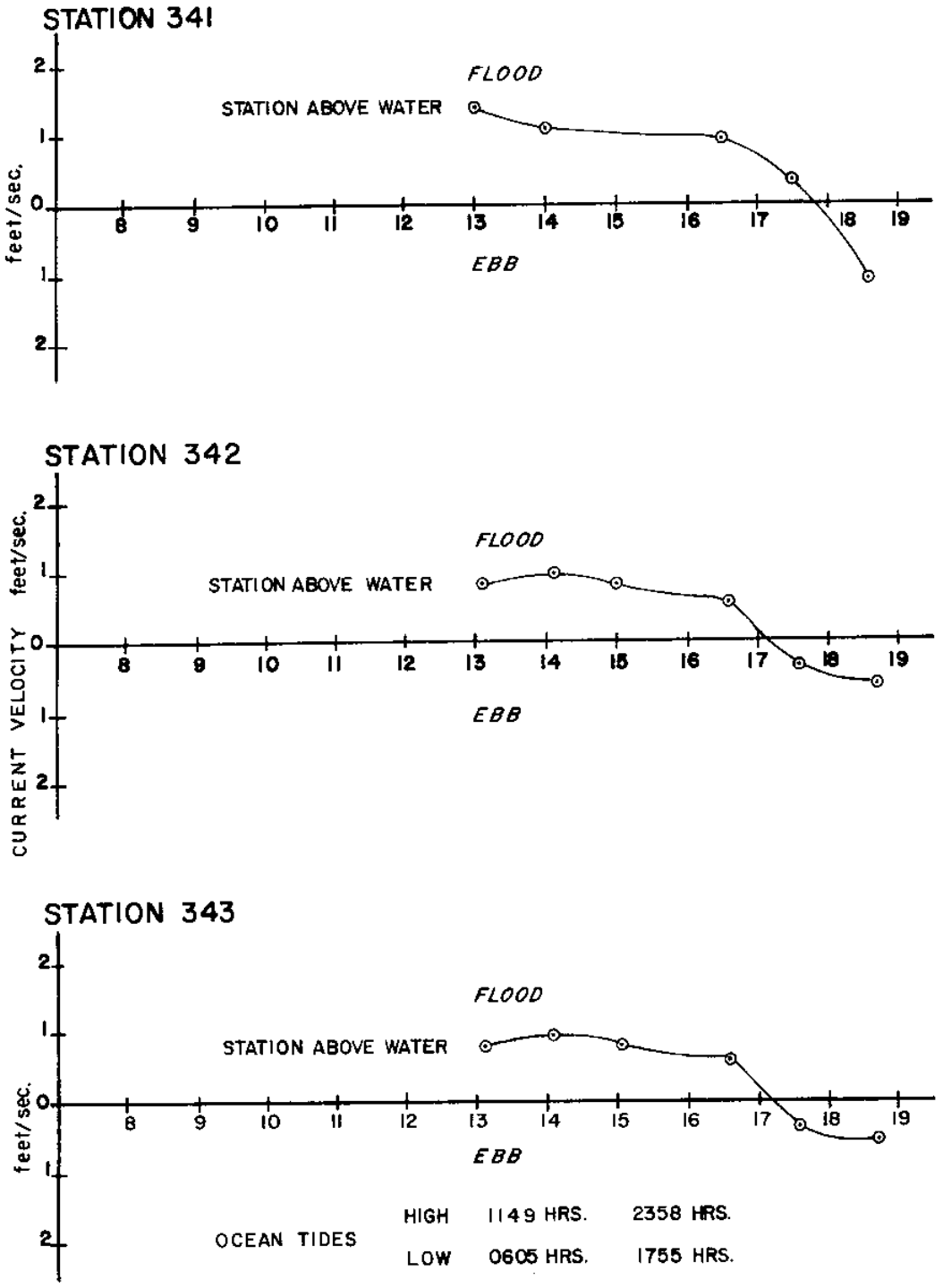

Fig. 38. Shoal Current Velocities Versus Time

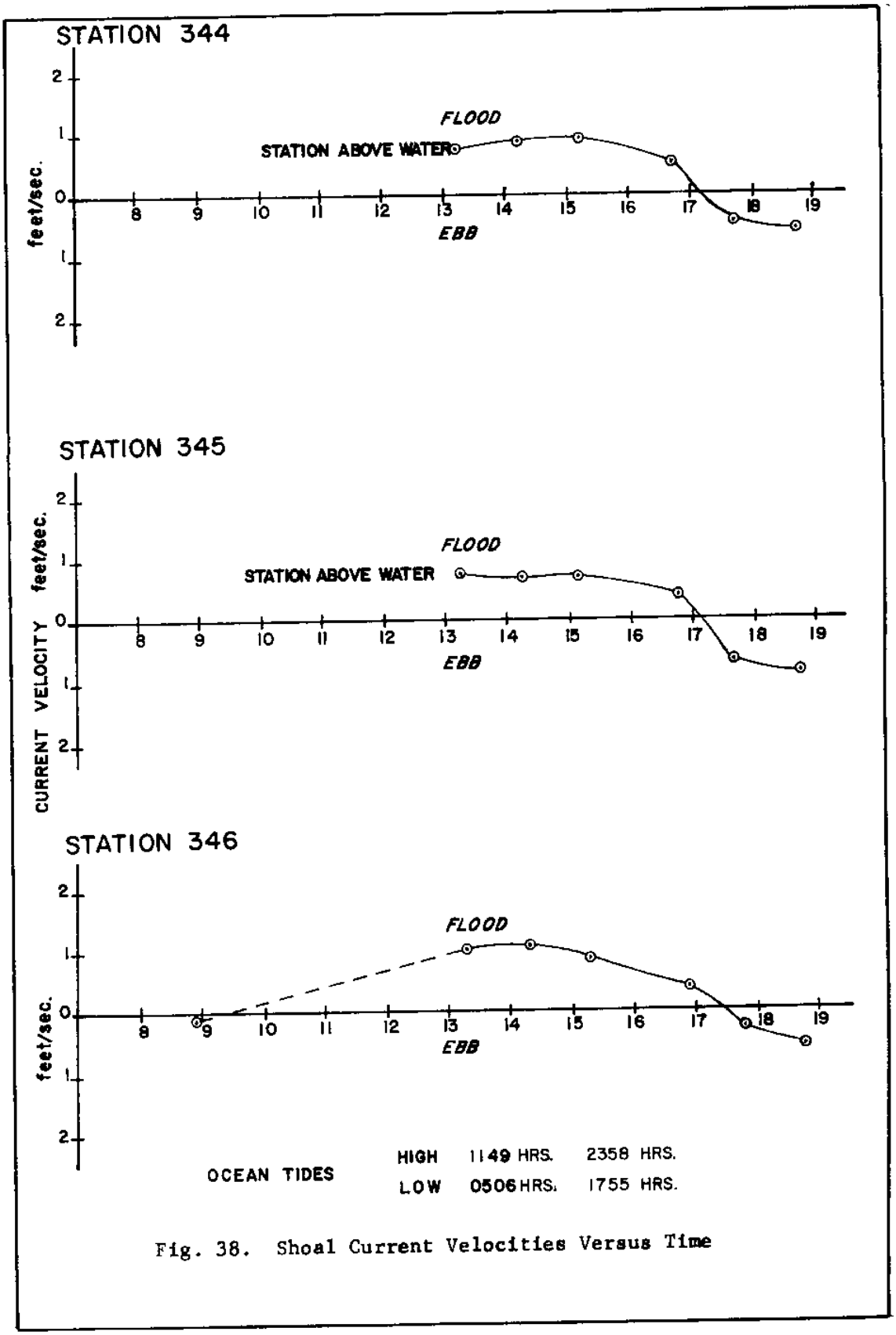

Fig. 38. Shoal Current Velocities Versus Time

the grid. At all stations where ebb currents were measured, the flood current duration exceeded the ebb duration. A summary of the maximum flood and ebb velocity measured and the durations of the flood and ebb cycles are shown in Table 12. Although a detailed bathymetry of the

TABLE 12

SUMMARY OF CURRENT STUDY DATA FOR SHOAL STUDY AREA

Station	Max Ebb (ft/sec)	Max Flood (ft/sec)	Flood Duration (hrs)	Ebb Duration (hrs)
300	1.12	.82	6.5	6.1
310	.29	1.02	6.8	5.8
320	.89	2.07	7.5	5.0
330	1.35	1.8	6.7	5.9
340	1.18	1.94	7.1	5.5
350	.98	2.03	7.4	5.2
360	.69	1.57	---	---
361	1.3	1.77	7.7	4.9
341	1.15	1.38	---	---
342	.62	.98	---	---
343	.59	1.15	---	---
344	.62	.89	---	---
345	.89	.75	---	---
346	.59	1.08	7.9	4.7

shoal is not available, the currents conform to the observed variations in depth across the shoal. The 341 to 346 grid line represented a shallow area in the shoal study area and the velocities were accordingly smaller. The principle direction of flow across the shoal grid was toward the north and northwest during the flood cycle and toward the northeast,

southwest and southeast during the ebb cycle. It is evident from the direction measurements that during the flood cycle water flowed across the shoal from the direction of the inlet mouth. On the ebb cycle, however, water appeared to disperse across the shoal towards channels adjacent to the shoal area to the east, south and southeast.

ANALYSIS OF DATA

Delta Growth Patterns

Analysis of the erosion and flood shoal growth data showed a close correlation between the rate of erosion and the growth rate of the shoals. A comparison was made between Chang's model delta study in which the sediment load was related to lateral, longitudinal and areal growth rates, and the growth patterns of the flood tidal shoals. The sediment load was assumed to be directly proportional to the erosion rate of the beaches. The comparison was made by using Figures 18 and 26. During the period of maximum erosion, October 1971, to June, 1975, there was a constant rate of areal, longitudinal and lateral growth of the flood tidal delta. The areal and lateral growth rates were greater during this initial period. This coincided with Chang's findings in which an increased sediment load caused more widening than lengthening of the model delta. During the short period from June, 1975, to November 1975, there was a rapid increase in lateral extent and area of the flood tidal delta. These changes were associated with a small net erosion during that period. This finding contradicted the findings from the October 1971, to June 1975, period and did not follow the trends found in Chang's model delta. From October, 1976, through March, 1977, there was continued lateral growth of the flood tidal delta. Slight areal growth and no additional landward growth occurred during that period, thus following the same trends seen in 1975.

Inlet Stability

To predict the stability of the inlet the temporal changes in inlet features and the relationship between inlet channel length and cross-sectional area were observed. Stability analysis provided a numerical estimate of the stability.

The rates of change in the inlet features, beaches and shoals, that were observed during the later portion of the study period indicated that the inlet system was relatively stable compared to the period following the opening. Although there was continued growth of the shoals, the rates were much smaller than in the early life of the inlet.

According to Bruun and Gerritsen (1960) the cross-sectional area of the inlet throat channel must increase with an increased elongation of the inlet channels or choking of the inlet channel will occur. In order to determine if Drum Inlet meets this criteria, the inlet channel width was assumed proportional to the cross-sectional area and the effective inlet channel length was assumed proportional to the flood shoal area. Comparing the change in throat width and shoals as in Figure 25, it is seen that there was a rapid increase in throat width associated with the areal growth through July,1975. It is difficult to account for the rapid increase and decrease in the inlet throat width that occurred between October,1973,and November, 1975. The inlet throat could have consisted of multiple shallow channels causing the appearance of a wide throat in the aerial photographs. If the multiple channels combined to form a single deep inlet gorge, there would have been a decrease in width in order to maintain an equilibrium cross-sectional area.

Constructing a line through the data that discounts the short term variations in the throat width, Figure 25 reveals a close correlation between areal growth of the flood tidal delta and the width of the inlet throat after the initial rapid changes early in the inlet life. This indicates that the changes necessary to prevent choking, discussed by Bruun and Gerritsen, did occur at Drum Inlet following the rapid initial changes that took place immediately after the opening of the inlet. Whether the expansion of the cross-section was rapid enough to keep pace with the growth of the shoals must be further analyzed using stability analysis.

It was determined that by the end of the study period the beaches, inlet throat and flood tidal shoals had reached a relatively stable configuration. This implies that there was sufficient flushing of sediments from inner channels and the inlet main channel to prevent the continued rapid rate of growth experienced during the early life of the inlet. The validity of this determination of stability can be easily checked using the dimensionalessratio of tidal prism to maximum net littoral drift, Ω/M , proposed by Bruun and Gerritsen (1960) and Bruun (1966) Using a tidal prism calculated by Vallianos[3] of 10,700 acre-feet and the maximum net littoral drift of 750,000 cubic yards in the southwesterly direction, results in a tidal prism to littoral drift ratio, Ω/M , equal to 23. Bruun indicates that ratios of Ω/M less than 100 generally represent inlets that are unstable and are characterized by extensive shoals. This indicates that shoaling will continue at Drum Inlet. Vallianos,[4] using historical correlations

---

[3] Limberos Vallianos, personal communication.

[4] Ibid.

between the Old and New Drum Inlet and the Ω/M ratio, predicted that the New Drum Inlet will follow the same trends as the Old Inlet. He predicted that the New Inlet will migrate in a southwesterly direction and close within the next 25-year period.

Sediment Characteristics and Movement in High and Low Energy Zones

A comparison between tracer particle movement velocities, and wave migration rates, shoal current velocities, and channel current velocities versus sediment characteristics provided insight into the relationship between sediment movement rates and flow energy.

A summary of information developed on current and sediment movement is presented in Table 13. Tracer particle rates in the low energy zone were based on samples taken from 1615 to 1730 hours on August 20.

TABLE 13

SUMMARY OF SEDIMENT MOVEMENT AND CURRENT DATA FOR THE HIGH AND LOW ENERGY ZONES

Average Sand Wave Migration Rate - 2 ft/day (0.08 ft/hr)		
Average Current Velocities on Study Shoal		
	Flood	Ebb
	1.4 ft/sec.	0.9 ft/sec.
Tracer Particle Movement Rates		
Low Energy Zone		
	Flood Direction	Ebb Direction
	72 ft/hr.	72 ft/hr.
High Energy Zone		
	North Beach	South Beach
	300 ft/hr.	289 ft/hr.

This was the sampling period following the introduction of the fire orange, blaze orange and lightening yellow tracer material. This period was used because it was probable that tracer movement was beyond the boundaries of the grid at later samplings making the movement rate impossible to determine. Rates were determined by dividing the distance to the tracer found furthest from the introduction line by the time from introduction. Rates in the high energy zone were based on samplings from 1518 to 1618 hours on August 22 for the north beach and 1135 to 1250 hours on August 22 for the south beach.

The high energy zone particle movement rates were over four times greater than for the low energy area. This indicated that large quantities of sand, under the influence of currents and ocean waves, moved towards the inlet mouth during the flood tidal current cycle. The movement of the sand wave across the shoal area offered insight into the difference between the particle transport and the bed load transport. The large particle rates indicated transport as suspended sediment. The discovery of tracer on the beach that had been introduced on the shoal study area indicated that substantial amounts of sediment in suspension moved from the shoals back out the inlet mouth.

A comparison of measured current velocities and sediment sorting and graphic mean grain size is presented in Table 14. These data indicate that the distributary channels experienced greater ebb than flood velocities. The largest currents and widest range of velocities at Station 3 corresponded to the largest mean particle size and the most poorly sorted of all samples taken. These data indicated that the high energy areas, the surf zone and inside the inlet mouth, served as storage or staging areas for sand moving in and out of the inlet mouth

TABLE 14

COMPARISON OF CURRENT VELOCITY AND
SEDIMENT CHARACTERISTICS LOCATION

Current Station*	Sediment Sampling Station**	Maximum Flood (ft/sec)	Maximum Ebb (ft/sec)	Average Flood (ft/sec)	Average Ebb (ft/sec)	Graphic Mean (ϕ)	Sorting (ϕ)
3	5	3.4	2.6	2.5	2.0	1.4	1.1
Shoal Grid	6	2.1	1.3	1.4	0.9	2.2	0.6
4	7	1.2	1.4	0.7	0.8	2.2	0.6
5	8	2.4	2.7	1.6	1.5	2.1	0.6

*See station locations, Fig. 39.

**See station locations, Fig. 32.

because of the ability of the wide range of currents to transport a wide range of grain sizes. Particle sizes were smaller and sorting better in the low energy areas. The currents in the low energy areas are only capable of transporting a narrow range of particle sizes.

The high energy zones served as sources and the low energy zones served as sinks facilitating the circulation of sand in the inlet system.

Sediment Budget

Comparisons were made between the net eroded volume from the north and south beach prior to October, 1976, the littoral drift volumes for the Drum Inlet area and the volume of sand deposited on the flood tidal shoals in order to evaluate the relative contributions of each sediment source and sink in the inlet system.

The volume of sediment deposited on the shoals was obtained by a mass calculation using a July,1976,photogrammetric contour map of the inlet shoals obtained from the U. S. Army Corps of Engineers, Wilmington District. The pre-inlet bottom contour in Core Sound was assumed to be a constant slope of 0.002 ft/ft from zero depth at the sound side of the barrier island to an 8 foot depth 4400 feet northwest of the island. The volume of material computed from the contour map was 2,100,000 cubic yards. This volume included the volume in the spoil areas northwest and southwest of the inlet mouth.

According to Vallianos,[5] the littoral drift volumes along Core Banks in the vicinity of Drum Inlet are currently estimated at about 1.25 million cubic yards per year of which approximately 750,000 and 500,000 cubic yards move southwesterly and northwesterly, respectively.

A summary of the volumes eroded from the beaches, the littoral drift rates, and shoal volumes are given in Table 15. The yearly beach erosion and flood shoal volumes were obtained by dividing the time from October,1971,to October,1976. This assumed that the erosion rate was uniform during that period. As determined in earlier discussion, this assumption was not valid, but it enabled a gross comparison to be made. This assumption and the inaccuracies involved in determining the shoal volumes, erosion rates and littoral drift volumes made the numbers presented here accurate within approximately 50 percent.

The shoal volume represented only 18 percent of the total, or yearly volume of sediment supplied to the system. The currents measured in the field at station 3 (figure 39) near the inlet mouth showed a

---

[5]Limberios Vallianos, personal communication.

TABLE 15

SUMMARY OF VOLUME CHANGES IN THE INLET SYSTEM

	Yearly Eroded Volumes (yd^3/yr)	Total Volume Eroded Through October 1976 (yd^3)
Sources:		
Littoral Drift		
Total	1,250,000	6,250,000
Southwesterly	750,000	3,750,000
Northeasterly	500,000	2,500,000
Beach Erosion		
North Beach	620,000	3,100,000
South Beach	480,000	2,400,000
Sink:		
Flood Tidal Shoals	420,000	2,100,000

flood current velocity 13 percent higher than the ebb current velocity. If the approximation that the bedload transport is proportional to the velocity to the fifth power (Bruun and Gerritsen, 1960), the flood, ebb current ratio indicates that 13 percent of the material supplied to the inlet mouth was trapped by the flood currents and 87 percent was bypassed. These percentages indicated that of the 2.77 million cubic yards supplied to the inlet yearly, 2.4 million cubic yards were bypassed and 360,000 cubic yards were trapped on the flood shoals. This volume is of the same order of magnitude as the calculated volume of 420,000 cubic yards. The ratio of northeasterly to southwesterly littoral drift volumes was used to determine the percentage of the bypassed material that moves north and south from the inlet. These percentages

indicated that 40 percent (960,000 cubic yards) of the bypassed material moved north and 60 percent (1.44 million cubic yards) moved south. A schematic diagram of the inlet bypassing and trapping system is shown in Figure 39.

This analysis does not account for sediment lost offshore, in the ebb tidal delta, contributions of beaches north and south of the study area of overwash.

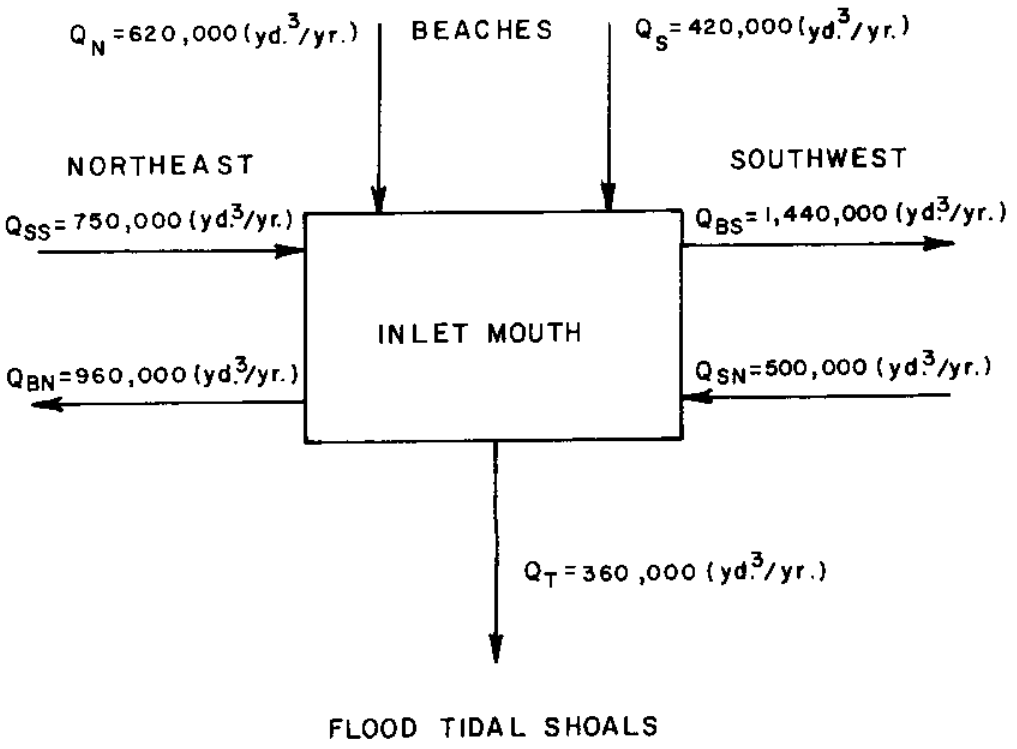

Q_{SS} = LITTORAL DRIFT VOLUME, SW. DIRECTION

Q_{SN} = LITTORAL DRIFT VOLUME, NE. DIRECTION

Q_{BN} = BYPASSED VOLUME, NE. DIRECTION

Q_{BS} = BYPASSED VOLUME, SW. DIRECTION

Q_T = VOLUME TRAPPED ON FLOOD TIDAL SHOALS

Q_N = VOLUME ERODED FROM NORTH BEACH

Q_S = VOLUME ERODED FROM SOUTH BEACH

Fig. 39. Schematic Diagram of Inlet Sediment Bypassing and Trapping System

CONCLUSIONS

The following conclusions were developed from this study: (1) A pattern of circulation of sediments in the inlet system was established. The hypothesis was developed from the results of the sediment tracer study in which it was found that movement of sand across the shoals was flood dominated. There was also evidence of substantial ebb movement of sand across the shoal areas. However, the amounts transported by the flood currents appeared to be much greater than for the ebb currents. Discovery of tracer on the beaches which had been introduced on the shoals indicated that there was substantial flushing of sediments from inner shoals and channels. The migration of sand waves across the shoal areas in the aerial photographs supported the findings of the tracer study. The domination of flood currents in the main channel and across the shallow shoal areas and the apparent ebb dominance in the distributary channels further supported the circulation hypothesis. Sediment deposited in the distributary channels from the shoals was carried to the main channel where it was redistributed by strong flood and ebb currents. The sediment may be moved out of the inlet back to the littoral system or carried back across the shoals completing the circulation pattern. The distributions of sand sizes indicated that the sand was distributed in the inlet system according to the hydraulic energy of the flows at each specific location. Areas of high energy, such as the surf zones on the

adjacent beaches and in the main channel where there was a wide range of current velocities, served as sources of sediment moving in and out of the inlet. These areas were looked upon as staging areas for sediments to be distributed throughout the entire inlet system.

(2) The stability of the inlet and the flood tidal shoals was fair. The growth rates of shoals was low compared to the rate of change early in the life of the inlet. Landward growth of shoals stabilized early in 1975. Other features, lateral extent, width of the inlet throat and aereal extent experienced only slight changes after January,1976. These data indicate a stabilization of the inlet system after January,1976. However, stability calculations indicated poor stability and continued shoaling. The conclusion is that shoaling will continue. The rate will be directly related to the severity of the environmental conditions affecting the inlet. An increase in the frequency of occurrence of severe coastal storms could accelerate the shoaling process by increasing the sediment load imposed on the inlet.

(3) The presence of the inlet caused severe erosion of 1.5 miles of the barrier island adjacent to the inlet. This was indicated by the location of nodal points 5000 feet north of the inlet and 3000 feet south of the inlet. The points were characterized by little change in beach position compared to other points in the study area. The points became evident after the initial rapid erosion following the opening of the inlet. According to the data, the south beach experienced more erosion than the north beach. There was very rapid erosion of the adjacent beaches following the opening of the inlet. This erosion can be attributed to the inlet attempting to reach an equilibrium configuration.

The overall net shoreline erosion during the study period was 5.5 million cubic yards.

(4) The sediment budget analysis provided order of magnitude volumes of the inlet shoaling rate. Approximately 13 percent of the material supplied to the inlet mouth was retained on the shoals. This indicated that shoal growth will probably continue at a rate from 360,000 to 420,000 cubic yards per year. As shoals grow and effective channel lengths continue to increase causing greater hydraulic resistance, more of the trapped sand will be deposited in the sound closer to the inlet throat causing migration and eventually, with a certain combination of environmental conditions cause choking.

Recommendations for Further Research

Recommendations for additional research include:

(1) a study of the effects of the flood tidal shoals on the circulation in Core Sound,

(2) a detailed sediment budget for Portsmouth Island and Core Banks, from Ocracoke Inlet to Cape Lookout to determine the total effect on the barrier islands of the presence of Drum Inlet and the sand trapping and bypassing mechanism of the inlet,

(3) a physical model study of tidal delta formation including effects of waves and unsteady flows, and

(4) development of a method to predict the rapid growth patterns of shoals due to man-made inlets.

LITERATURE CITED

Bruun, P., 1966. Tidal Inlets and Littoral Drift. Oslo, Norway: University Book Company.

Bruun, P., and Gerritsen, F., 1960. Stability of Coastal Inlets. Amsterdam, Netherlands: North Holland Publishing Company.

Dean, R. G., and Walton, T. L., 1975. "Sediment Transport Processes in the Vicinity of Inlets with Special Reference to Sand Trapping," Esturine Research, Vol. II. New York: Academic Press. pp. 129-149.

Escoffier, F. F., 1977. "Hydraulics and Stability of Tidal Inlets," General Investigation of Tidal Inlets, Report 13. U.S. Army, Corps of Engineers, Coastal Engineering Research Center, Ft. Belvoir, VA.

Escoffier, F. F., 1940. "The Stability of Tidal Inlets," Shore and Beach, Vol. 8, No. 4, pp. 114-115.

Folks, R. L., 1974. Petrology of Sedimentary Rocks. Austin, Texas: Hemphill Publishing Company.

Hayes, M. O , 1975. "Morphology of Sand Accumulation in Estuaries," Esturine Research, Vol. II. New York: Academic Press. pp. 3-22.

House Document No. 414, 75th Congress, 2nd Session, 1937. "Drum Inlet, North Carolina."

Isophording, W. C., 1970. "Fortran IV Program for Calculation of Measure of Central Tendency and Dispersion on IBM 360 Computer," Journal of Geology, Vol. 78, pp. 626-628.

Jarrett, J. T., 1976. "Tidal Prism - Inlet Area Relationships," General Investigation of Tidal Inlets. Report 3, U.S. Army, Corps of Engineers, Coastal Engineering Research Center, Ft. Belvoir, VA.

Johnson, J. W., 1973. "Characteristics and Behavior of Pacific Coast Tidal Inlets," Journal of the Waterways, Harbors and Coastal Engineering Division, ASCE, Vol. 99, No. WW3, pp. 325-339.

Machemehl, J. L., Chamber, M., and Bird, N., 1977. "Flow Dynamics and Sediment Movement in Lockwoods Folly Inlet, North Carolina," University of North Carolina Sea Grant Publication, No. UNC-SG-77-11, North Carolina State University, Raleigh, N.C.

Masterson, R.P., Machemehl, J.L., and Cavaroc, V.V., 1973. "Sediment Movement in Tubbs Inlet, North Carolina," North Carolina State University Center for Marine and Coastal Studies, Report No. 73-Z, Raleigh, N.C.

Moffitt, F. H., 1977. "History of Shore Growth from Aerial Photographs," Air Photography and Coastal Problems, Vol. II. Edited by M. T. El-Ashry, Dowden, Hutchinson and Ross, Inc., Stroudsberg, PA, pp. 51-55.

Nummendal, D., Oertel, G. F., Hubbard, D. K., and Hine, A.C., 1977. "Tidal Inlet Variability - Cape Hatteras to Cape Canaveral," Fifth Symposium of Waterway, Port, Coastal and Ocean Engineering, Division of ASCE, Coastal Sediments '77. pp. 543-562.

O'Brien, M. P., 1966. "Equilibrium Flow Areas of Tidal Inlets on Sandy Coasts," Proceedings of the Tenth Coastal Engineering Conference, Vol. 1, pp. 676-686.

O'Brien, M.P., 1975. "Notes on Tidal Inlets on Sandy Coasts," University of California Hydraulic Engineering Laboratory, Report No. HEL-24-5, Berkeley, CA.

O'Brien, M. P., and Dean, R. G., 1972. "Hydraulics and Sedimentary Stability of Coastal Inlets," Proceedings of the Thirteenth Coastal Engineering Conference, Vol. 2, pp. 761-780.

Schuum, S. A., 1977. The Fluvial System, Wiley Interscience. New York: John Wiley and Sons.

Silvestor, R. M., and La Cruz, C. R., 1970. "Pattern Forming Forces in Deltas," Journal of the Waterways and Harbors Division, ASCE, Vol. 96, No. WNZ, pp. 201-217.

Snell, C. M., and Gillespie, R. H., 1973. "Project Drum Inlet: Explosive Excavation in Saturated Sand," U.S. Army, Corps of Engineers, Waterways Experiment Station T.R. No. #-73.5.

Stafford, D. B., 1968. "Development and Evaluation of a Procedure for Using Aerial Photographs to Conduct a Survey of Coastal Erosion." Ph.D. Thesis, Department of Civil Engineering, North Carolina State University, Raleigh, N.C.

U.S. Army, Corps of Engineers, 1973. Shore Protection Manual, Vol. II, Chapter 5, Coastal Engineering Research Center, Ft. Belvois, VA.

U.S. Department of Commerce, NOAA, Nos, 1977. "Tide Tables, High and Low Water Predictions," 1977. East Coast of North and South America including Greenland, Washington, D.C.

U.S. Naval Weather Service Command, 1975. "Summary of Synoptic Meteorological Observations," Vol. 3, North American Coastal Marine Arcs, National Climatic Center, Asheville, N.C.

Walton, T.L., Jr., 1973. "Littoral Drift Computations along the Coast of Florida by Means of Ship Wave Observations," University of Florida Coastal and Oceanographic Engineering Laboratory, Report No. 15.

Yang, C. T., 1976. "Minimum Unit Stream Power and Fluvial Hydraulics," Journal of the Hydraulics Division, ASCE, Vol. 102, No. HY 7, pp. 919-934.

APPENDIX A

FLOURESCENT TRACER STUDY METHODS AND ANALYSIS

APPENDIX A

FLOURESCENT TRACER STUDY METHODS AND ANALYSIS

Tracer Dying Method

The tracer dying technique described by Machemehl, Chambers and Bird (1977) was used in this study. Three thousand pounds of native sand was collected from three locations in the inlet close to the areas where the dyed tracer was to be introduced. The locations are shown in Figure 40. Location SL1 was near grid point N·O (Figure 41) or the north beach. SL2 was near grid point 366 (Figure 43) adjacent to the shoal study area and SL3 was near grid point 300 (Figure 43) adjacent to the shoal study area. Five hundred pounds of tracer sand of each color was produced. The sand from SL1 was dyed Arc Yellow and Signal Green. Sand from Location SL2 was dyed Fire Orange and Horizon Blue. Sand from Location SL3 was dyed Blaze Orange and Lightening Yellow. Specific gravity test and sieve analysis were used to check the validity of the tracer method. It was found that the dying process did not change the particle size distribution of the sand. Specific gravities of the dyed and undyed sand were 2.6 and 2.7, respectively. From these tests, it can be said that the dying process did not alter the basic sediment properties of the sand.

Tracer Introduction and Sampling

Prior to introduction of the tracer into the two energy zones, a grid was laid out on the study shoal and on the beach north and south of the inlet. The locations of these grids are shown in Figure 40. Blow-ups of the individual grids are shown in Figures 41, 42, and 43. The grid in the high energy zone on the north and south beach was set by locating numbered survey stakes just above the high water line on the beach. An attempt was made to locate grid points in the surf zone by using 50 pound concrete anchors and one gallon containers marked to indicate the grid location. This was a failure because the waves and currents quickly moved the anchors down the beach. During the sampling the seaward distances from the numbered stakes were estimated. The north and south beach grids were 1400 and 900 feet long, respectively, and core samples were taken up to 100 feet seaward.

The grid system for the low energy area, hereafter called the shoal study area, was a 700 feet square area marked at 100 feet intervals with 50 pound concrete anchors and one gallon container marked to indicate the location. These grid markers stayed in place with no problems. The location of all grid points was surveyed with a transit and stadia rod using Corps of Engineers horizontal control points for reference.

The tracer was introduced on the north and south beaches by raking it into the beach approximately one hour before high tide. On the shoal study area the tracer was introduced along grid lines in

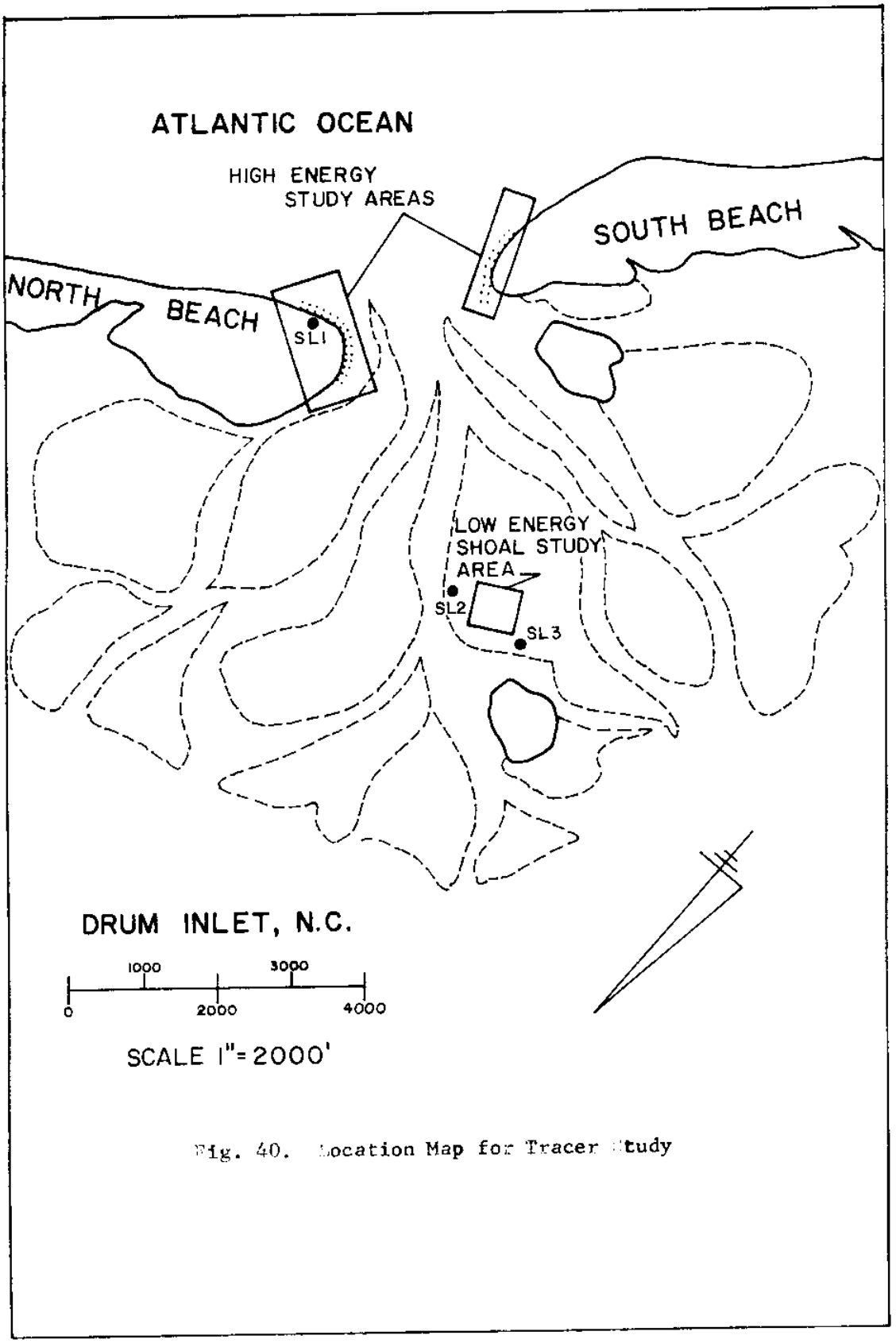

Fig. 40. Location Map for Tracer Study

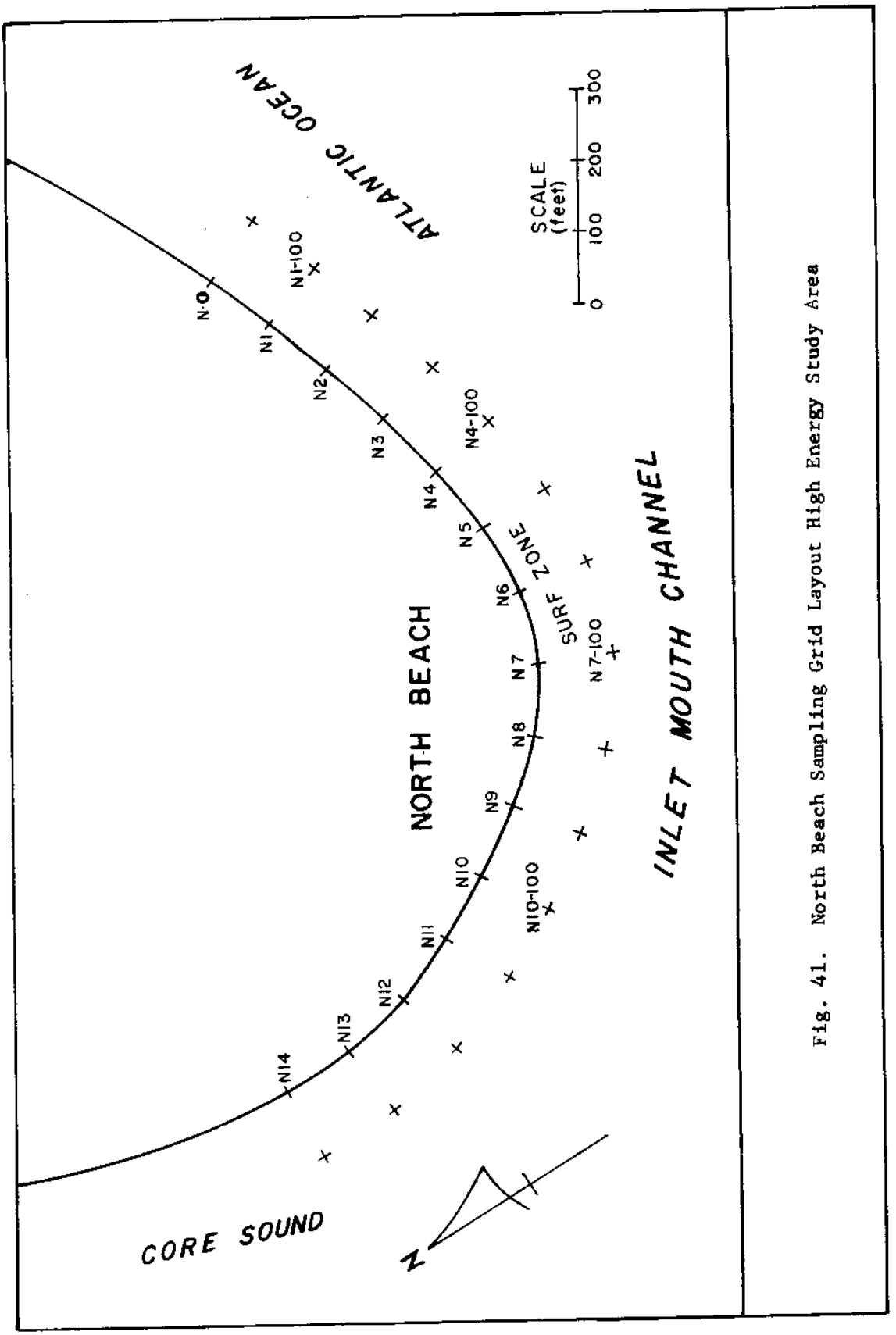

Fig. 41. North Beach Sampling Grid Layout High Energy Study Area

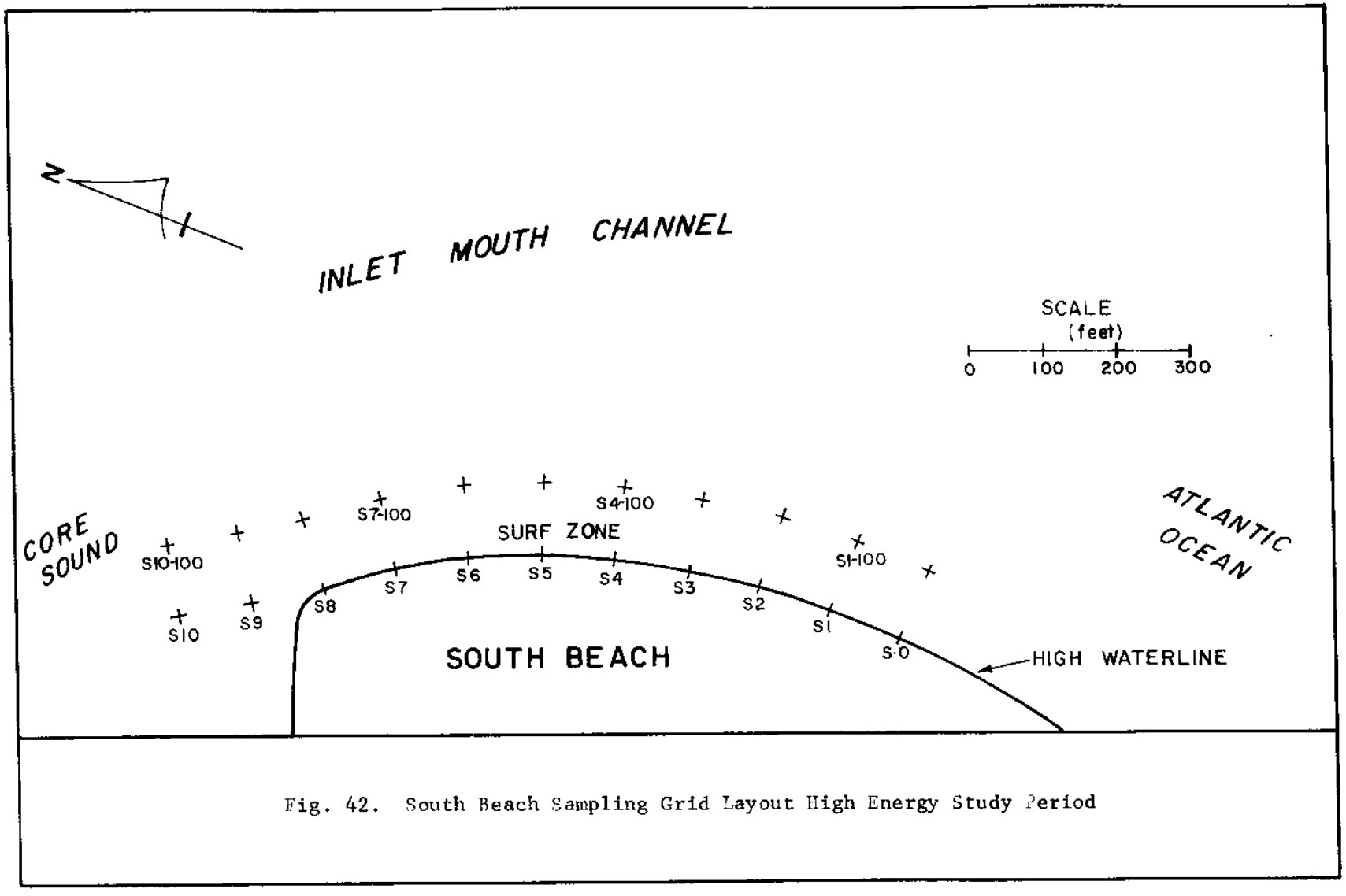

Fig. 42. South Beach Sampling Grid Layout High Energy Study Period

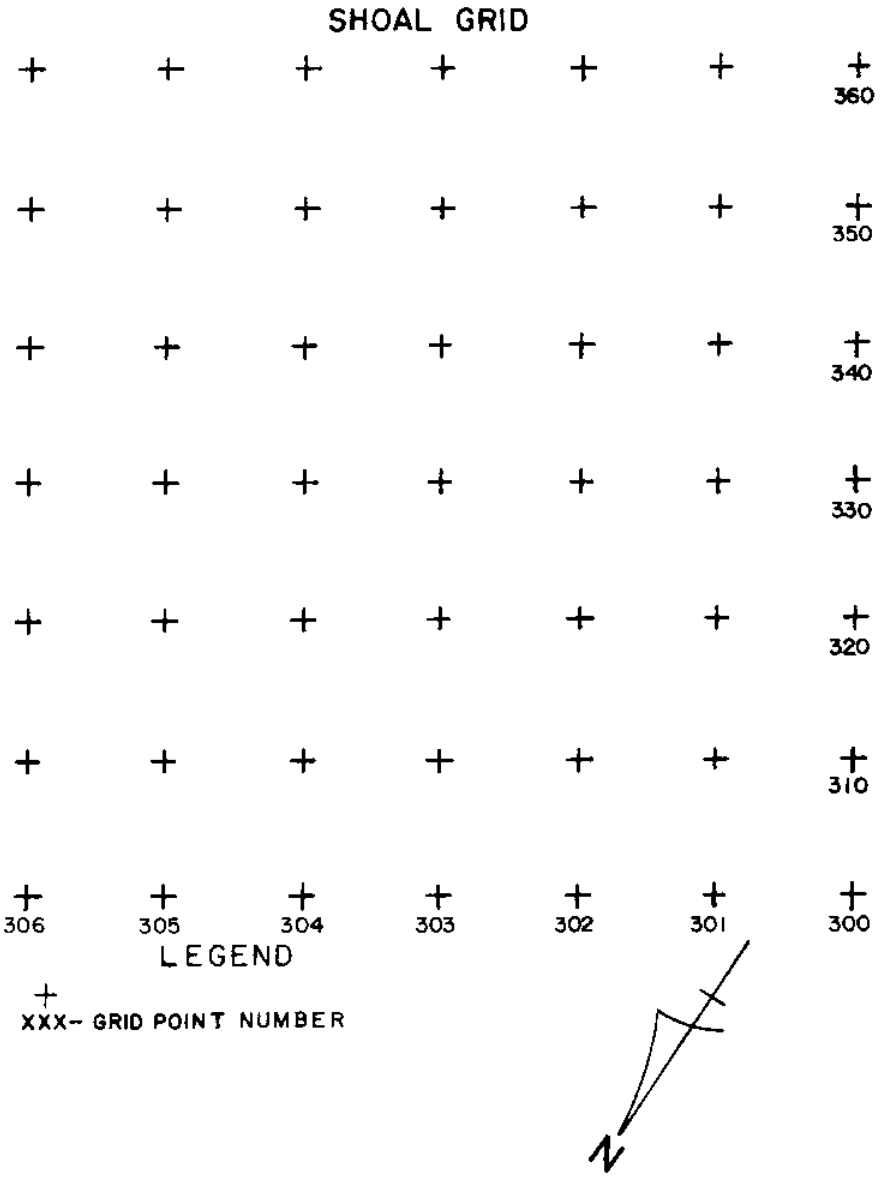

Fig. 43. Grid Layout for Shoal Study Area

50 pound cold water soluable bags. The bags quickly dissolved and released the tracer.

Sampling over the grids was done by forcing a 2-inch diameter, plexiglass, cylindrical tube into the bed approximately 4-6 inches deep and removing a core sample. The method was chosen because it was necessary to account for the incorporation of the tracer sand into the bed. Each sample was approximately 13 cubic inches and weighed approximately 1.0 pounds after drying. Core sampling on the north and south beaches was near each grid stake and at estimated distances from the stakes into the surf-zone. Sampling over the shoal study area was near each grid point and halfway between grid points.

The analysis of the core samples consisted of air drying the sand, spreading each sample out on a pan under a long wave ultraviolet light and counting the number of tracer particles of each color present. The results were recorded according to sampling location, time of sampling period and tracer color. Due to the tremendous number of samples that were accumulated, those taken at the half points on the shoal study area were not analyzed.

A timetable for the introduction of the tracer material into the study areas and the following sampling periods is shown in Table 16. The introduction and sampling times are referenced with the high and low ocean tide times.

TABLE 16

TIME TABLE OF OCEAN TIDES AND INTRODUCTION AND SAMPLING OF TRACER

Date/Time	Activity
August 18	
0239	Low Tide
0902	High Tide
1200	Introduced Horizon Blue Tracer
August 19	
Bad Weather - No Work	
0322	Low Tide
0951	High Tide
1554	Low Tide
2200	High Tide
August 20	
0410	Low Tide
1047	High Tide
1000-1200	Introduced Blaze Orange, Lightening Yellow and Fire Orange Tracer
1600	Low Tide
1615-1730	Sampled Shoal Area
2255	High Tide
August 21	
0506	Low Tide
1100-1200	Sampled Shoal Area
1149	High Tide
1300-1700	Sampled Over Shoal
1755	Low Tide
2358	High Tide
August 22	
0607	Low Tide
1140	Introduced Signal Green Tracer on South Beach
1200	Introduced Arc Yellow Tracer on North Beach
1208-1340	Sampled North Beach
1135-1450	Sampled South Beach
1255	High Tide
1902	Low Tide
August 23	
0107	High Tide
0715	Low Tide
0820-0900	Sampled North Beach
0950-1010	Sampled South Beach
0810-0940	Sampled Shoal Area
1402	High Tide
2009	Low Tide

Tracer Test Analysis - Low Energy Study Area

August 18 sampling period

After introduction of horizon blue tracer along grid points 342-344 on the shoal study area, the material appeared to move along troughs of bed ripple formations. There was no clumping of the tracer. After 1.5 hours, core samples showed tracer incorporated into the bed. After approximately 2 hours, the tracer had assumed the forms of the secondary bedforms. There was visual evidence that the combination of small waves and current was causing some of the tracer to become suspended in the flow across the shoal area.

Horizon blue. Data from sampling approximately 2 hours after the introduction showed very little movement. There was some evidence of tracer movement in the northwest (flood) direction. No tracer was found that would indicate any ebb movement. Data from the sampling period is shown in Figure 44.

August 20 sampling period

Blaze orange tracer was introduced between grid points 322 and 324, lightening yellow between 313 and 333 and fire orange between 362 and 364.

Fire orange. The fire orange tracer was introduced only to measure flood movement. After approximately 5 hours, there was a pattern of flood movement. There is only trace evidence, but a tongue-like pattern was evident. This is illustrated by the fire orange data in Figure 45.

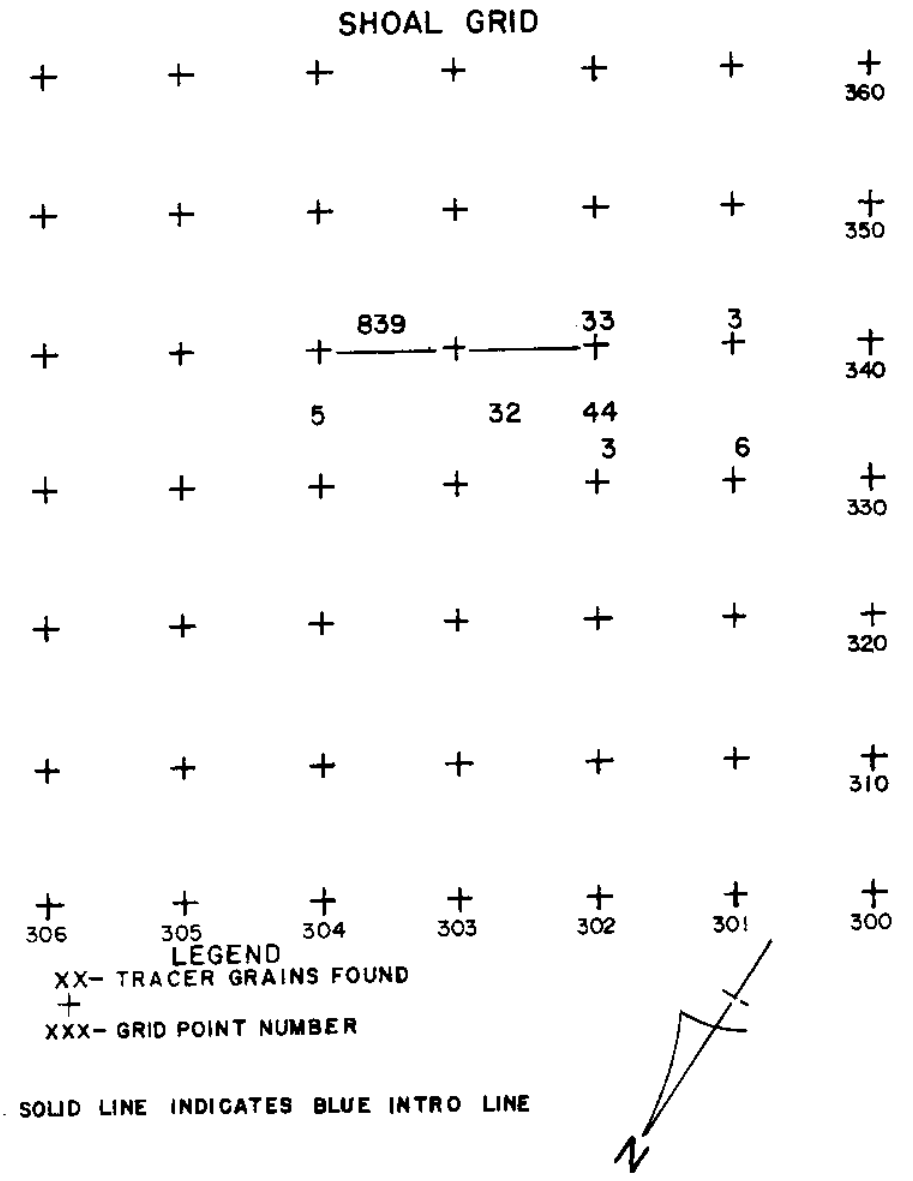

Fig. 44. Horizon Blue Tracer Found During Sampling on August 18 between 1100 and 1400 hours

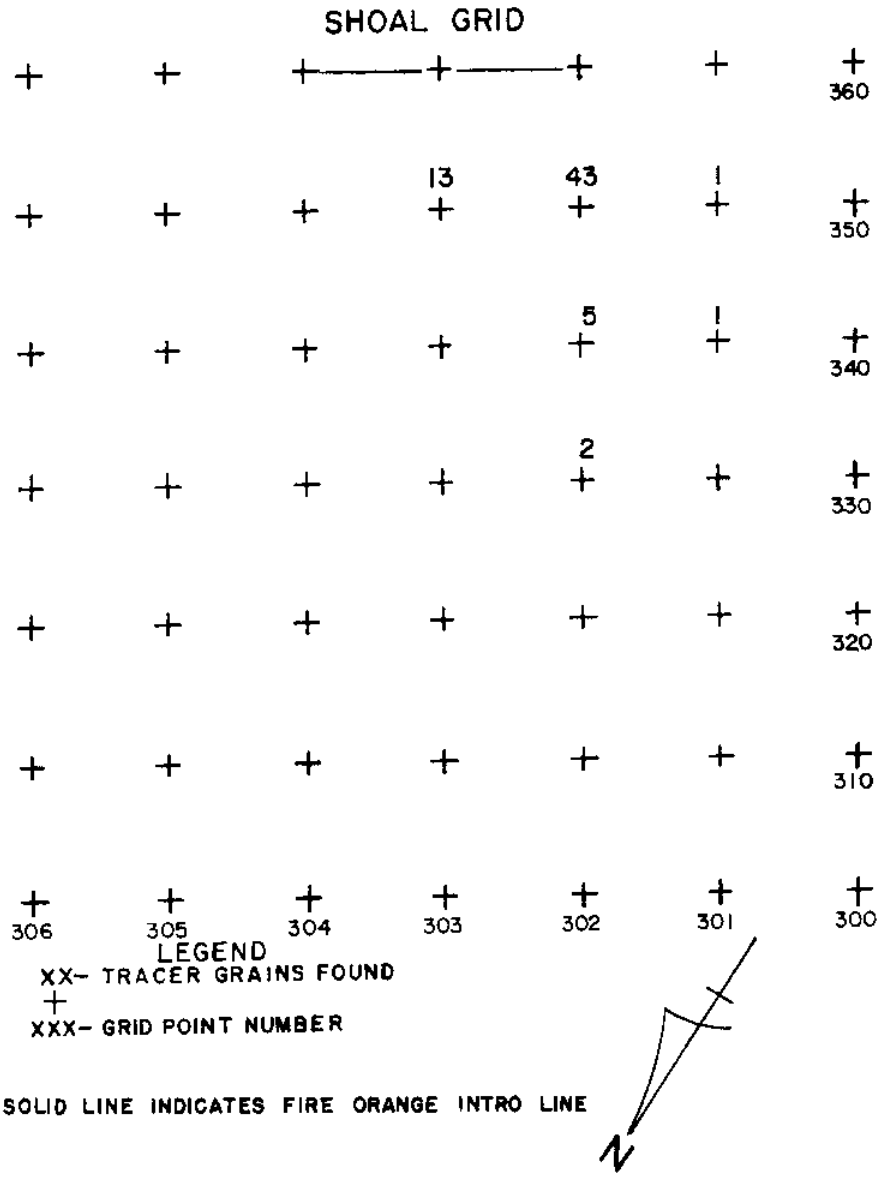

Fig. 45. Fire Orange Tracer Found During Sampling on August 20 between 1615 and 1730 hours

Blaze Orange. Approximately five hours after introduction there was evidence of ebb and flood movement. There was substantial movement in the ebb direction. The movement that occurred was probably in suspension. There were no patterns to the movement of the tracer by this sampling period. Data for the blaze orange movement is presented in Figure 46.

Lightning Yellow. After approximately five hours, the movement of lightning yellow tracer was only in trace amounts. This data is shown in Figure 47. There is evidence of both flood and ebb movement.

Horizon Blue. There was not enough blue tracer found during this sampling period to indicate any substantial movement or patterns of movement beyond those found during the August 18 sampling period. Horizon blue data for this period is presented in Figure 48.

August 21 sampling period

Fire Orange. After two complete tidal cycles, a definite pattern of movement of the tracer was evident. Figure 49 is the data from the earlier of two samplings during this period and one can see a definite flood oriented "tongue-like" pattern of tracer across the shoal area. There is also evidence of some northerly trace movement which is also flood oriented. There is continued evidence of the previous patterns in data of the sampling later on 21 August. As shown in Figure 50, a pattern of northerly movement in trace amounts had developed. After two and one-half tidal cycles, the movement patterns of the fire orange tracer indicated a definite sand body moving across the shoal study area.

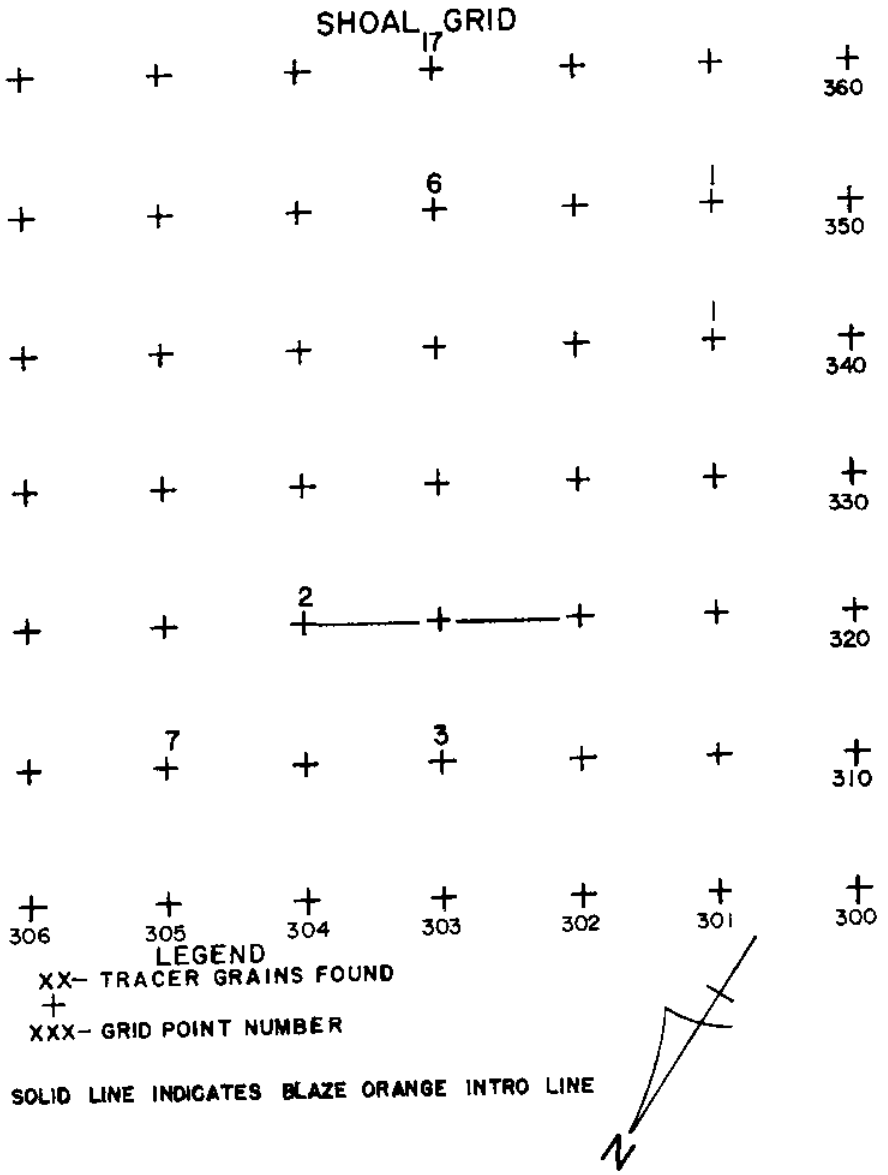

Fig. 46. Blaze Orange Tracer Found During Sampling on August 20 between 1615 and 1730 hours

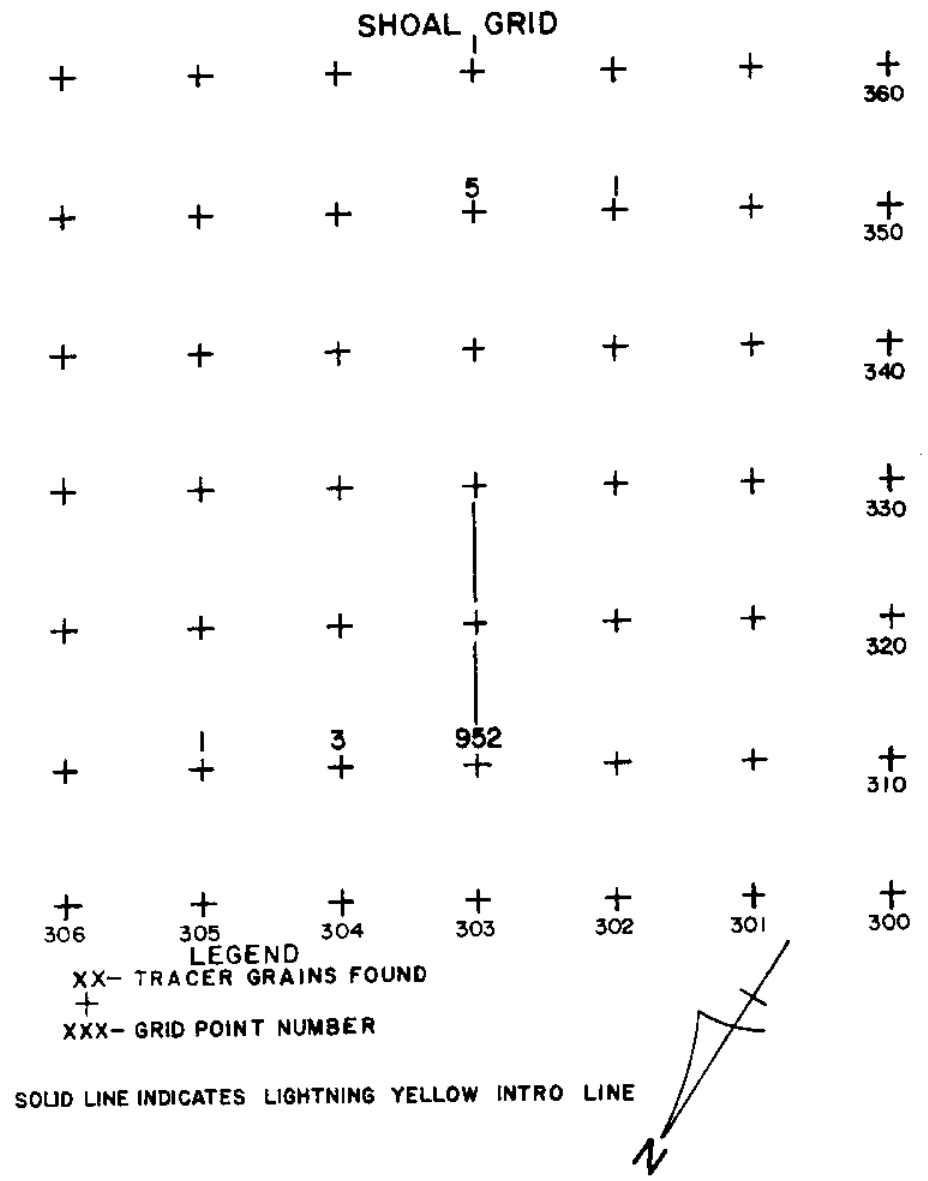

Fig. 47. Lightning Yellow Tracer Found During Sampling on August 20 between 1615 and 1730 hours

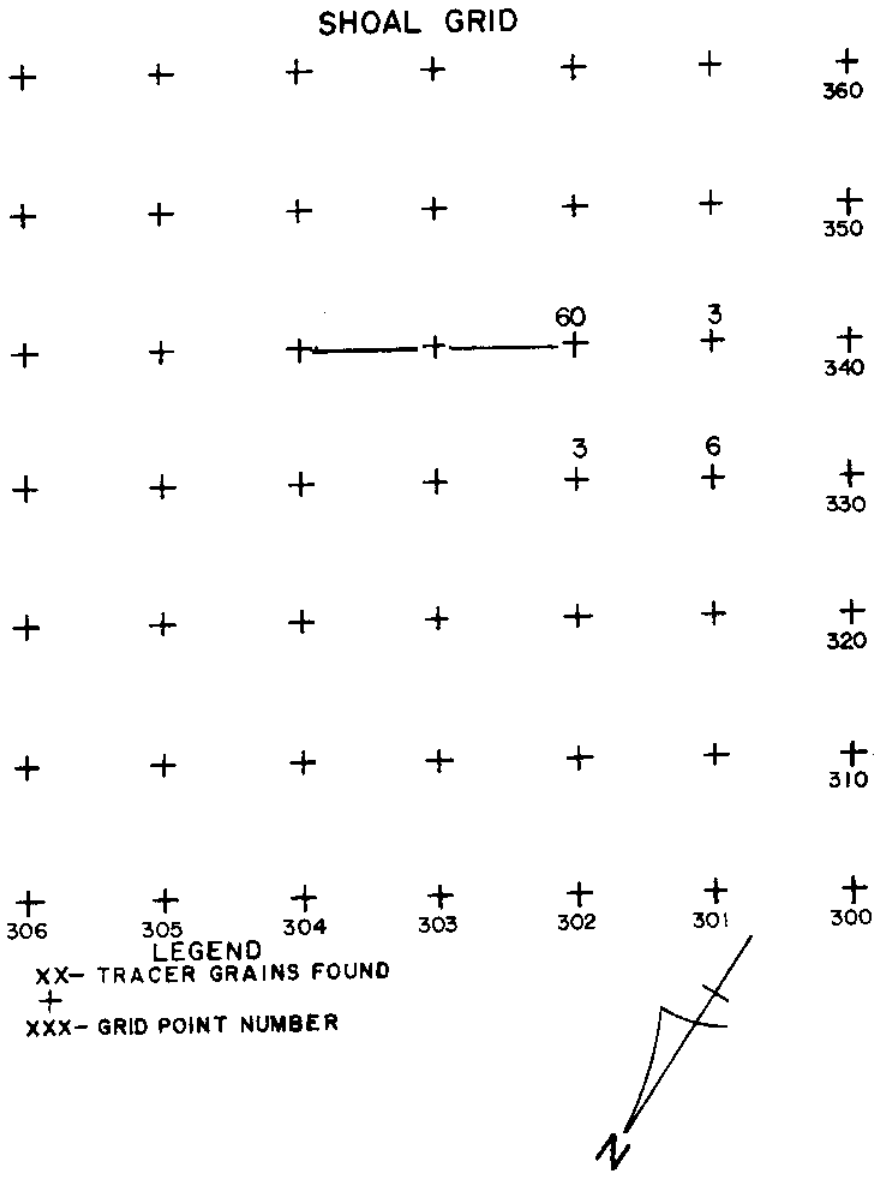

Fig. 48. Horizon Blue Tracer Found During Sampling on August 20 between 1615 and 1730 hours

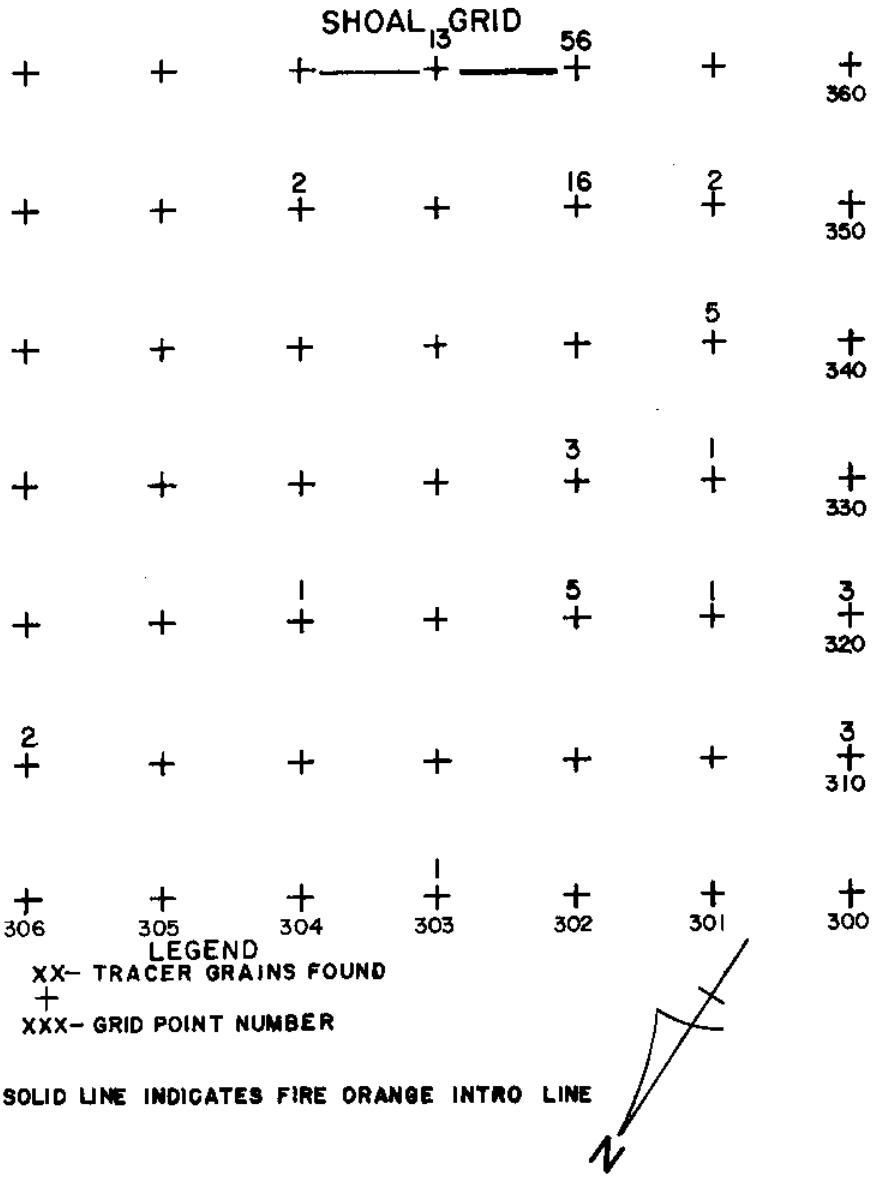

Fig. 49. Fire Orange Tracer Found During Sampling on August 21 between 1100 and 1300 hours

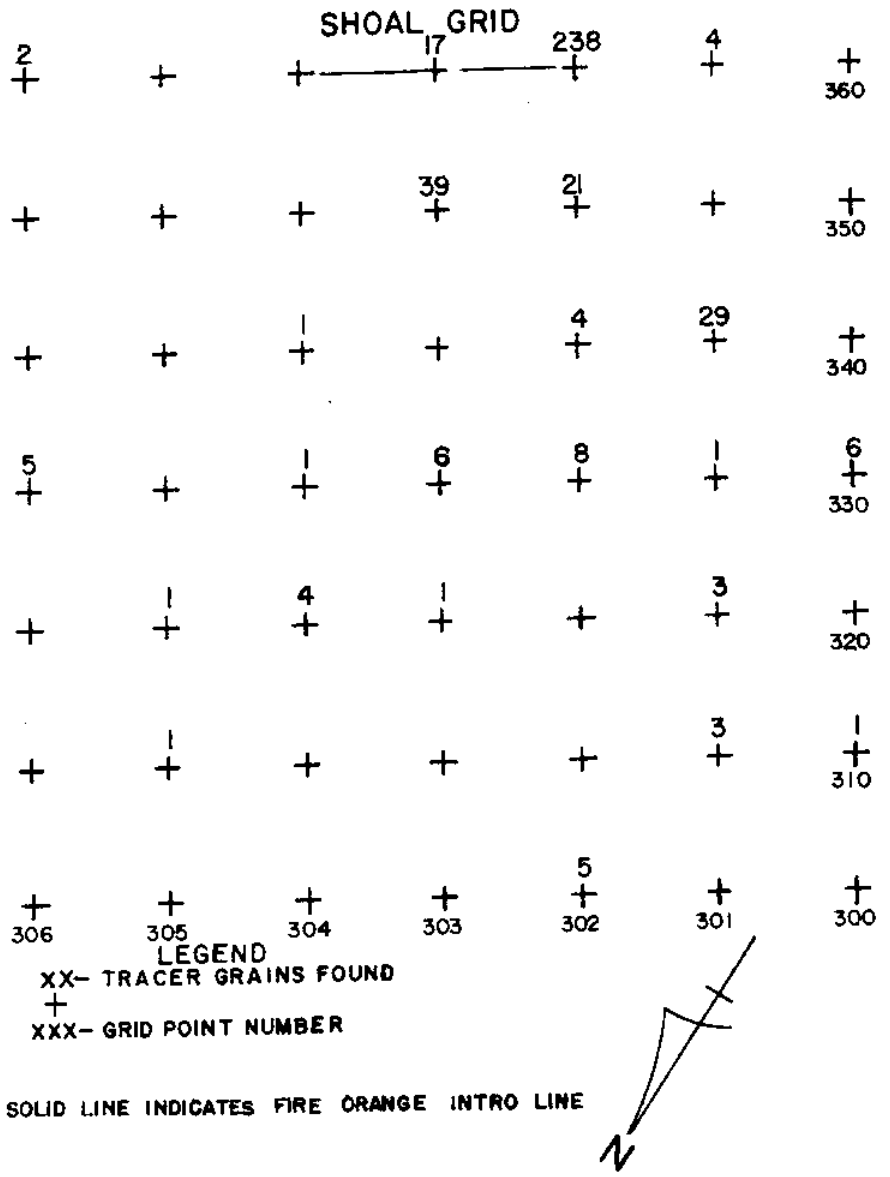

Fig. 50. Fire Orange Tracer Found During Sampling on August 21 between 1730 and 1945 hours

Blaze Orange. The sampling data from the 1100 to 1300 sampling period indicated tracer movement in both ebb and flood directions. Substantial amounts of tracer were found south of the intro line, forming a tongue-like pattern oriented in a southerly direction. Some trace amounts were found east of the introduction line. The data in Figure 51 indicates that, after two complete tidal cycles, the blaze orange was well dispersed with evidence of an ebb oriented body of sand moving south and a flood oriented sand body oriented northwest of the intro line. Only trace amounts of tracer were found in samples collected during the 1730 to 1945 sampling period. As indicated in Figure 52, there was no evidence of the same movement patterns present in the earlier samples on August 21.

Lightning Yellow. Data from the 1100 to 1300 sampling period indicated wide dispersion of the tracer. The dominate direction appeared to be westerly, but trace amounts were found in all parts of the grid. Figure 53 shows the wide spread dispersion of the lightning yellow tracer after two tidal cycles. The sampling from 1730 to 1945 showed a net westerly movement of tracer. Shown in Figure 54, the westerly orientation of the tracer confirmed the earlier dominate westerly direction.

Horizon Blue. Data from the 1100 to 1300 sampling period showed dispersion of the blue tracer over the grid. Figure 55 shows stronger movement in the northwest flood oriented direction. There was a northwest oriented pattern indicated by the tracer found in the 1730 to 1945 sampling. This pattern is evident in Figure 56. This pattern confirms the northwest movement found in the earlier sampling.

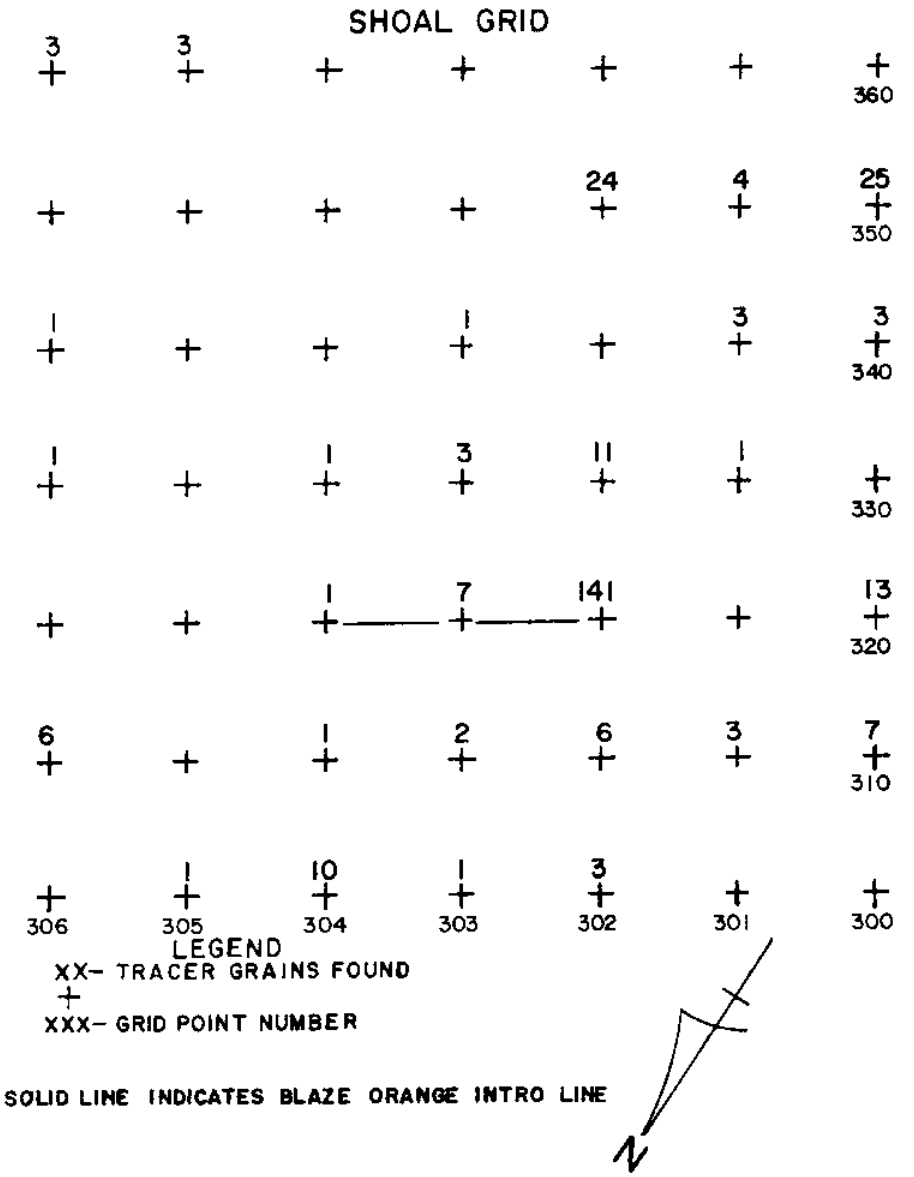

Fig. 51. Blaze Orange Tracer Found During Sampling on August 21 between 1100 and 1300 hours

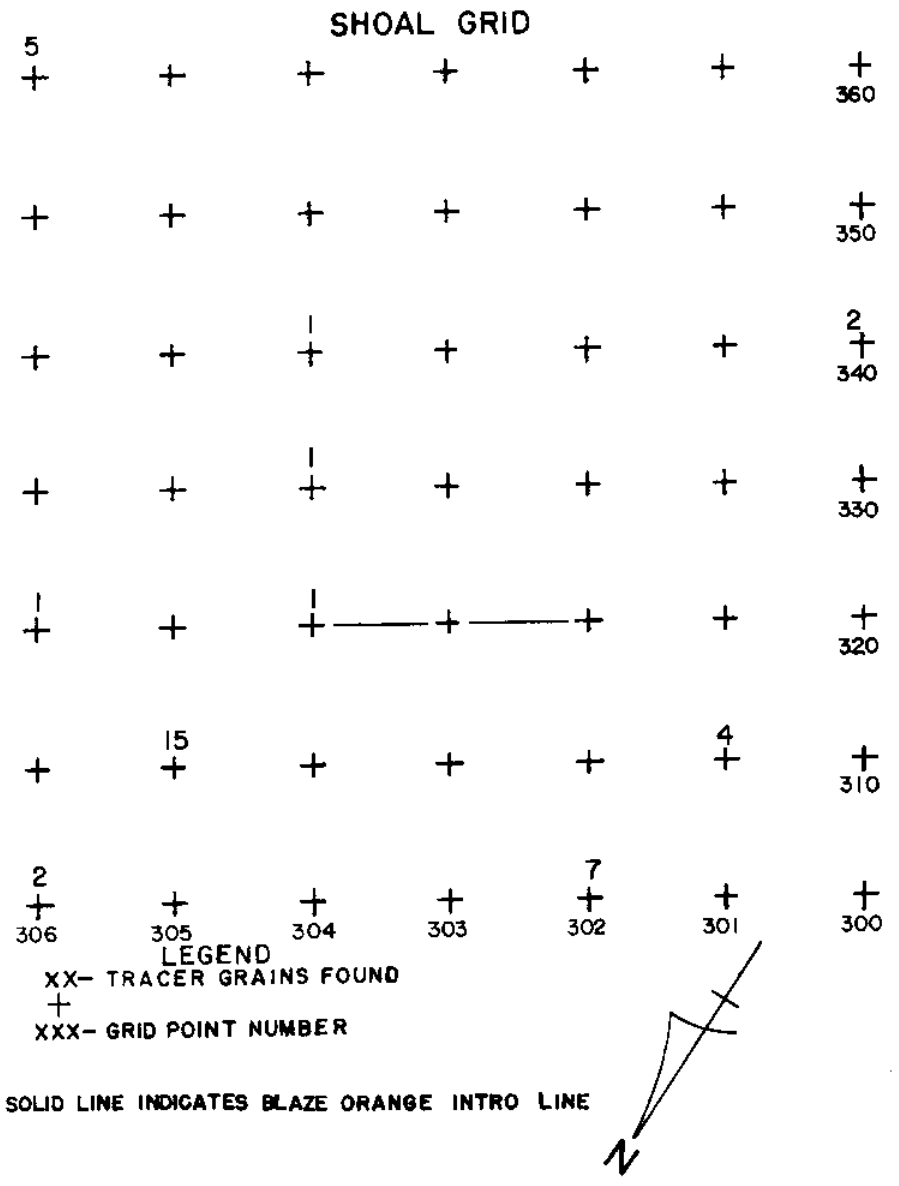

Fig. 52. Blaze Orange Tracer Found During Sampling on August 21 between 1730 and 1945 hours

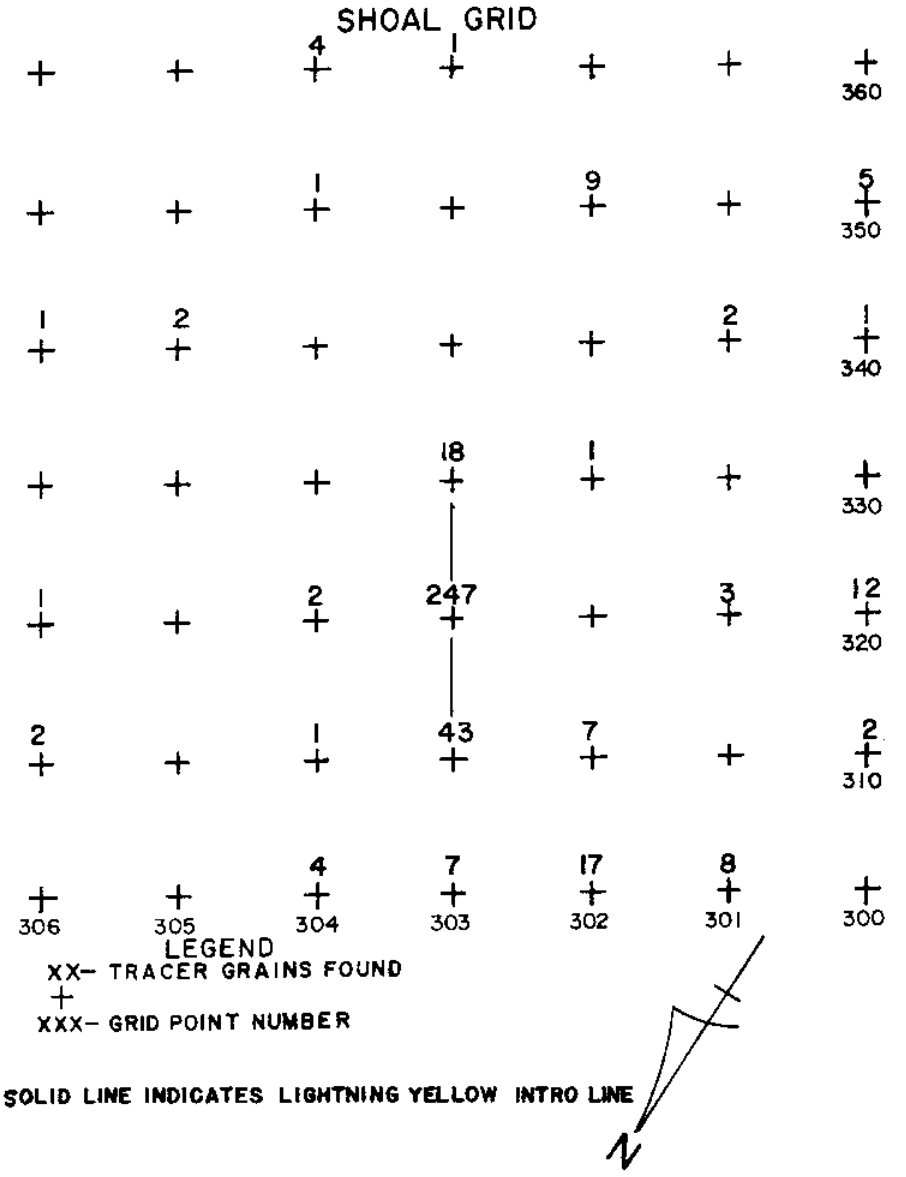

Fig. 53. Lightning Yellow Tracer Found During Sampling on August 21 between 1100 and 1300 hours

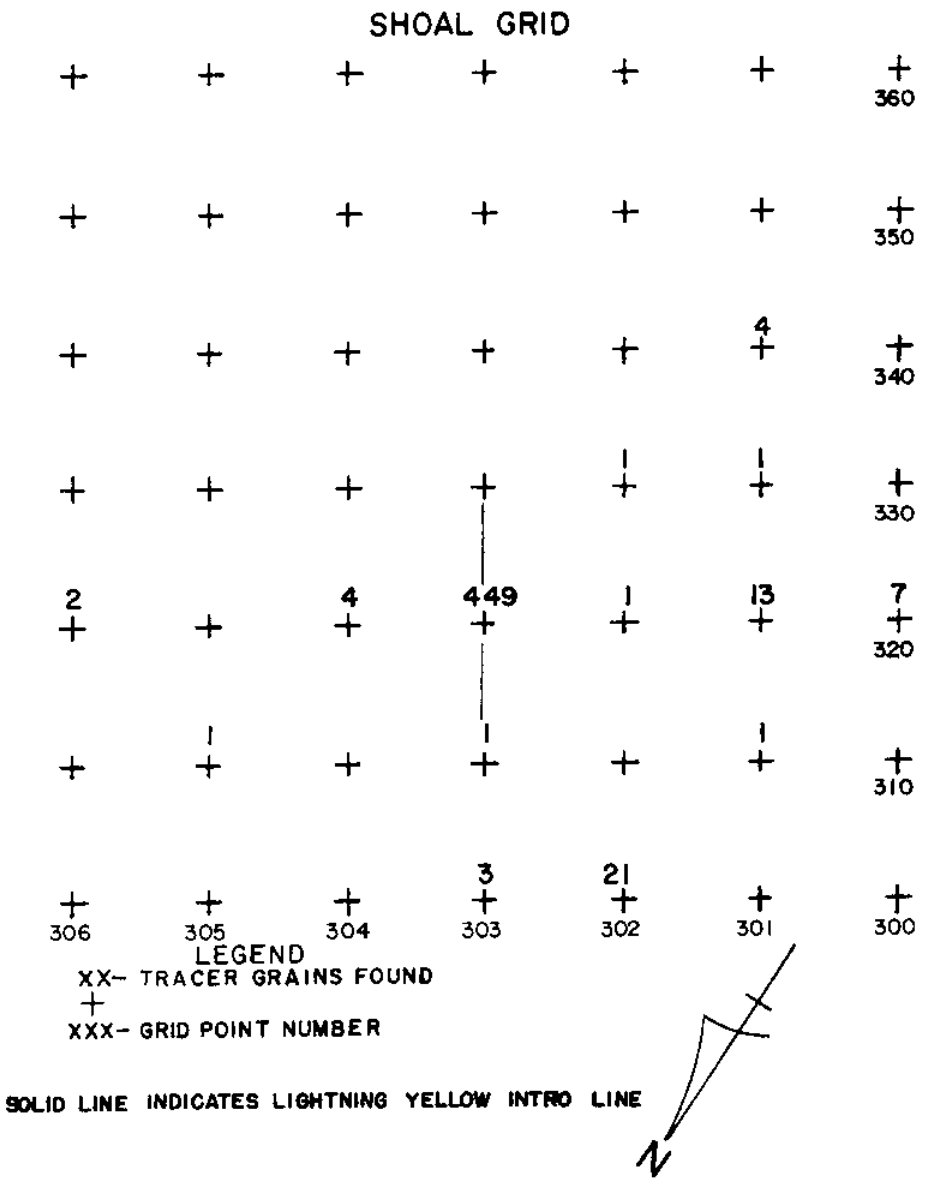

Fig. 54. Lightning Yellow Tracer Found During Sampling on August 21 between 1730 and 1945 hours

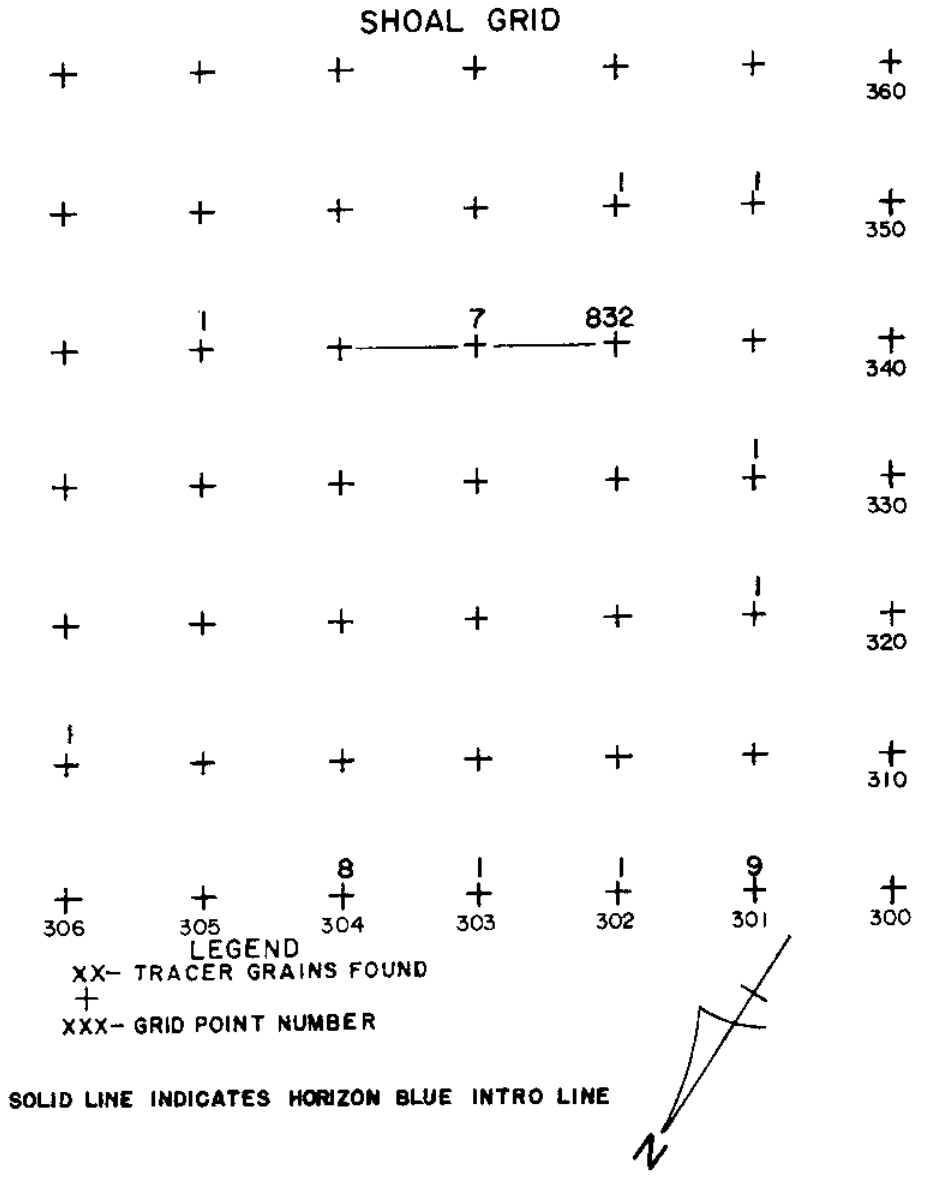

Fig. 55. Horizon Blue Tracer Found During Sampling on August 21 between 1100 and 1300 hours

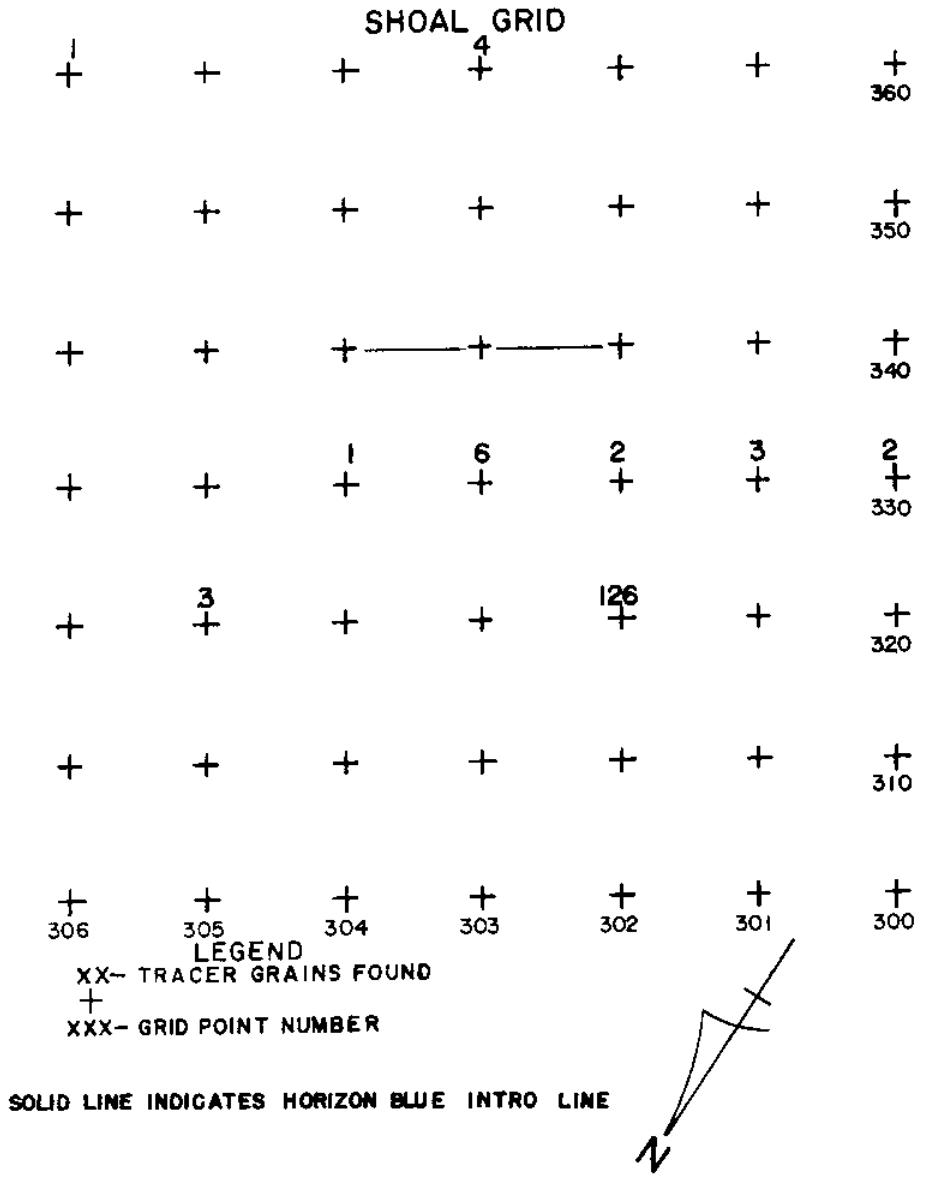

Fig. 56. Horizon Blue Tracer Found During Sampling on August 21 between 1730 and 1945 hours

August 23 sampling period

Fire Orange. After five tidal cycles the northwest oriented tongue of tracer was evident. Figure 57 shows the dispersion of the fire orange tracer. The pattern of movement was unchanged from the previous samplings.

Blaze Orange. Data from the August 23 sampling showed flood oriented movement of tracer in the northwesterly direction and ebb oriented movement in the southerly and southeasterly directions. Figure 58 shows the tracer distributions that indicates equal movement in both ebb and flood directions.

Lightning Yellow. Tracer material was found at only eight locations during this sampling period. It can be seen in Figure 59 that no patterns are evident, but there is evidence of movement in both ebb and flood directions.

Horizon Blue. Data from the August 23 sampling showed tracer found at six locations. No tracer was found south or southeast of the intro line. Only trace amounts were found in the northeasterly direction, indicating a flood dominance. Figure 60 shows the blue tracer found during this sampling period.

Tracer Test Analysis - North Beach High Energy Study Area

August 22 sampling period

After introduction of the Arc Yellow tracer along the N·D line perpendicular to the beach, there was immediate transport of tracer down the beach towards the inlet in large quantities. The rapid movement is represented by tracer counts found after introduction in

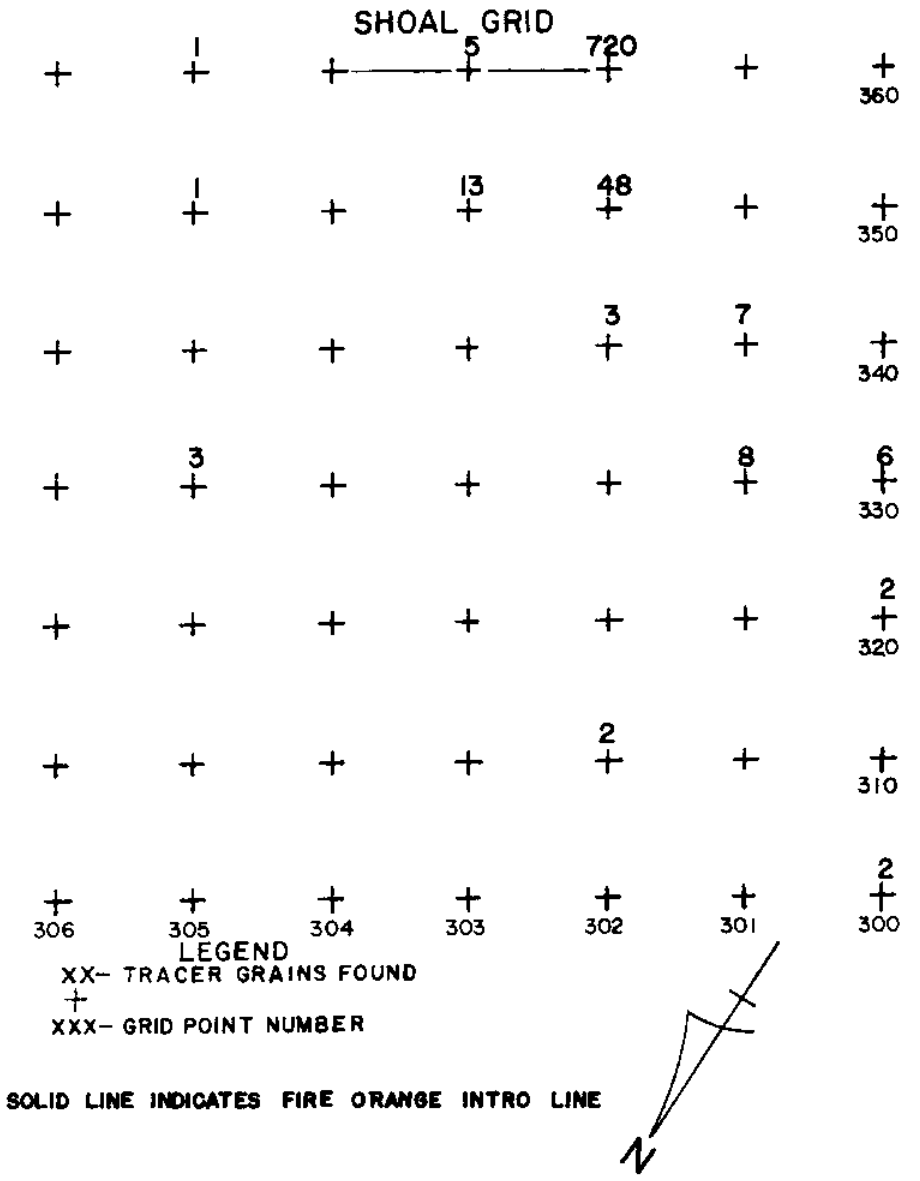

Fig. 57. Fire Orange Tracer Found During Sampling on August 23 between 0810 and 0945 hours

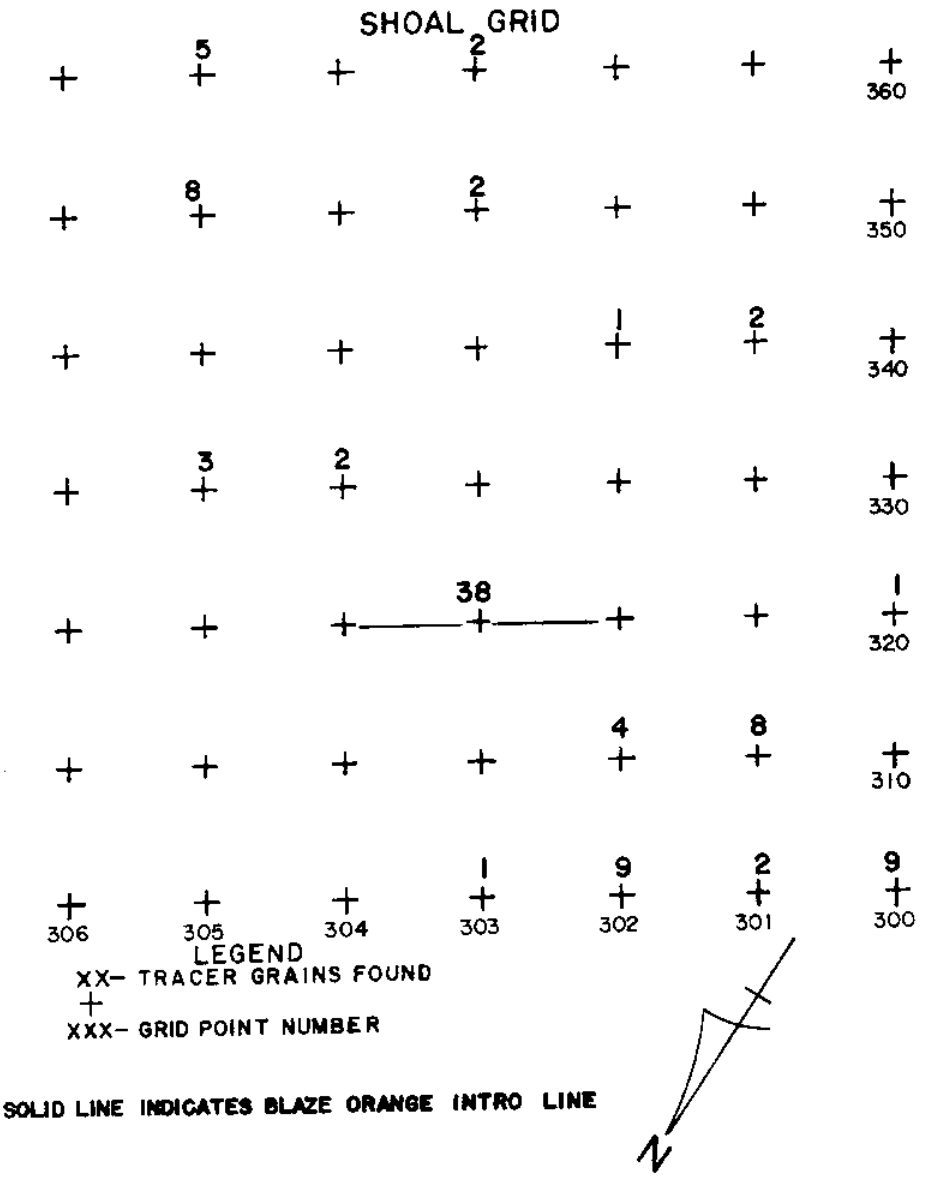

Fig. 58. Blaze Orange Tracer Found During Sampling on August 23 between 0810 and 0945 hours

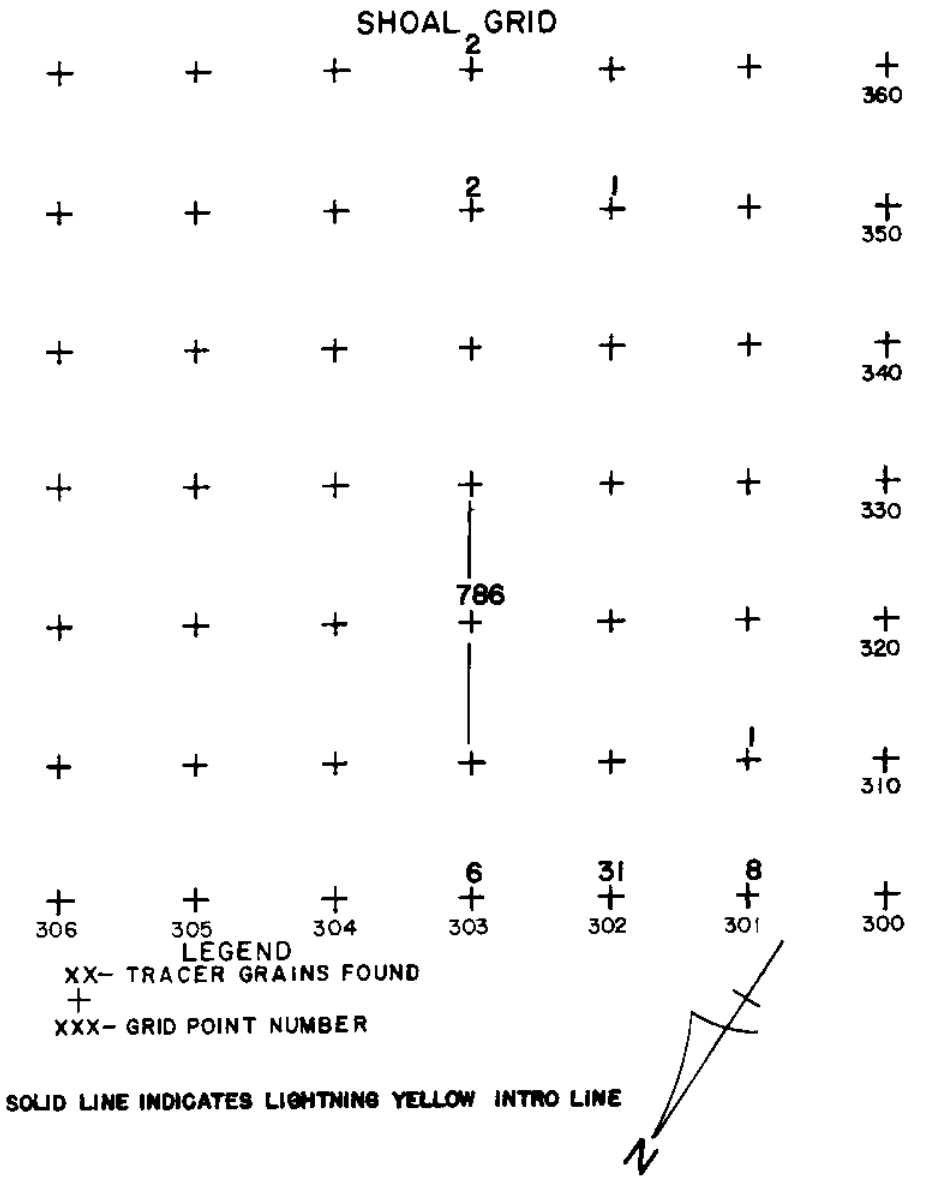

ig. 59. Lightning Yellow Tracer Found During Sampling on August 23 between 0810 and 0945 hours

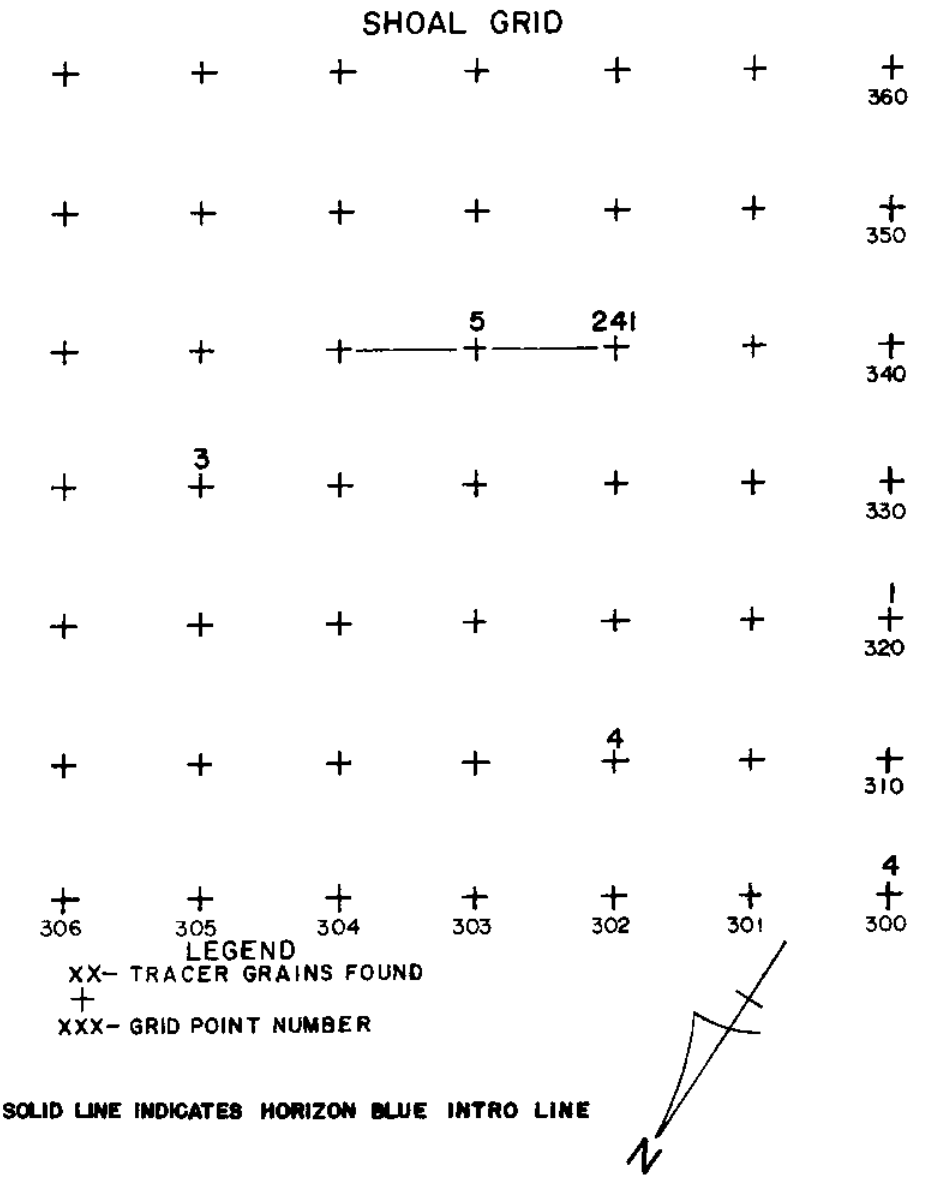

Fig. 60. Horizon Blue Tracer Found During Sampling on August 23 between 0810 and 0945 hours

Figure 61. Movement was mainly in suspension. There was a tendency for the sediment to remain on top of the water, not breaking the surface tension. This would account for the quantities of tracer found. As illustrated in Figure 62, the tracer dispersed further into the surf zone as it moved down the beach. Data from the final sampling on August 22 from 1518 to 1618 showed continued rapid movement toward the inlet throat. The tracer was more concentrated further out in the surf zone than in the two previous samplings. There was no evidence at that time of the movement of the tracer as a sand body (Figure 63).

Of special interest was the presence of fire orange trace particles in samples taken on the north beach grid during the 1518 to 1618 sampling period. This indicated that material from the shoal moved in suspension out the inlet in the ebb currents. The locations where the fire orange tracer was found are shown in Figure 64.

August 23 sampling period

After one and one-half tidal cycles, there was uniform distribution of tracer down the beach in the surf zone between 60 and 100 feet from the grid stakes. As seen in Figure 65, there was an absence of tracer particles on the introduction line, only small numbers for the first 200 feet and last 100 feet, and a fairly even distribution between these points. These factors would indicate the movement of the tracer as a sand body toward the inlet throat.

As in the sampling period of August 22, trace amounts of fire orange tracer were found on the north beach. the locations of the fire orange tracer particles are shown in Figure 66.

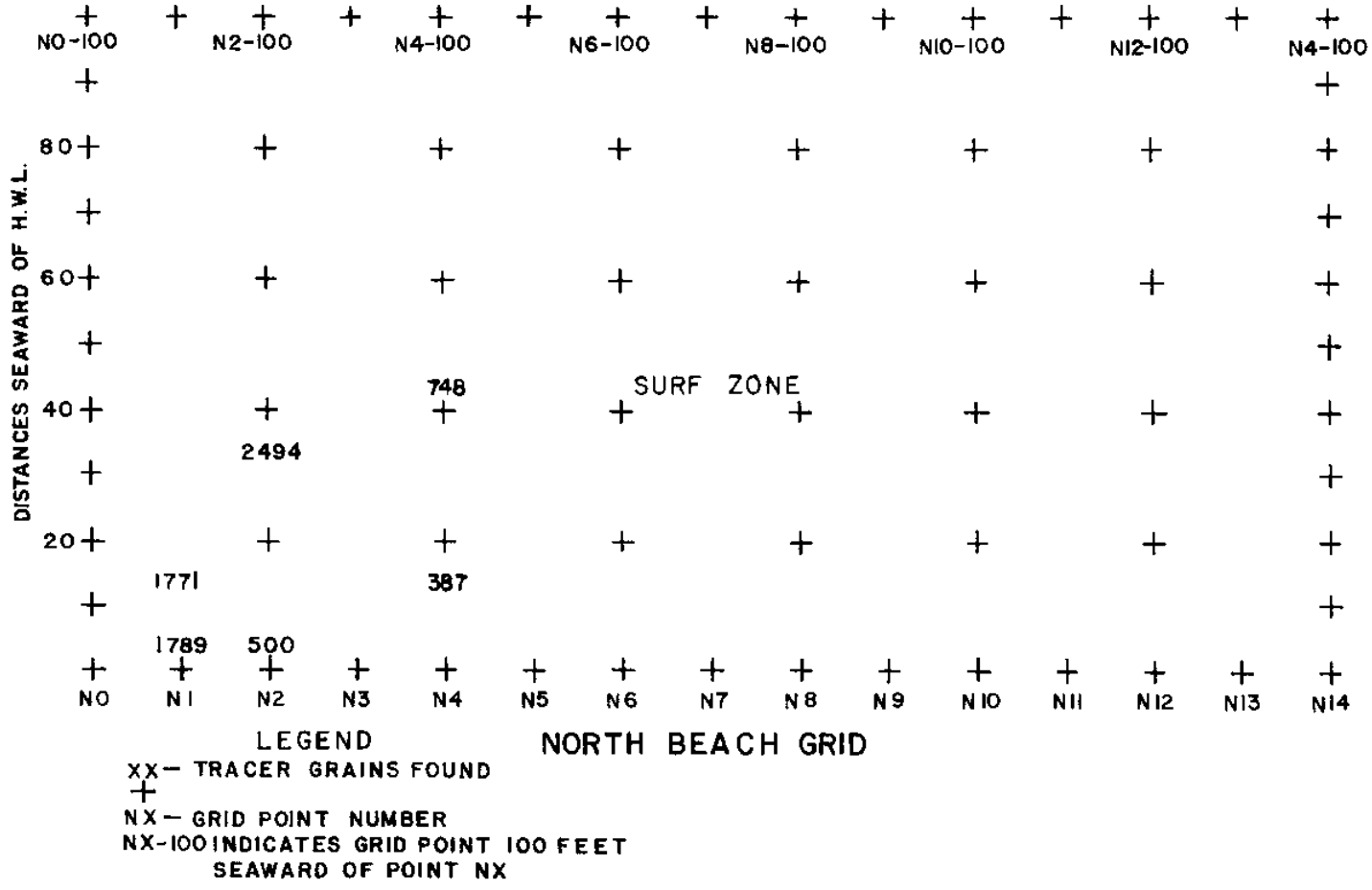

Fig. 61. Arc Yellow Tracer Found on the North Beach Grid on August 22 between 1208 and 1340 hours

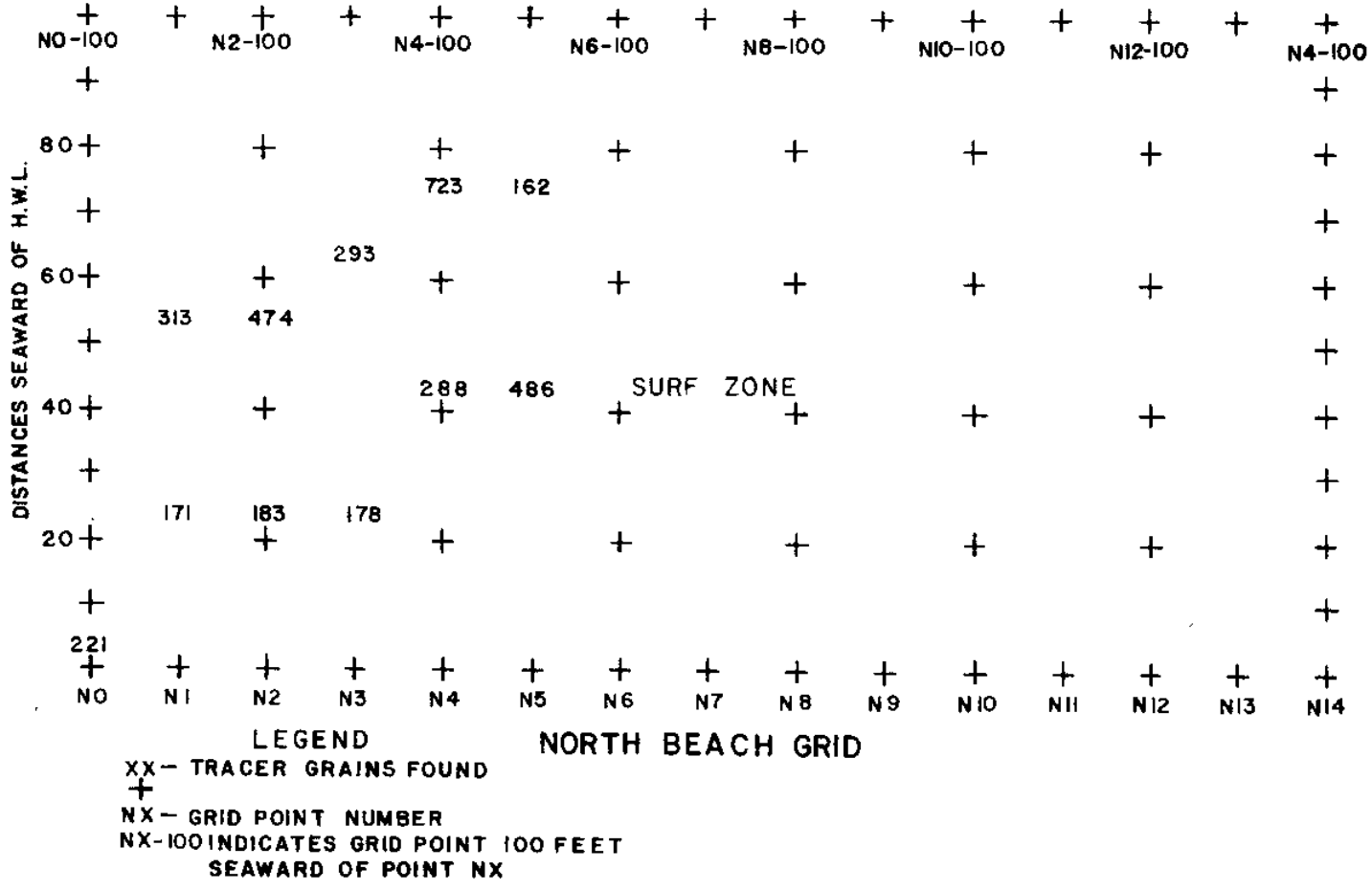

Fig. 62. Arc Yellow Tracer Found During Sampling on August 22 between 1320 and 1340 hours

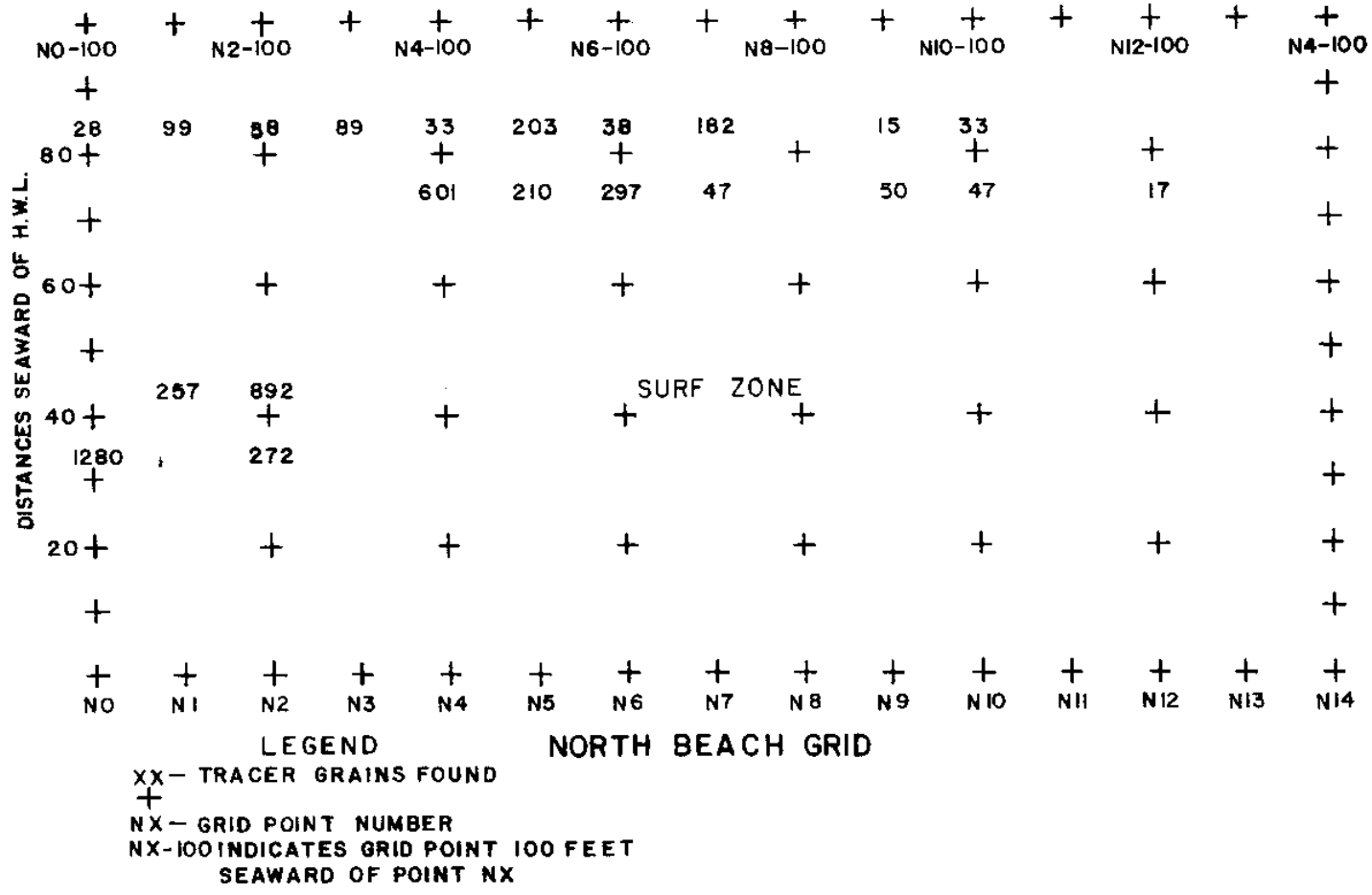

Fig. 63. Arc Yellow Tracer ound During ampling on August 22 between 1518 and 1618 hours

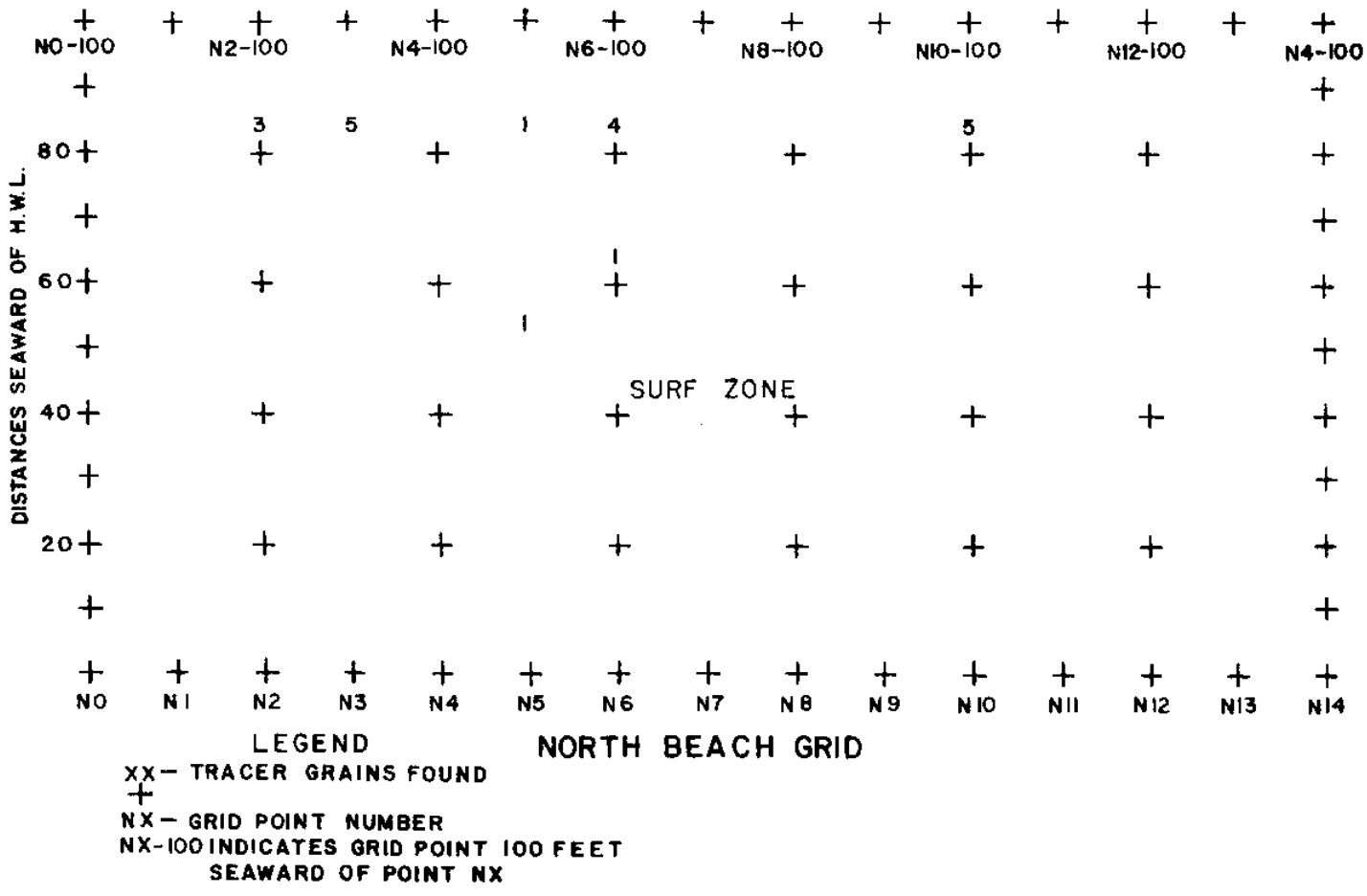

Fig. 64. Fire Orange Tracer Found During Sampling on August 22 between 1518 and 1618 hours

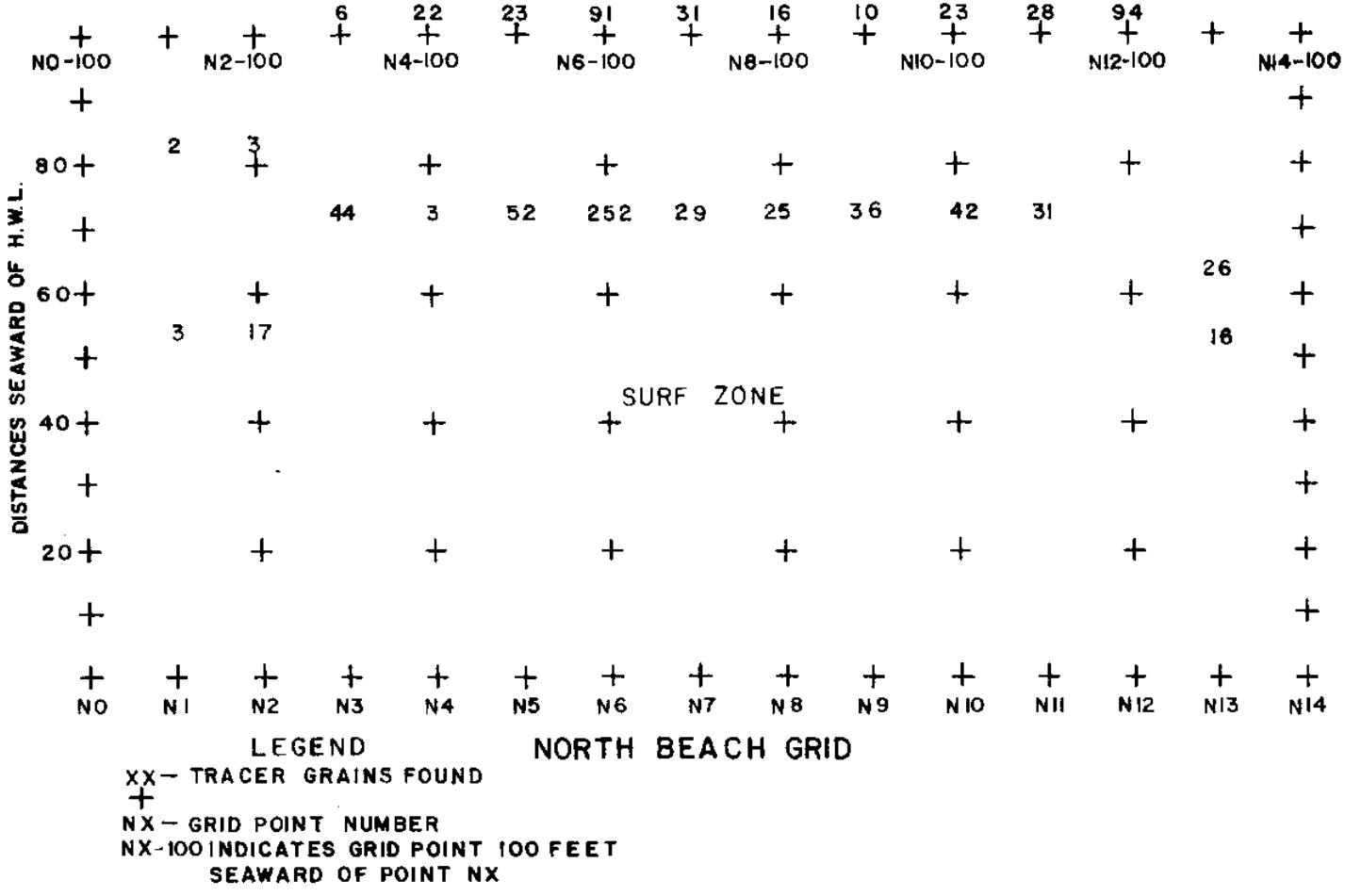

Fig. 65. Arc Yellow Tracer Found During Sampling on August 23 between 0820 and 0900 hours

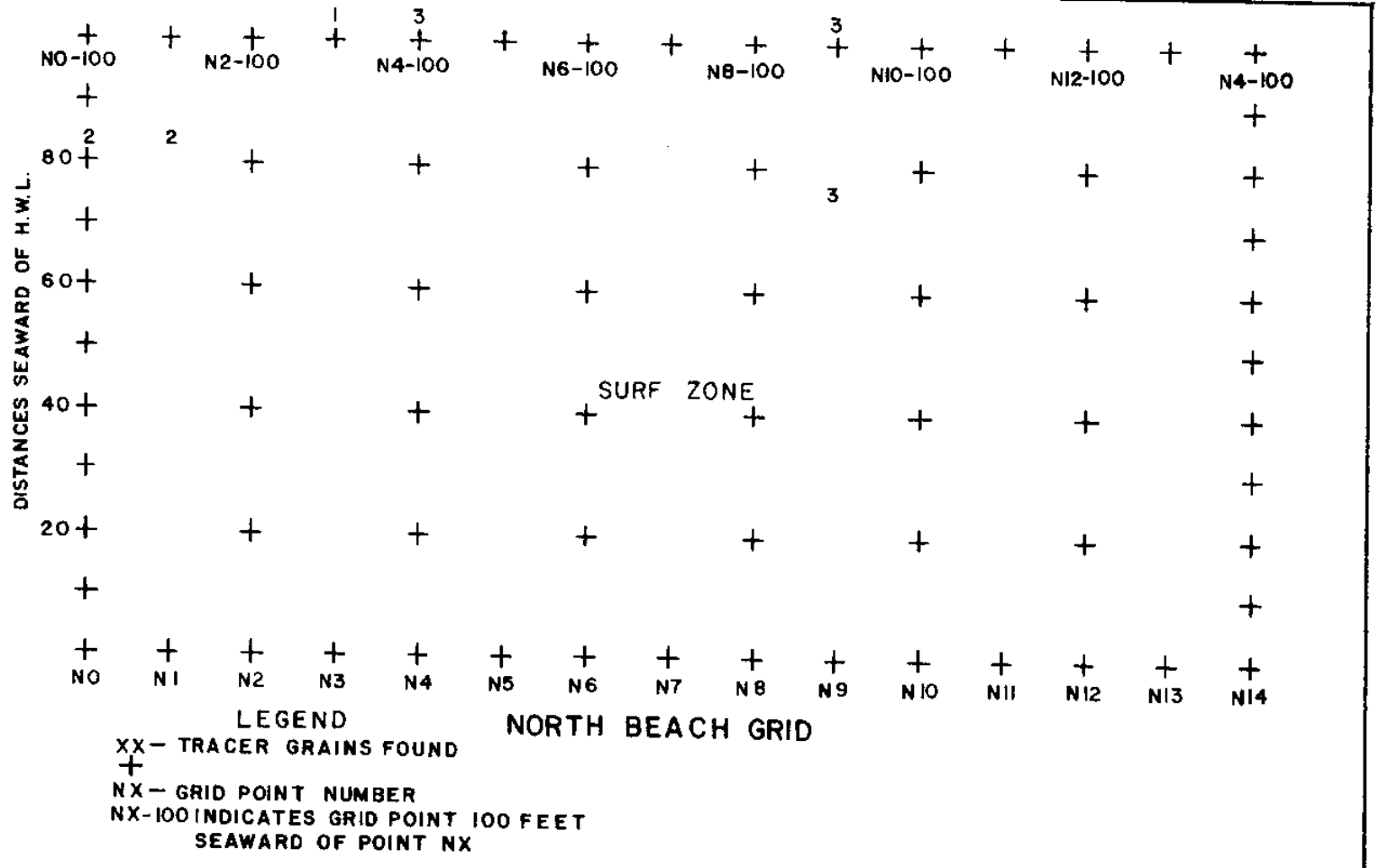

Fig. 66. Fire Orange Tracer Found During Sampling on August 23 between 0820 and 0900 hours

Tracer Test Results - South Beach High Energy Study Area

August 22 sampling period

Within 1 hour and 20 minutes after the introduction of Signal Green tracer, it moved 900 feet down the beach. Figure 67 shows the distribution of tracer over the grid during the first sampling period. The distribution of tracer over the grid was fairly uniform 100 feet into the surf zone. Later sampling from 1320 to 1405 showed large amounts of tracer moving down the beach. The data for that sampling period is shown in Figure 68. The large numbers from grid points S·O to 56 indicate that the tracer was moving as a body towards the inlet.

Trace amounts of fire orange tracer material were also found on the south beach. The locations of these particles is shown in Figure 69.

August 23 sampling period

After one and one-half complete tidal cycles, the green tracer was fairly evenly distributed on the beach. No samples were collected 100 feet into the surf zone, so no data is available for that area. Figure 70 shows the small amount of tracer found at the intro point and the even distribution on the beach. This indicated the movement of sand as a body toward the inlet.

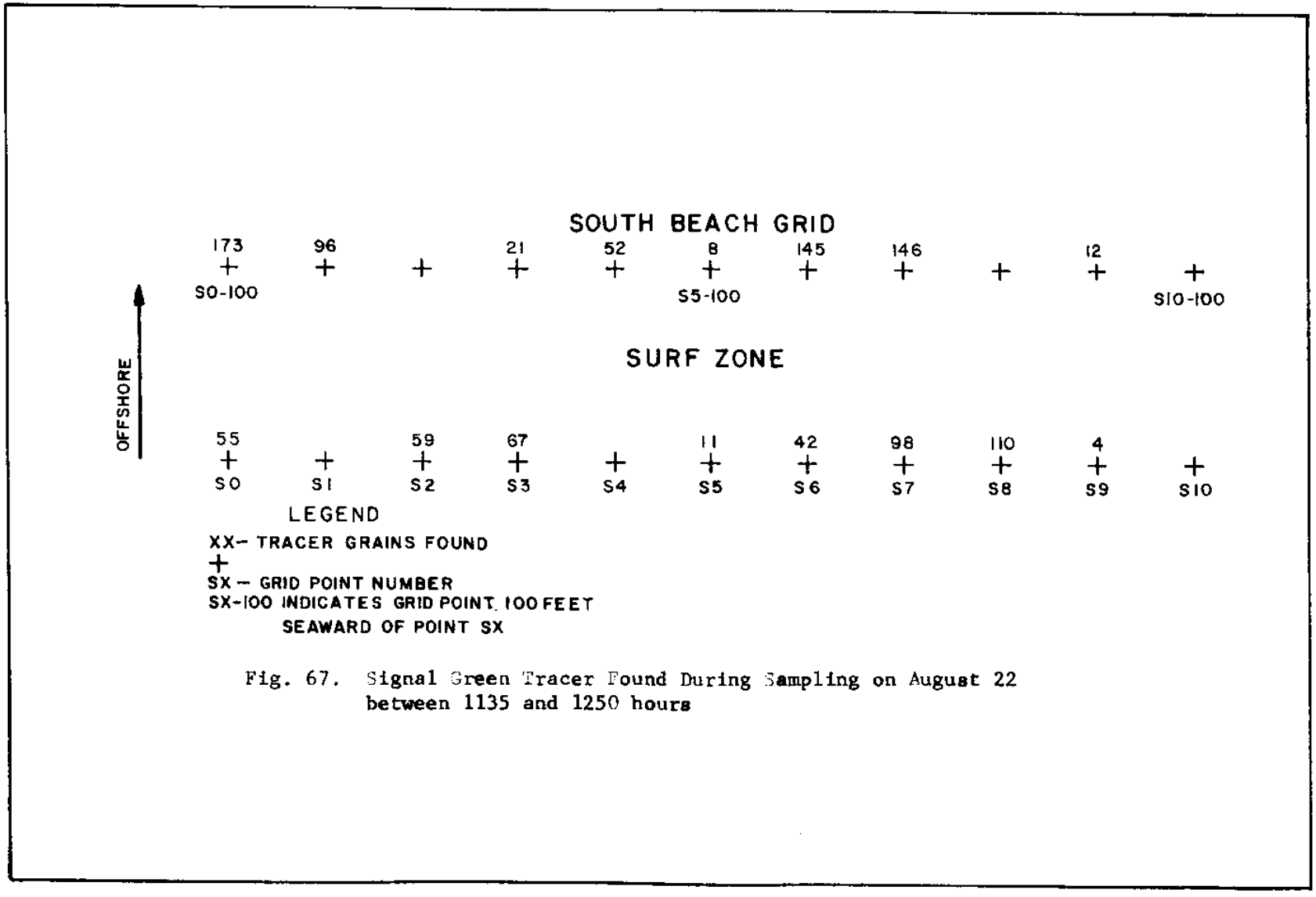

Fig. 67. Signal Green Tracer Found During Sampling on August 22 between 1135 and 1250 hours

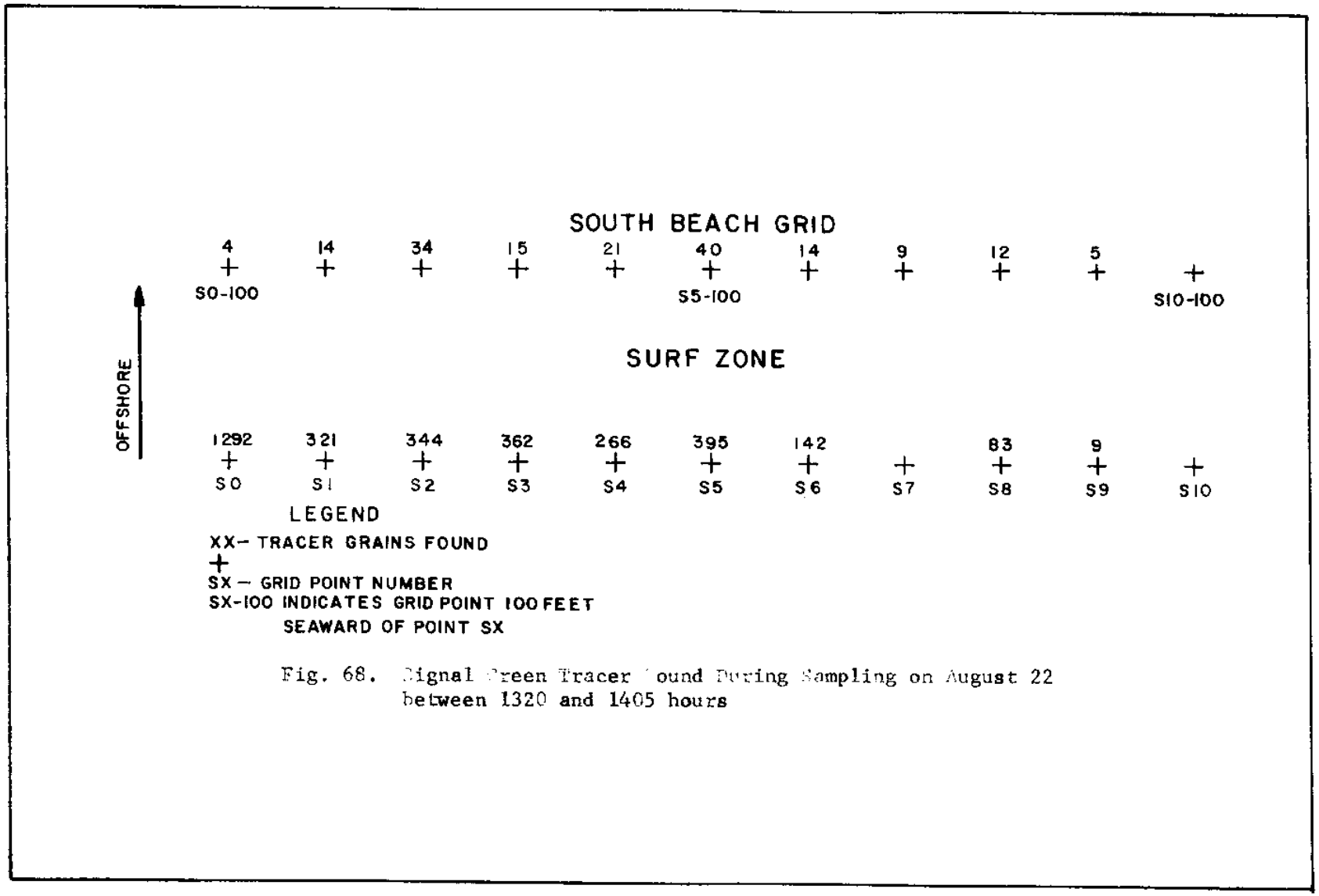

Fig. 68. Signal Green Tracer Found During Sampling on August 22 between 1320 and 1405 hours

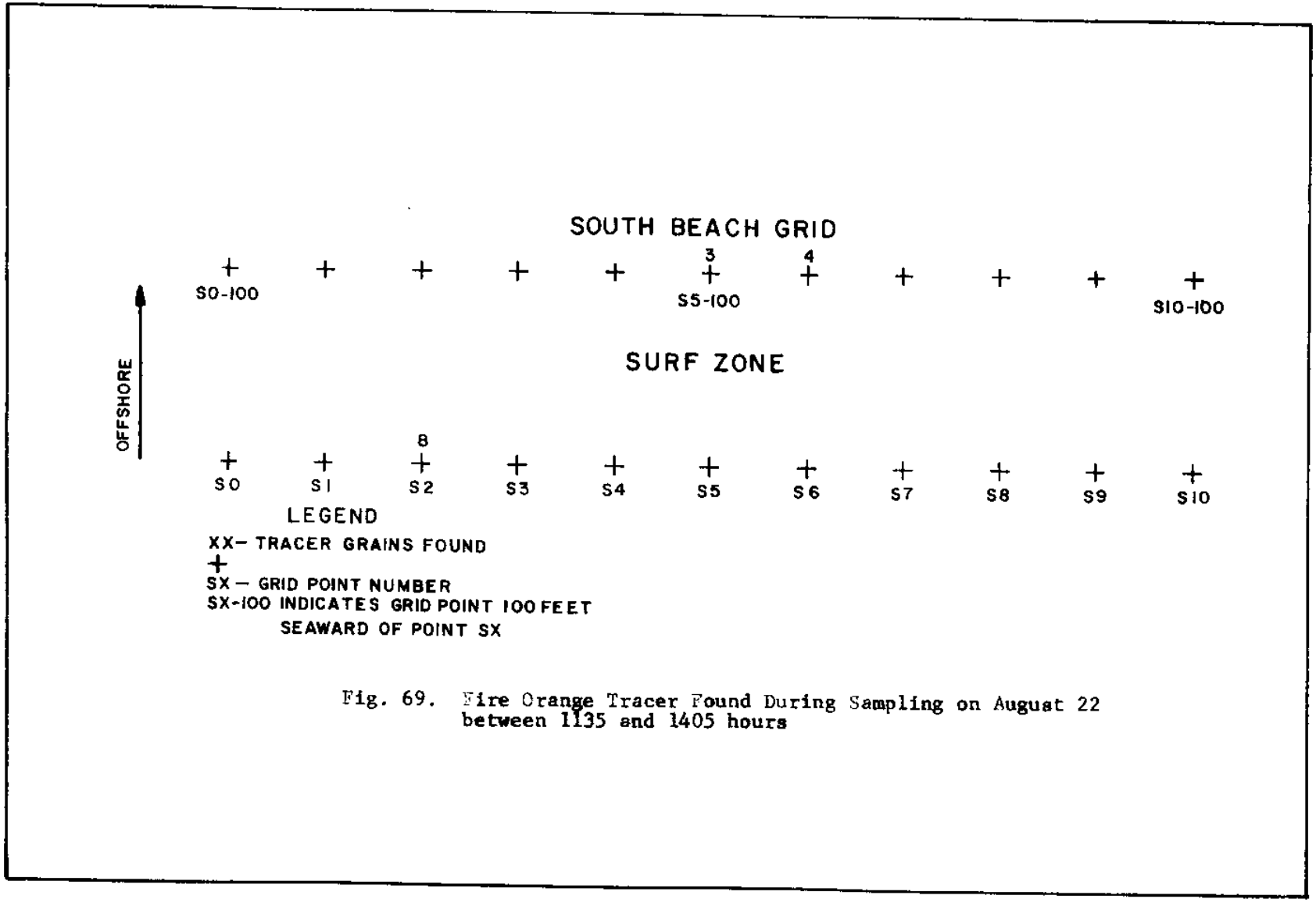

Fig. 69. Fire Orange Tracer Found During Sampling on August 22 between 1135 and 1405 hours

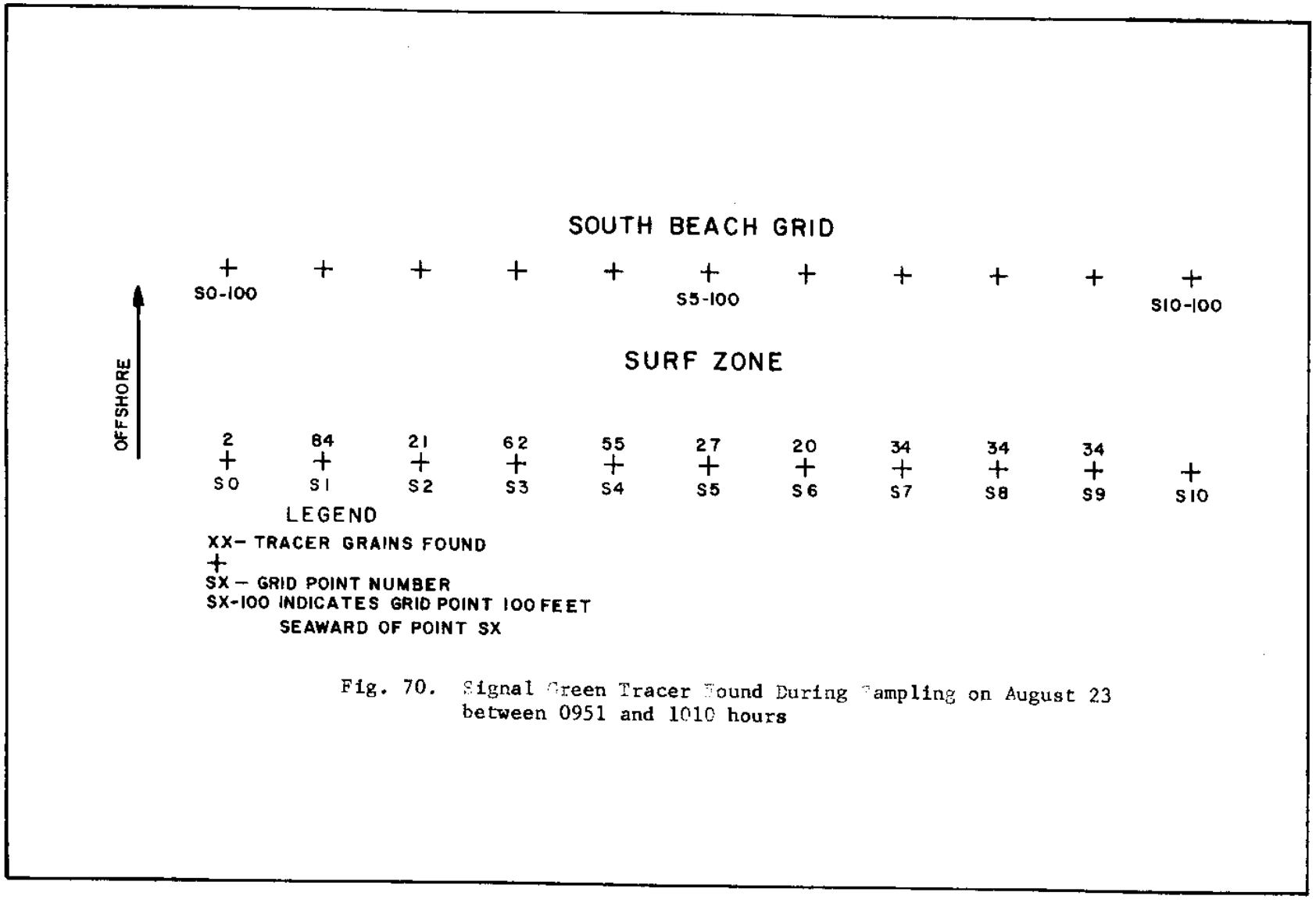

Fig. 70. Signal Green Tracer Found During Sampling on August 23 between 0951 and 1010 hours

APPENDIX B

SEDIMENT CHARACTERISTIC DATA

APPENDIX B

SEDIMENT CHARACTERISTIC DATA

TABLE 17

PHI, MILLIMETER, INCHES CONVERSION TABLE

Phi (ϕ)	mm*	Inches	Phi (ϕ)	mm*	Inches
0.5	0.7071	0.0278	1.8	0.2872	0.0113
0.6	0.6598	0.0260	1.9	0.2679	0.0105
0.7	0.6156	0.0242	2.0	0.2500	0.0098
0.8	0.5743	0.0226	2.1	0.2333	0.0092
0.9	0.5359	0.0211	2.2	0.2176	0.0086
1.0	0.5000	0.0197	2.3	0.2031	0.0080
1.1	0.4665	0.0184	2.4	0.1895	0.0075
1.2	0.4353	0.0171	2.5	0.1768	0.0070
1.3	0.4061	0.0160	2.6	0.1649	0.0065
1.4	0.3789	0.0149	2.7	0.1539	0.0061
1.5	0.3536	0.0139	2.8	0.1436	0.0057
1.6	0.3299	0.0130	2.9	0.1340	0.0053
1.7	0.3078	0.0121	3.0	0.1250	0.0049

STATION I

GRID PT. S0

M_Z = 0.9 ϕ

S = 1.1 ϕ

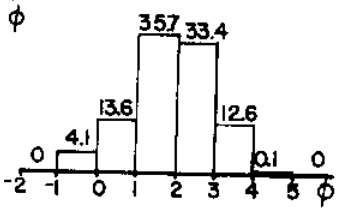

GRID PT. S0-100

M_Z = 1.9 ϕ

S = 0.7 ϕ

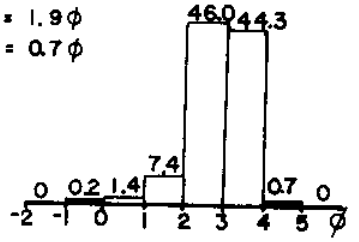

GRID PT. S 5

M_Z = 2.0 ϕ

S = 0.6 ϕ

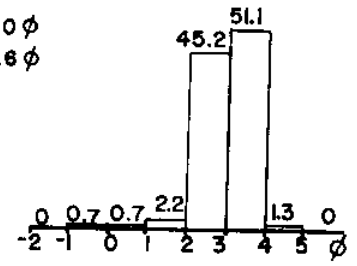

GRID PT. S5-100

M_Z = 1.7 ϕ

S = 0.8 ϕ

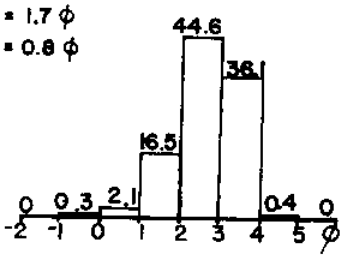

GRID PT. S10

M_Z = 2.3 ϕ

S = 0.6 ϕ

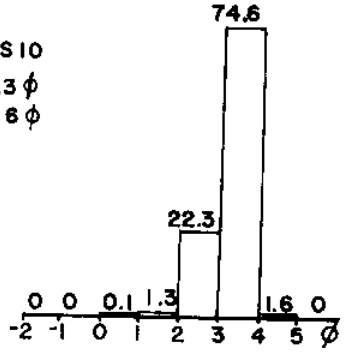

Fig. 71. Histograms for Sediment Samples Analysed

STATION 2

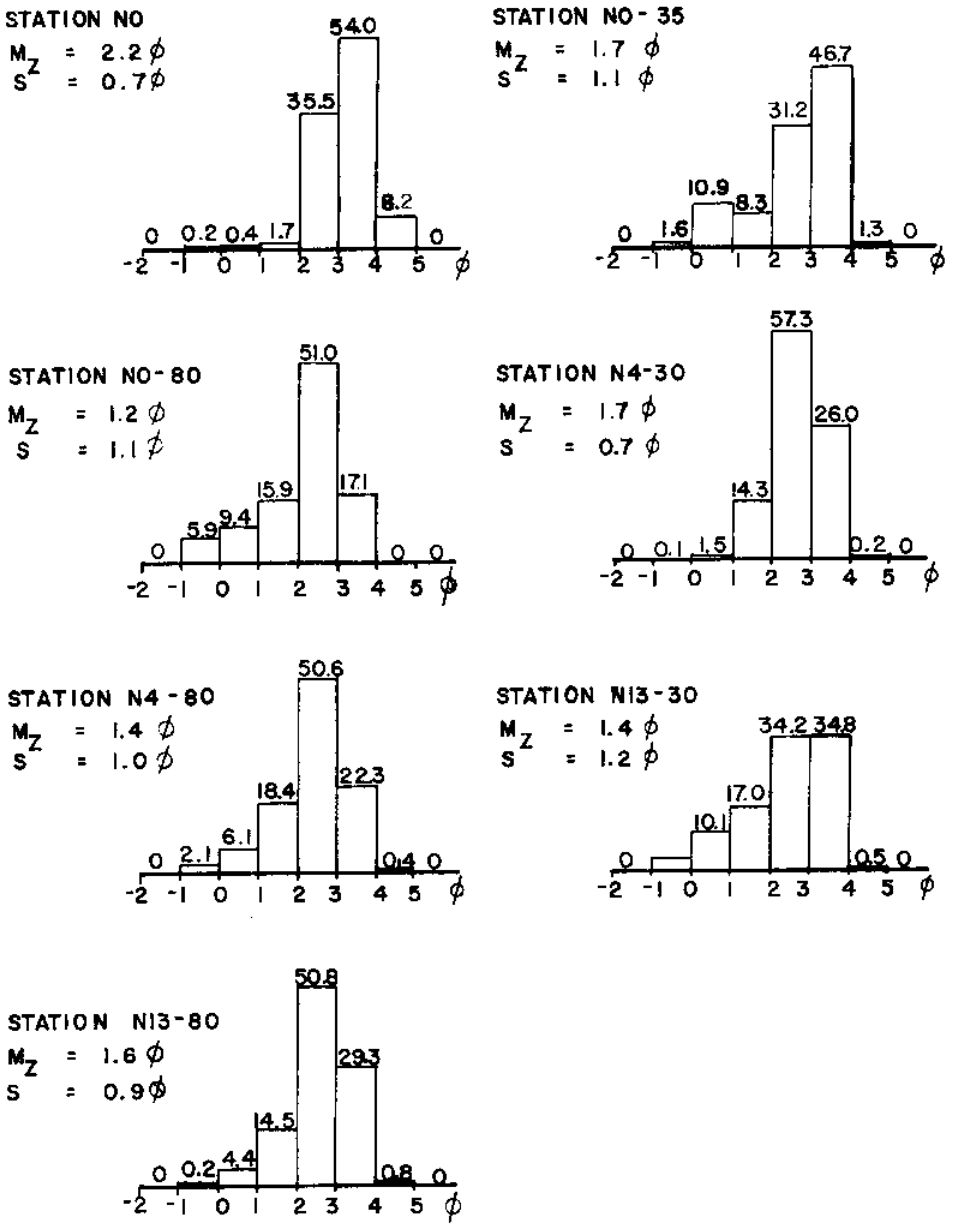

Fig. 71. Histograms for Sediment Samples Analyzed

STATION 4

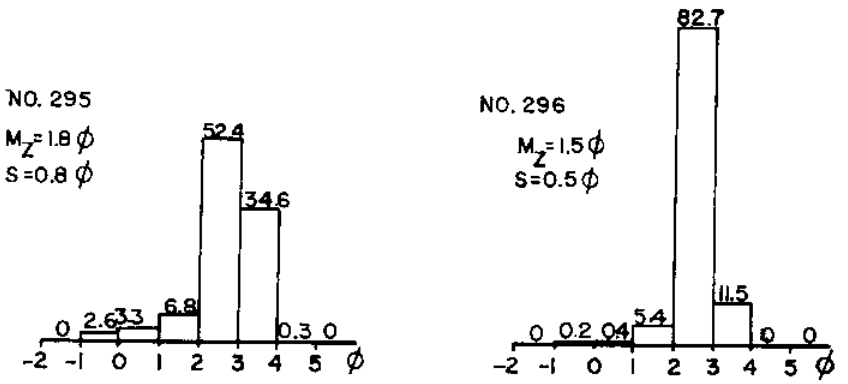

STATION 5

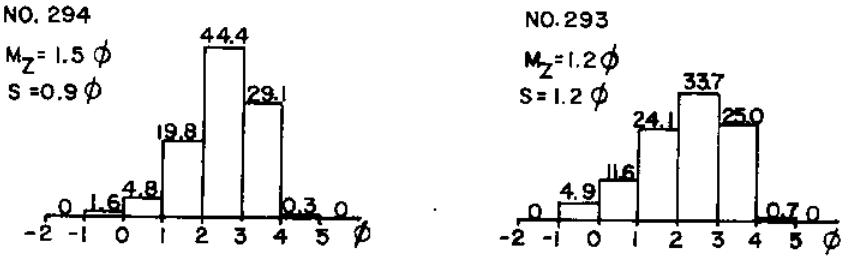

Fig. 71. Histograms for Sediment Samples Analyzed

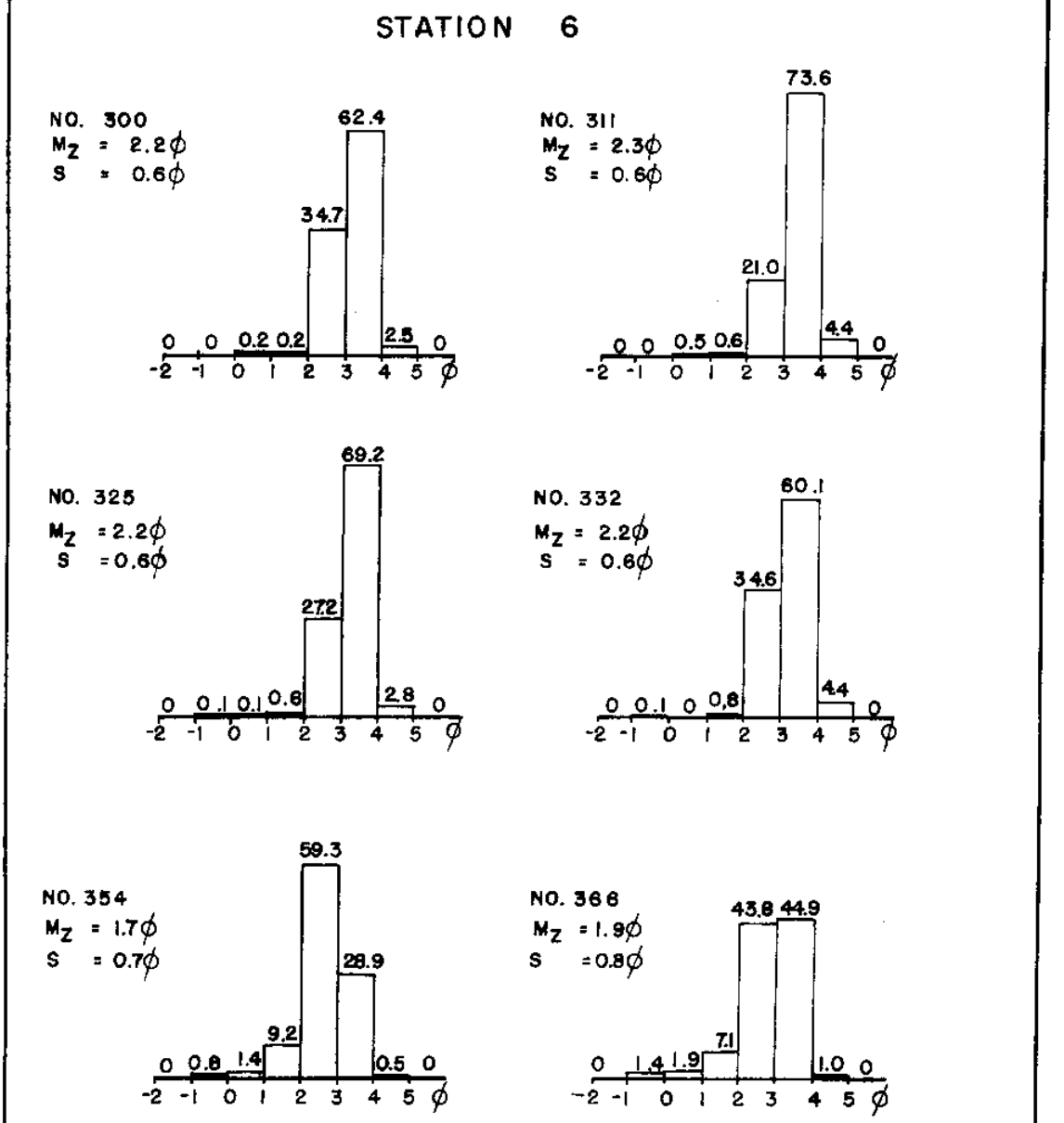

Fig. 71. Histograms for Sediment Samples Analyzed

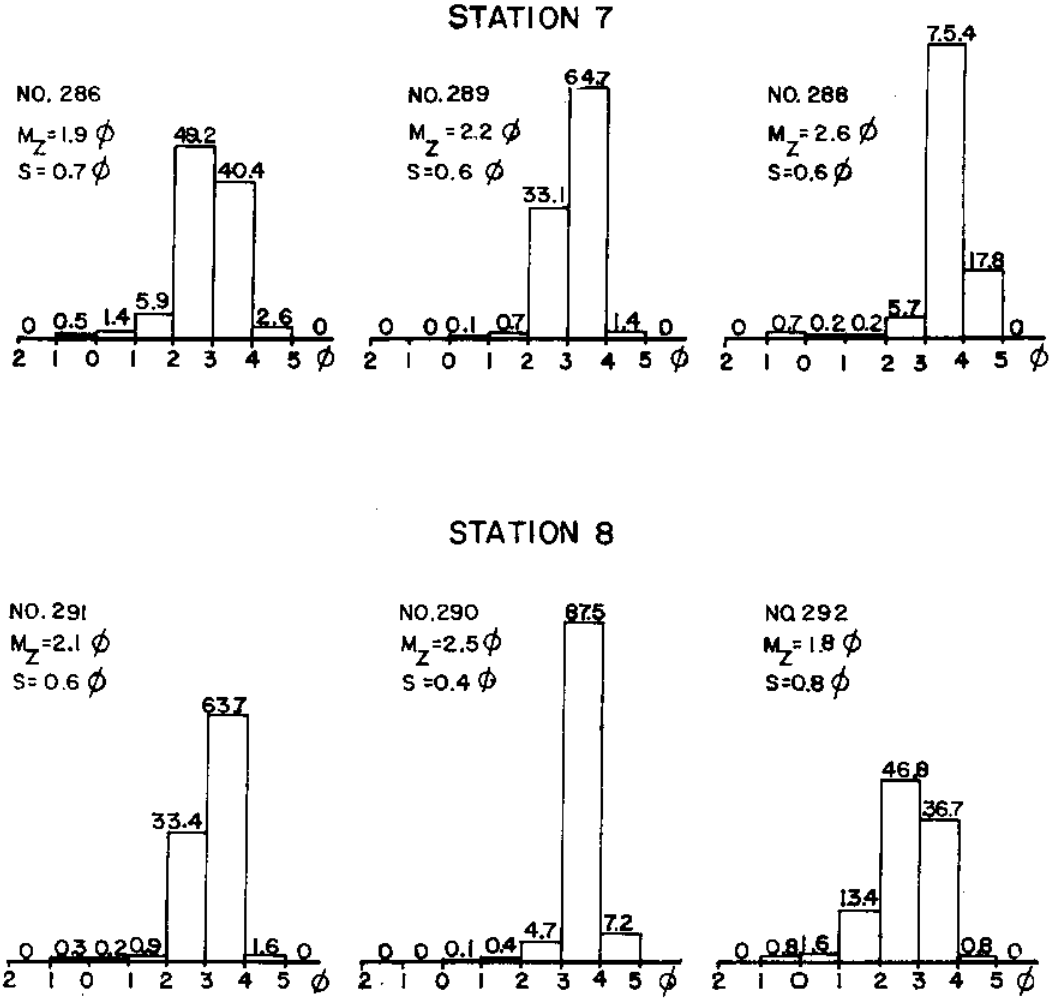

Fig. 71. Histograms for Sediment Samples Analyzed

APPENDIX C

CURRENT STUDY METHODS AND DATA

APPENDIX C

CURRENT STUDY METHODS AND DATA

TABLE 18

CURRENTS IN ADJACENT CHANNELS

Station	Time	Velocity (ft/sec)	Direction	Flow
2	840	0.62	NE	E
	912	0.62	NE	E
	955	0.42	NE	E
	1030	0.22	SW	F
	1107	1.09	SW	F
	1230	1.69	SW	F
	1325	1.81	SW	F
	1410	2.05	SW	F
	1503	2.12	SW	F
	1540	1.71	SW	F
	1622	1.34	SW	F
	1700	0.66	NE	E
	1823	1.22	NE	E
2	1900	1.20	NE	E
3	830	2.30	SSE	E
	920	1.71	SSE	E
	1006	1.41	SSE	E
	1037	0.36	NNE	F
	1113	2.05	NNE	F
	1240	3.01	NNE	F
	1330	3.38	NNE	F
	1420	3.30	NNE	F
	1512	3.40	NNE	F
	1555	3.01	NNE	F
	1630	2.37	NNE	F
	1712	1.27	NNE	F
	1830	2.23	SSE	E
3	1912	2.57	SSE	E

TABLE 18--Continued

Station	Time	Velocity (ft/sec)	Direction	Flow
4	815	1.08	NE	E
	937	0.60	NE	E
	1016	0.27	NE	E
	1047	0.59	SW	F
	1120	1.22	SW	F
	1253	0.90	SW	F
	1345	1.02	SW	F
	1430	0.91	SW	F
	1520	0.55	SW	F
	1607	0.26	SW	F
	1640	0.15	SW	F
	1720	0.36	NE	E
	1845	1.38	NE	E
4	1920	1.32	NE	E
5	904	1.69	E	E
	947	1.15	E	E
	1025	0.40	E	E
	1053	1.00	W	F
	1126	1.94	W	F
	1305	2.14	W	F
	1350	2.39	W	F
	1435	2.10	W	F
	1530	1.71	W	F
	1612	1.13	W	F
	1647	0.49	W	F
	1730	0.49	E	E
	1850	2.48	E	E
5	1930	2.65	E	E

TABLE 19

SHOAL CURRENTS

Location	Time	Current (ft/sec)	Direction	Flood or Ebb (F or E)
300	0810	0.72	80	E
	0935	0.56	S95E	E
	1215	0.69	S135W	F
	1330	0.82	N70W	F
	1431	0.79	N55W	F
	1559	0.49	N60W	F
	1700	0.33	N35W	F
	1812	0.82	N40E	E
	1857	1.12	N80E	E
310	0940	0.52	S135E	E
	1219	0.89	N125N	F
	1332	1.02	N50W	F
	1435	0.98	N60W	F
	1502	0.82	N60W	F
	1704	0.49	N85W	F
	1815	0.79	SE	E
	1900	0.72	E	E
320	0944	0.00	-	S
	1222	1.61	W	F
	1335	2.07	N55W	F
	1438	1.87	N55W	F
	1606	1.28	N60W	F
	1702	0.62	N40W	F
	1819	0.89	N45E	E
	1902	0.79	S100E	E
330	0830	1.12	E	E
	0948	0.79	N75E	E
	1225	1.54	W	F
	1340	1.61	N65W	F
	1442	1.80	N60W	F
	1609	1.02	N60W	F
	1711	.30	N40W	F
	1822	1.18	NE	E
	1904	1.35	E	E
340	0833	1.02	ESE	E
	0957	0.49	S11oE	E
	1229	1.87	N85W	F
	1343	1.94	N50W	F
	1445	1.71	N60W	F
	1614	1.18	N60W	F

TABLE 19--Continued

Location	Time	Current (ft/sec)	Direction	Flood or Ebb (F or E)
340	1715	0.39	N50W	F
	1825	0.85	N70E	E
	1906	1.18	E	E
350	0835	0.56	S120E	E
	0957	0.23	S110E	E
	1232	1.9	W	F
	1346	1.9	N50W	F
	1448	2.03	N60W	F
	1618	1.18	N55W	F
	1718	0.30	N40W	F
	1827	0.75	W	E
	1909	0.98	S115E	E
360	0838	Too Shallow	-	-
	1236	1.59	S95W	E
	1350	1.57	N60W	F
	1451	1.44	N60W	F
	1622	1.25	N60W	F
	1720	0.0	-	-
	1830	0.59	N75E	E ?
	1911	0.69	S115E	E
361	0840	1.28	S130E	E
	0959	-	-	-
	1240	1.57	W	F
	1356	1.74	N50W	F
	1454	1.77	N60W	F
	1626	0.89	N60W	F
	1724	0.33	N15W	F
	1832	1.08	N80E	E
341	1300	1.38	N35W	F
	1459	1.15	N60W	F
	1632	0.92	N50W	F
	1730	0.30	N15W	F
	1837	1.15	N75E	E
342	0852	-	-	-
	1305	0.79	N45W	F
	1406	0.98	N50W	F
	1502	0.79	N65W	F
	1637	0.56	N50W	F
	1733	0.39	N05E	E
	1840	0.62	N30E	E

TABLE 19--Continued

Location	Time	Current (ft/sec)	Direction	Flood or Ebb (F or E)
343	0852	-	-	-
	1307	1.15	N50W	F
	1410	-	-	-
	1505	1.12	N60W	F
	1604	0.59	N45W	F
	1736	0.33	N05E	E
	1842	0.59	E	E
344	0852	-	-	-
	1310	0.72	N55W	F
	1412	0.85	N45W	F
	1509	0.89	N60W	F
	1644	0.56	N30W	F
	1739	0.46	N05E	E
	1844	0.62	N75E	E
345	0852	-	-	-
	1315	0.75	N60W	F
	1415	0.66	N50W	F
	1512	0.69	N55W	F
	1648	0.36	N45W	F
	1743	0.72	N05E	E
	1846	0.89	N70E	E
346	0853	0.33	S125E	E
	1319	1.05	N50W	F
	1417	1.08	N60W	F
	1515	0.85	N55W	F
	1657	0.36	N50W	F
	1745	0.30	N35E	E
	1848	0.59	E	E